Universidad Abierta Interamericana (Argentina)
Università degli Studi di Palermo. Dipartimento di Scienze e Tecnologie Biologiche Chimiche e Farmaceutiche (STEBICEF) (Italy)

TITLE:

"Polyurethane mesh and breast implant in a rat model"

DOCTOR
Sandra Filiciani MD

TUTOR
Argentinian Tutor: Prof. Gagliardi Enrique Pedro MD, PhD. (Argentinian Catholic University)
Italian Tutor: Prof. D'Amore Antonio, PhD. (RiMED Foundation, University of Pittsburgh)
Prof. Caradonna Fabio, PhD. (Università degli Studi di Palermo)

COORDINATOR
Argentinian: Prof. Alicia Mattiazzi Md, PhD
Italian: Prof. Bruno Pignataro, PhD

DOUBLE DEGREE IN CO-TUTELA
PhD in Medicine Universidad Abierta Interamericana (Argentina)
PhD in Technology and Sciences for Human Health. Università degli Studi di Palermo (Cycle 36, Italy)

YEAR OF TITLE 2024

ACKNOWLEDGE

I want to express my sincere gratitude to all those who have contributed to completing this thesis. Their support and guidance have been invaluable throughout this period.

I am mainly grateful to *UAI* and *UNIPA* for creating this opportunity and allowing me to be the first PhD student in Co-tutela Argentina-Italy. Special thanks to RiMed Foundation and Cardiovascular Tissue Engineering D'Amore Lab Italy for providing their laboratory.

This endeavor would not have been possible without the Directors: *Professor Alicia Mattiazzi, Md. Ph.D.(*Cardiovascular Research Emeritus, CONICET) director of the Argentinian PhD program; *Dr. Bruno Giuseppe Pignataro* (Full Professor UNIPA), Italian coordinator of the PhD program; and Dr. Fabio Caradonna, Associate Professor UNIPA, co-tutela coordinator, and even my tutor, for building and maintaining this co-tutela program.

I deeply appreciate my Argentinian supervisor, Enrique Pedro Gagliardi, MD, PhD (Plastic Surgeon, Consulting Professor at Catholic Argentina University UCA). His guidance and expert advice have been instrumental in shaping this thesis.

Words cannot express my gratitude to special persons who are my Co-Tutors: *Dr. Antonio D'Amore* (Bioengineer, Group leader, and head of the tissue engineering program Fondazione RiMED, Associate Professor at the University of Pittsburgh), for allowing me to be part of the D'Amore Lab, conducting and believing in this project. His insightful feedback, patience, and support encouraged me to grow in this research. Extremely beautiful, the Argentinian flag and his love for our country. I extend my profound gratitude to the remarkable woman whose brilliance, dedication, and mentorship have deeply influenced this thesis, *Dr. Laura Modica de Mohac* (Pharmacy and Post Doctoral Researcher); from our first encounter, her guidance, knowledge and support have not only shaped this research but also enriched my understanding of bioengineers and every step of the process.

Really especially thanks to all my Italian colleagues: *Dr. Marzio Di Giuseppe* and *Patrizia Caruso, PhD* students, both Mechanical Engineer, for teaching me the mechanical tests; Dr. Arianna Adamo (Pharmaceutical Biotechnology); *Dr. Victor Balashov* (Postdoctoral Researcher), and *Flaviana Falci* PhD. Student (Bioenginieer), of those who I learned histological process; *Melika Malekhosseini, PhD student (Bio-Nanomaterials)* and *Gallina Matteo, MSc* (Pharmacy), for helping me with electrospinning and mesh fabrication; *Dr. Federica Cosentino* (Scientist in numerical models) who taught me the process and analysis programs; *Dr. Pietro Terranova* (Mechanical Engineer) constructing breast implant models; *Dr. Joan D. Laubrie Soto* (Bio-Mechanical Engineer) for sharing the Chilean mate; the PhD students and Bioencineer: *Elisa Lazalaco*, *Enrica Romano, Marta Baccarella* and *Di Caccamo, Beatrice*, always helping with the research and accommodation. Scientists in Cardiovascular Tissue Engineering at D'Amore Lab Ri.MED. I want to express my heartfelt gratitude; they were like my family, friends, teachers, students, and children; they helped me to do this research.

I am deeply indebted to Argentinian colleague *Franco Chiaraluce, MD*. (Pathologist) for his enthusiasm and dedication to evaluate and analyze the histology also on the weekend; *Jorge D'Angelo MD*. Professor (Plastic Surgeon), *Dr. Ariel Quiroga, Dr. Carla Comanzo, Dr. Marina Vera* (all Professors and Researchers of CONICET UAI, UNR), who helped me with the rat's surgery and housing; *Alejandra Martinez* and *Diego Parenti,* (Histotechnology Technician in UNR) performing the process of staining**.**

Dra. Florencia Fernandez (UAI) managed every activity strategically and efficiently in Argentina. Marta Alarcon, a Statistician, made this research's statistical analysis and interpretation possible.

I want to express my deepest gratitude to my husband, *Guillermo,* to my children, *Maru* and *Fede; Cata, Nico, Dechi, and my mom*. Their unwavering love, support, and understanding throughout this academic journey have been my pillars of strength. I am truly blessed to have them in my life.

CONFLICT OF INTEREST

The author declares that she has no conflicts of interest that could have appeared to influence the work reported in this paper.

FUNDING

This research was financially supported by the Autor, UAI, which provided part of the travel; RiMed Foundation, which conducted all the experiments in Italy; and UAI and Universidad Nacional de Rosario UNR, which conducted in vivo experiments.

SUMMARY

Breast implants are used for aesthetic and reconstructive purposes to enhance the size and shape of the breast. The submuscular pocket provides upper pole coverage. However, the lateral and inferior pole could be covered only by the thin skin, predisposing to ptosis, bottoming out, and implant extrusion. Better results can be achieved by using mesh to implant support. Whether it is biological or synthetic meshes, there are also some potential drawbacks, such as infection or rejection. The mesh degradation can be problematic since rapid absorption can cause implant bottoming out, or long-lasting durability can produce a continued foreign body reaction.

Hypothesis: PCUU + Tecoflex™ (PCUU-T) nanofiber mesh could stimulate tissue ingrowth with reduced scar formation and provide mechanical support in breast implant procedures compared to other synthetic meshes.

Objective: To evaluate the use of biodegradable Poly (carbonate- urethane) urea (PCUU) plus non-degradable Tecoflex™ (PCUU-T) nonwoven mesh as a scaffold in association with a breast implant and its behavior in a small animal preclinical study in comparison with commercial mesh Ultrapro™.

Method and Material: 1) Five synthetic meshes were evaluated through the thickness, density, mechanical, and porosity tests. 2) Different blends of PCUU+T concentration were prepared and underwent several tests (thickness, density, degradation, porosity, and mechanical tests). 3) An in vivo study was conducted with n=18 adult female Wistar rats (70 days old). Experiments were divided into three groups (6 rats each), receiving PCUU+T mesh on the left side and Ultrapro™ mesh on the right side on the subdermal dorsal pockets: Smooth group (S) received smooth mini-breast implants per side; Texture group (T) received textured implants per side, and Mesh group (M) was a control group that received mesh without implants. The rats' weight was measured, and blood was collected before and after surgery to assess toxicity. Postoperative complications were analyzed with clinical exam and by ultrasound. After euthanasia on day 63, the block were removed for histological and bacteriological evaluation.

Results: Ultrapro™ mesh represented the best characterization mesh. The 50:50 PCUU+T blend was selected (thickness 374 μm, weight 46.33mg, anisotropic ratio 2.14, porosity 4.71). Rats' weights increased by 21% from the preoperative to 63 days ($P<0,05$). 89% of the rats have no complications. No presence of seroma was identified. Bacteriology was 88% negative, 6% presented *Staphylococcus epidermidis*, and 6% *Corynebacterium*. No giant cells were found on the PCUU-T in all groups; they were only present in the Ultrapro™ most with smooth implants. PCUU-T mesh showed significantly fewer plasmacytes and lymphocytes than Ultrapro™. Eosinophils were higher on control skin. Mast cells were significantly lower on the PCUU-T. Ultrapro™ had a greater amount of inflammatory cells. Group M showed significantly more numbers of vessels than the control skin. Vascular congestion and hemosiderin deposits were observed with Ultrapro™. The vascular component on the PCUU-T was similar to the control group M. The collagen concentration on PCUU-T showed less collagen formation than Ultrapro™, whatever the implant surface. Hematological parameters were similar in the pre and postoperative measures.

Conclusion: This research developed a novel nanofiber partially biodegradable electrospun PCUU-T nonwoven mesh. This designed mesh was used as a scaffold in association with a breast implant in a rat model and compared with partially absorbable Ultrapro™ mesh in the respective dorsum of a rat model.

The outcomes of the novel mesh were associated with the lowest foreign body response, without giant cell formation, a good degree of new collagen deposition, and matrix

remodeling. It is suitable for native tissue integration, healing, and remodeling tissue, with a good anisotropy ratio to provide future support for breast implant-base reconstruction.
Keywords: Poly(carbonate- -urethane) urea, Tecoflex, Ultrapro, mesh, biomaterial, electrospinning, breast implant-base reconstruction.

SINTESI

Le protesi al seno sono dispositivi medici utilizzati per scopi estetici e ricostruttivi al fine di migliorare le dimensioni e la forma del seno. La tasca sotto muscolare rappresenta la sede opportuna per il posizionamento delle protesi nel polo superiore. Tuttavia, in alcuni casi, il polo laterale e inferiore risultano coperti solo da uno strato sottile di pelle, predisponendo alla ptosi, al cedimento e all'estrazione dell'impianto. In molti casi, migliori risultati estetici e clinici possono essere ottenuti utilizzando una maglia per il supporto dell'impianto. Che si tratti di maglie biologiche o sintetiche, ci sono anche alcuni potenziali svantaggi nell'utilizzarle nella chirurgia basata sugli impianti mammarie, principalmente il rischio di infezione o rigetto. Il degrado della maglia può essere problematico poiché l'assorbimento rapido può causare il cedimento dell'impianto o la durabilità a lungo termine può produrre una continua reazione del corpo estraneo.
Ipotesi: Lo sviluppo di una maglia fibrosa in PCUU + Tecoflex™ (PCUU-T) potrebbe stimolare la crescita del tessuto con ridotta formazione di cicatrici e fornire supporto meccanico nei procedimenti di impianto mammarie rispetto ad altre maglie sintetiche.
Obiettivo: Valutare l'uso della maglia non tessuta in PCUU-T come impalcatura in associazione con un impianto mammario ed il suo comportamento in uno studio preclinico su piccoli animali in confronto con la maglia commerciale Ultrapro™.
Metodo e Materiale: 1) Cinque maglie sintetiche sono state valutate attraverso test di spessore, densità, meccanici e di porosità. 2) Diverse concentrazioni di PCUU+T sono state preparate e sottoposte a vari test (spessore, densità, degradazione, porosità e test meccanici). 3) Uno studio in vivo è stato condotto con n=18 ratti Wistar femmine adulte (70 giorni di età). Gli esperimenti sono stati divisi in tre gruppi (6 ratti ciascuno), ricevendo maglia PCUU+T sul lato sinistro e maglia Ultrapro™ sul lato destro nei taschini dorsali sotto muscolari: Il primo gruppo Liscio (S) ha ricevuto mini-impianti mammarie lisci per lato; il secondo gruppo Texture (T) ha ricevuto impianti testurizzati per lato, e il terzo gruppo Maglia (M) è stato un gruppo di controllo che ha ricevuto solo la maglia senza impianti. Il peso dei ratti è stato misurato e il sangue è stato prelevato dalla coda prima e dopo l'intervento chirurgico per valutare la tossicità. Le complicanze postoperatorie sono state analizzate con esame clinico e mediante ecografia. Dopo l'eutanasia al giorno 63, il blocco è stato rimosso per valutazione istologica e batteriologico.
Risultati: La maglia Ultrapro™ ha rappresentato le migliori caratterizzazioni delle maglie. La miscela 50:50 PCUU+T (spessore 374 µm, peso 46,33 mg, rapporto anisotropo 2,14, porosità 4,71). Il peso dei ratti è aumentato del 21% dal preoperatorio ai 63 giorni ($P<0,05$). L'89% dei ratti non ha avuto complicazioni. Nessuna presenza di seroma è stata identificata clinicamente e mediante ecografia. La batteriologia dopo l'eutanasia è stata negativa all'88%, il 6% ha presentato Staphylococcus epidermidi e il 6% Corynebacterium. Non sono state trovate cellule giganti sul lato PCUU-T in tutti i gruppi; erano presenti solo nella maglia Ultrapro™ e avevano una significativa associazione con gli impianti mammarie lisci. Inoltre, la maglia PCUU-T ha mostrato significativamente meno plasmaciti e linfociti rispetto a Ultrapro™. Una lieve fibrosi è

stata riconosciuta sulla periferia di Ultrapro™. Gli eosinofili erano più elevati sulla pelle di controllo, il gruppo di impianti testurizzati sul lato PCUU-T ha mostrato più eosinofili rispetto a Ultrapro™. I mastociti erano significativamente inferiori sul lato PCUU-T rispetto a Ultrapro™. Ultrapro™ aveva una maggiore quantità di cellule infiammatorie. Il gruppo M ha mostrato significativamente più numeri di vasi rispetto alla pelle di controllo. Congestione vascolare e depositi di emosiderina sono stati osservati nella maglia Ultrapro™. Il componente vascolare sul PCUU-T aveva caratteristiche molto simili al gruppo di controllo M. Il risultato ha identificato una buona integrazione nella maglia PCUU-T. La concentrazione di collagene su PCUU-T ha mostrato una formazione di collagene inferiore rispetto a Ultrapro™ indipendentemente dalla superficie dell'impianto. I parametri ematologici erano simili nelle misurazioni pre e postoperatorie.
Conclusioni: Questa ricerca ha sviluppato una nuova maglia non tessuta nano fibrosa parzialmente biodegradabile di PCUU-T. Questa maglia progettata è stata utilizzata come impalcatura in associazione con un impianto mammarie in un modello di ratto e confrontata con la maglia parzialmente assorbibile Ultrapro™ nel dorso di un modello di ratto. I risultati della nuova maglia sono stati associati alla più bassa risposta del corpo estraneo, senza formazione di cellule giganti e con un buon grado di deposizione di nuovo collagene e rimodellamento della matrice. Adatta per l'integrazione del tessuto nativo, la guarigione e il rimodellamento del tessuto, con un buon rapporto di anisotropia per fornire supporto futuro per la ricostruzione basata sull'impianto mammarie.
Parole chiave: Poli (carbonato-urea-uretano), Tecoflex, Ultrapro, maglia, biomateriale, elettrofilatura, ricostruzione basata sull'impianto mammarie.

RESUMEN

Los implantes mamarios son dispositivos médicos utilizados con fines estéticos y reconstructivos para mejorar el tamaño y la forma de la mama. El bolsillo submuscular es una buena opción para proporcionar cobertura de polo superior. Sin embargo, en algunos casos, el polo lateral e inferior podría ser cubierto solo por la piel delgada, predisponiendo a la ptosis, deslizamiento hacia fuera, y la extrusión del implante. Se pueden lograr mejores resultados utilizando malla para utilizar como soporte. Ya se trate de mallas biológicas o sintéticas, también hay algunos inconvenientes potenciales para su uso en la cirugía basada en implantes mamarios, principalmente el riesgo de infección o rechazo. La degradación de la malla puede ser problemática, ya que la rápida absorción puede causar que el implante se ptose o una durabilidad duradera puede producir una reacción continua del cuerpo extraño.
Hipótesis: La malla de nanofibras PCUU + Tecoflex™ (PCUU-T) podría estimular el crecimiento de tejidos con formación reducida de cicatrices y proporcionar apoyo mecánico en los procedimientos de implante mamario en comparación con otras mallas sintéticas.
Objetivo: Evaluar el uso de Poli (carbonato-urea-uretano) (PCUU) biodegradable, más Tecoflex™ no degradable (PCUU-T) malla no tejida, como un andamio en asociación con un implante de mama y su comportamiento, realizando en un estudio preclínico en animal en comparación con la malla comercial Ultrapro™ .
Método y Material: 1) Se evaluaron cinco mallas sintéticas a través de las pruebas de espesor, densidad, mecánica y porosidad. 2) Se prepararon diferentes mezclas de concentración de PCUU+T que fueron sometidas a varias pruebas (espesor, densidad, degradación, porosidad y pruebas mecánicas). 3) Se realizó un estudio en vivo con n=18 ratas Wistar hembras adultas (70 días). Los experimentos se dividieron en tres grupos (6

ratas cada uno), recibiendo malla PCUU + T en el lado izquierdo y malla Ultrapro™ en el lado derecho en los bolsillos dorsales subdérmicos: El primer grupo Smooth (S) recibió mini-implantes mamarios lisos por lado; el segundo grupo Texture (T) recibió implantes texturizados por lado, y el tercer grupo Mesh (M) fue un grupo de control que recibió malla sin implantes. Se midió el peso de las ratas y se recogió sangre de la cola antes y después de la cirugía para evaluar la toxicidad. Las complicaciones postoperatorias se analizaron con examen clínico y ecografía. Después de la eutanasia del día 63, el block fue retirado para su evaluación bacteriológico e histológica.

Resultados: La malla Ultrapro™ represento la mejore malla para estudiar. La mezcla 50:50 PCUU+T (espesor 374 μm, peso 46.33 mg, anisotrópia 2.14, porosidad 4.71). El peso de las ratas aumentó un 21% desde el preoperatorio a 63 días ($P<0,05$). El 89% de las ratas no presentan complicaciones. No se identificó clínicamente ni por ultrasonido la presencia de seroma. La bacteriología después de la eutanasia fue 88% negativa, 6% presentó Staphylococcus epidermidis y 6% Corynebacterium. No se encontraron células gigantes en el lado PCUU-T en todos los grupos; solo estaban presentes en la malla Ultrapro™ y tenían una asociación significativa con implantes mamarios lisos. Además, la malla PCUU-T mostró significativamente menos plasmacitos y linfocitos que Ultrapro™ . Se reconoció fibrosis leve en la periferia de Ultrapro™ . Los eosinófilos fueron más altos en la piel de control, el grupo de implantes de textura en el lado PCUU-T mostró más eosinófilos que Ultrapro™ . Los mastocitos eran significativamente más bajos en el lado PCUU-T que Ultrapro™ . Ultrapro™ tenía una mayor cantidad de células inflamatorias. El grupo M mostró un número significativamente mayor de vasos que la piel de control. Se observó congestión vascular y depósitos de hemosiderina en la malla Ultrapro™. El componente vascular en el PCUU-T tenía características muy similares al grupo control M. El resultado identificó una buena integración en la malla PCUU-T. La concentración de colágeno en PCUU-T mostró menos formación de colágeno que Ultrapro™ sea cual sea la superficie del implante. Los parámetros hematológicos fueron similares en las medidas pre y postoperatoria.

Conclusión: Esta investigación desarrolló una nueva malla no tejida PCUU-T de nanofibra parcialmente biodegradable. Esta malla diseñada se utilizó como andamio en asociación con un implante de mama en un modelo de rata y se comparó con la malla Ultrapro™ parcialmente absorbible.

Los resultados de la nueva malla se asociaron con la menor respuesta de cuerpo extraño, sin formación de células gigantes y un buen grado de deposición de colágeno y remodelación de la matriz. Adecuado para la integración de tejido nativo, curación y remodelación de tejido, con una buena relación de anisotropía para proporcionar apoyo futuro para la reconstrucción de la base del implante de mama.

Palabras claves: Poli(carbonato-urea-uretano), Tecoflex, Ultrapro, malla, biomaterial, electrospinning, reconstrucción de implante de mama-base.

Table of Contents

INTRODUCTION

Many changes in breast skin elasticity are common occurrences, especially after significant life events like childbirth, breastfeeding, weight loss, sequelae after aesthetic surgeries, or skin-sparing mastectomy for breast cancer.

Breast implants are medical devices used for both aesthetic and reconstructive purposes to enhance the size and shape of the breast. It presents a great challenge to obtain an aesthetic result.

The submuscular breast implant technique is a good option to give volume and provide the upper pole implant coverage. However, in some cases, the lateral and inferior pole could be covered only by the thin skin, predisposing to ptosis, bottoming out or implant malposition, and even more, implant extrusion.

Better results can be achieved by using synthetic or biological mesh to implant support and coverage. The mesh is placed underneath the skin, helping to create a more natural-looking breast shape and providing additional support to the implant to rebuild the breast. Nevertheless, meshes have different structures, morphologic, mechanical characteristics, thickness, and weight; there could also be some potential drawbacks to using them in breast implant-based surgery. One concern is the risk of mesh infection or rejection, which can lead to complications and additional surgeries. Mere degradation can be a problem since rapid absorption can cause the implant to fall out, and malposition altering the natural-looking breast or long-lasting durability can produce a continued foreign body reaction.

To produce an “optimal” mesh, it was necessary to evaluate and analyze the available meshes in the market for breast reconstruction and compare them with the literature. The safety and effectiveness of surgical mesh in breast surgery, including augmentation or reconstruction, have not been determined by the FDA.[1]

Biological or synthetic meshes are fabricated to induce tissue integration, or they may be developed to house or attract cells, which, in turn, assist in inducing tissue integration. Several key characteristics make a current biomaterial suitable for tissue engineering applications. Biomaterials could be absorbable or degradable and, therefore, facilitate new tissue integration with native tissue over time. The shape and texture of the material do not have to resemble that of natural tissue, but it should induce the growth of new tissue resembling native tissue. Cellular affinity is another important aspect of a biomaterial. Biomaterial must interact favorably with cellular components without

negative impacts such as tumorigenicity or toxicity. Some elements of porosity or surface texture are helpful and potentially allow cellular ingrowth into the material, transfer nutrients and waste products, stimulate vascular network into the scaffold, and induce the differentiation of multipotent cells.[2]

Many surgical mesh products are cleared for the repair and reinforce soft tissue where weakness exists.

This thesis presents experimental in vivo model research about a novel mesh fabrication. Different concentrations of biodegradable Poly(carbonate-urethane) urea (PCUU) and Tecoflex™ (a non-degradable medical grade polyurethane), named PCUU-T, were used. Each different blend was evaluated with specific tests (thickness, weight, degradation, mechanical, and porosity tests) to achieve the optimal mesh and compared with five synthetic meshes used in breast reconstruction. Experimental surgery was performed in 18 Wistar rats. The Ultrapro™ chosen commercial mesh and PCUU-T were located in their respective subdermal dorsal pockets, covering smooth and textured mini-breast implants. Rats were clinically examined for 9 weeks, and explantation was performed by removing in block skin, mesh, capsule, and implant after euthanasia (day 63). That material was intensively examined using histology and bacteriology.

Could PCUU-T mesh stimulate improved tissue ingrowth, with less scar formation and similar strength compared to other synthetic meshes?

Could PCUU-T mesh develop a minimal inflammatory reaction, good revascularization cell repopulation, and collagen deposition, with minimal foreign body reaction?

Could PCUU-T mesh decrease the rates of complications such as bacterial contamination, infections, and explantation compared to other materials?

THEORETICAL FRAMEWORK

What is research but a blind date with knowledge?
William Harvey

Chapter I. BREAST IMPLANT

The term Breast Implant (BI) describes any implantable prosthetic device that the contour, shape, or size of a breast for aesthetic or reconstructive reasons.

1. Natural History

In 1895, in Germany, Vincenz Czerny performed the first documented breast augmentation surgery on a 41-year-old woman who had a tumor removed from her left breast, using autologous lipoma tissue from her back.[3] During the first half of the 20th century, emulating Czerny, paraffin injections were made, glass balls, ivory to wool, and sponges were introduced.[4,5]

The year 1961 marked a major medical breakthrough and a milestone in the history of breast surgery. Frank Gerow and Thomas Cronin designed the first silicone breast implant using silicone by the Dow Corning Corporation; these had a thin silicone outer shell, a thick silicone elastomer (~0.75 mm) sell filled with thick viscous polydimethylsiloxane (PDMS) silicone gel, composed of 50% low molecular weight chain components which are more fluid, and 50% high molecular weight chain components which are more viscous) and Dacron fixation patches on the posterior aspect to maintain their position.[6]

In 1962, Timmie Jean Lindsey was the first woman to receive silicone implants.[7]

In 1964, saline filler implants were introduced by Henry Jenny and Laboratories Arion in France.[6]

In 1969, Ashley introduced anatomically shaped implants covered in polyurethane foam (PU), which were found to have significantly reduced the high rate of capsular contracture.[8]

In 1976, Heyer-Schulte introduced a second generation of "double lumen" implants to overcome the rupture of silicone implants. These implants comprised a silicone-filled core enclosed by an outer shell filled with salt.[9] Thanks to this, a third generation of implants was introduced in the 1980s.

In 1982, Radovan introduced tissue expanders that are used throughout the body, including in breast reconstruction.[10] In 1984, Becker manufactured a "double reverse light" implant also known as the Becker™ permanent expander, a double chamber expander with an external lumen of silicone gel and saline internal lumen, inflatable, which led to the possibility of having an adjustable single stage breast reconstruction.[11]

In the late 1980s, reports also emerged of in vitro degradation of PU, which could lead to the formation of 2,4-toluene diamine (2,4-TDA), known to be carcinogenic in animals, and raising concerns about its potential carcinogenicity in humans.[12,13] The FDA, after conducting a risk analysis, concluded that these were acceptable cancer risks and recommended that women with PU implants should not have their devices removed based solely on concerns about 2.4-AD cancer.[14,15]

Due to the increase in adverse events in patients with breast implants in the medical literature, in 1988, the FDA decided to designate breast implants as class III medical devices, with the Federal Register of 24 June 1988 (53 FR 23856): This meant that manufacturers needed rigorous FDA approval to demonstrate that their devices were medically safe before they could be sold and marketed.[16]

From the FDA legislative changes of 1988 onwards, a fourth generation of breast implants was developed with stricter manufacturing and quality control criteria. They included thick layers of external elastomer (~0.5 mm), in some cases like previous generations of implants, and a cohesive (manufacturer-specific) gel filler thought less likely to break and filter silicone.[17] They were more commonly round and with moderate cohesive gel filling and began to implement texturing of external layers with different processes, including techniques called "salt loss" and "printing stamping" to allow greater integration by tissue growth into the irregular spaces of the roof.

In the early 1990s, Dow Corning was involved in a lawsuit involving more than 12,000 women participating in a class action.[18] By 1991, there was still not enough data to prove the safety or dangers of silicone in the human body, such as connective tissue disease, neurological diseases, cancer, and more. The FDA temporarily banned silicone breast implants in the US in January 1992.

In June 1993, a fifth generation of breast implants was introduced to the market; different countries in Europe released imports to a variety of implant manufacturers and types of implants. Some brands such as Allergan™ (BioCell surface), Eurosilicone™, GC Aesthetics™, Silimed™, and others, began to produce texturization, either by spraying, dipping, or spraying thin salt crystals on the silicone cover before curing, and supposedly

removed after rinsing with water without brushing.[19] This texturization was thick and somewhat different from that created by other manufacturers, such as Mentor™ (siltex surface), generating a finer homogeneous exterior texture through a pressurized printing stamping technique.[20,21]

In this period, the fear of health problems related to silicone favored the development of filling alternatives such as Trilucent™ implants LipoMatrix™. Health Care Products and Medicines Regulatory Agency (MHRA) found that oil decomposition was associated with cancer and birth defects; in 2000, Trilucent™ implants were withdrawn from the market.[22]

In the USA, scientific evidence was accumulating enough studies and clinical trials to refute claims that silicone implants were related to breast cancer and connective tissue diseases and the FDA lifted the prohibition in 2006 under the condition that manufacturers (Allergan™ and Mentor™) should conduct post-approval studies to characterize the long-term performance and safety of the devices.[23,24,25,26,27]

B-Lite™ implants were introduced in 2018 by Polytech™.[28] Lightweight breast implants are designed to be 30% lighter compared to traditional silicone implants. B-Lite™ implants achieve their lighter weight by incorporating inert, high purity, hollow, and borosilicate glass microspheres chemically bound and encapsulated by the silicone cohesive gel network, resulting in a lower overall density.[29,30]

3D bioprinting has become the latest technology innovation for breast implants, a convergence of biology and engineering technologies. Cells and growth factors are used as the 'ink' to create structures that resemble natural tissues like fat and blood vessels. [31]

CollPlant™ 2020 developed a 3D Bioprinted injectable breast implant using human collagen type I (rhCollagen) to regenerate breast tissue. Healshap™ company worked on customized and absorbable hydrogel containing human cells, 3D printed breast implant bioprosthesis in combination with delayed lipofilling to regenerate women's tissue. Both are still in experimental preclinical research.[32,33]

The first phase of human trials was conducted in Australia using 3D-printed absorbable PCL scaffolding for breast reconstruction.[34] The implant functions as a scaffolding guide for breast tissue engineering that can lead to fatty ingrown patient tissue from lipofilling surgical sessions.[35]

2. Implant Composition

a) Saline-filled breast implants

Contains an outer cover of silicone filled with a sterile physiological solution (saline). It comes in different shapes and sizes and has smooth or textured surface coverings. There are two types, the unstructured saline-filled does not support the shell or control movement of the saline filler, and the structured saline-filled breast implant is a round, smooth-surface, dual-lumen with an internal structure.[36] FDA-approved saline-filled breast implants in 2000 and 2014 respectively and are available in the USA.[37,38]

b) Silicone Gel-filled breast implants

Silicone BI has a silicone outer shell that is filled with silicone gel. They come in different sizes and have either smooth or textured shells. The PDMS is the basis of both the gel and shell of breast implants. The shell is produced from liquid components and an amorphous "fumed" silica (SiO_2) filler. The gel is a weakly cross-linked material that forms a 3-dimensional polymer network. Cross-linking occurs due to the reaction of vinyl groups present in the copolymer chains (dimethyl- and methyl vinyl-siloxane). Increasing the degree of PDMS cross-linking can lead to stronger and stiffer shell and gel materials.[39]

3. Implant Surface

All implant surfaces are made of a silicone elastomer, a chemically and mechanically resistant material. The cover has a well-defined structure and is manufactured manually by adding different layers (3 to 5) on top of each other to increase its resistance against breakage or become waterproof to the silicone, making it difficult to migrate.[40]

They can have different aspects, with different degrees of roughness or texture, ranging from one imperceptible to the eye and touch (they are considered smooth) to a surface texture or deeper, more noticeable, achieved by different mechanisms (called textured), or also a third category that is coated with micropoliurethane foam (mPU) known worldwide as polyurethane implants.[40]

Barr et al. (2017) divided breast implants according to surface roughness in Nano (75 µm), Meso (<15 µm), Micro (10-75 µm), and Macro (>75 µm).[41] The ISO-14607:2018 classification divides the surfaces according to their average roughness in Smooth (<10 µm), Micro (10-50 µm), and Macro (>50 µm).[40]

4. Implant Shape

The shape can be round with a symmetrical curved front side and a round flat back or base. Different heights, projections, or profiles with varied diameters (low, moderate, high, extra high) and different percentages of silicone filling are available.

The anatomical shape, such as a drop or tear, with the upper half having a smaller projection than the lower pole's higher projection. They have an asymmetrical curved front side and a flat, round, or more often, elliptical back base. Anatomic implants can achieve a natural look. These implants are filled with a highly cohesive gel to maintain their anatomical shape and are textured or PU to prevent their rotation by their adhesion.[42]

To avoid complications like seroma formation or breast implant-associated anaplastic large-cell lymphoma (BIA-ALCL) that are possibly associated with textured and polyurethane implants, alternative implants with advanced bioengineered smooth surfaces and anatomical shapes were developed. These implants have a fixation system to prevent rotation.[43]

5. Complications

Most breast augmentation procedures are performed without significant complications.

However, complications can arise after any surgical procedure, and the inherent risks of breast augmentation, either aesthetic or reconstructive, include capsular contracture, infection, wound dehiscence and implant loss, implant rupture, seroma, hematomas, implant malposition, or rippling.

Other very rare complications such as Breast Implants Associated to Anaplastic Large Cell Lymphoma, (BIA-ALCL), Breast Implant-Associated Squamous Cell Carcinoma, (BIA-SCC), the Autoimmune Syndrome Induced by Adjuvants (ASIA)[44], and Breast Implant Illness (BII) are also mentioned as potential risk.[45] Several complications can lead to prolonged sequelae, with subsequent treatment, as well as compromise the aesthetic outcome. Therefore, it can be associated with patient dissatisfaction and significant financial costs. Our description focuses on the most significant issue that arises when using a breast implant with mesh as seroma and infection.

In the literature, the use of synthetic meshes and ADM together with silicone implants is described as having a low postoperative complication rate, high patient acceptance and satisfaction, and a low incidence of postoperative morbidity.[46]

a) Seroma

It is a term used to indicate a serous clear fluid collection, which can develop in extensive soft tissue dissection immediately after surgery or one year after surgery (late seroma).[47] The serum is the result of the inflammation and increasing vascularization as the body prepares to heal the injury (Figure 1).

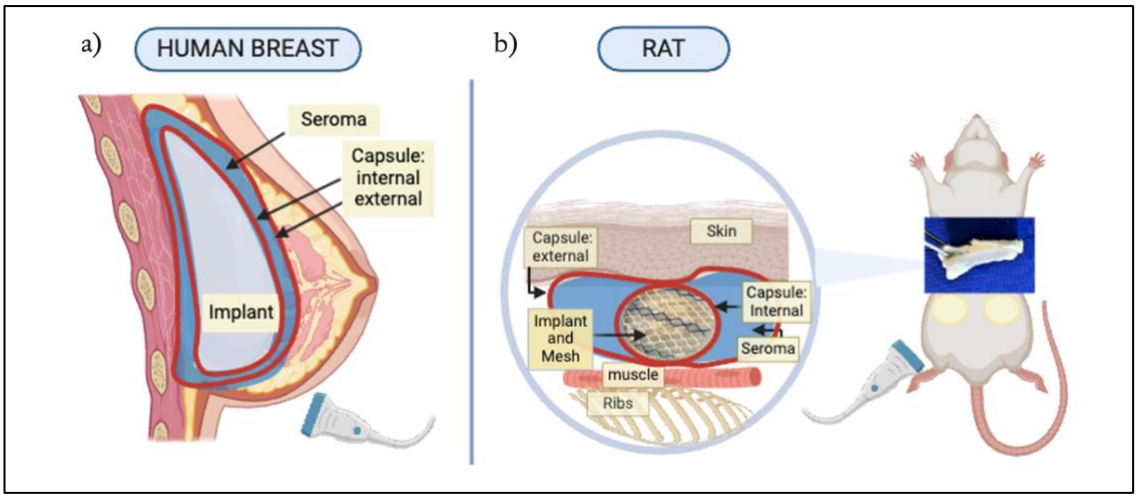

Figure 1: a) Schematic representation of the seroma in the human breast with sub-glandular implant. The seroma is surrounded by 2 capsules produced by the body (internal and external). b) Block of rat biopsy of skin and mesh. Magnification view representation, subcutaneous mini breast implant, and mesh surrounded by internal capsule, seroma, and external capsule.

Source: Own design and execution in BioRender™ (SF)

Their origin is typically caused by surgical trauma and subsequent acute inflammatory response, resulting in exudation. This condition is caused by a combination of several factors. During surgical operations, electrocautery damage, injury of lymphatic and capillary vessels, and the presence of dead space could be the cause.[48]

Most commonly occur following surgeries with excess skin and fat removal, mastectomy breast tissue excision, lymphatic disruption, and at the donor site after harvesting the latissimus dorsi muscle for reconstructive purposes.[49] Breast implants as a foreign body, mainly textured surfaces, can produce fluid collection. In surgeries where synthetic mesh or biological matrix is used, it could be a factor in seroma formation due to the excessive inflammatory reaction.[50]

Laboratory testing can classify fluid as serous if it has no cells and a low amount of protein (<2.0 g/dl). On the other hand, if the fluid contains cells and protein (>2.9 g/dl), it is an exudate. If the effusion fluid mostly consists of white blood cells, it indicates inflammation.[51]

Seroma in Cosmetic breast implant surgery: The incidence rate of seroma formation is 1 to 2% in some series.[52] Early seroma formation is defined as periprosthetic fluid

accumulation within the first postoperative year, whereas the late form is any moment beyond that time. Seroma is a significant problem for the surgeon and patient, causing anxiety and discomfort. It is followed by frequent outpatient visits, follow-up treatment, increased costs, and possibly impeded aesthetic outcomes. High Body Mass Index, large implant size, sub-glandular pocket, and smoking are factors significantly associated with seroma development, while age is not. Body Mass Index over 30 is the strongest indicator of seroma development.[53]

The mildly textured surfaces can cause some irritation and a mild seroma, but the more aggressive textured surfaces can cause some adherence of the capsule to the implant, assuming that the problem can be produced by mechanical damage.[47]

Biocell textured implants developed late seroma and/or a double capsule. A more plausible theory may be that the initial adherence of the capsule to the textured implant becomes separated, with minor trauma resulting in two rough surfaces that create a seroma because of the shear forces involved.[47,54] Guidelines for the management of late seroma after breast implant placement are available to rule out anaplastic large-cell lymphoma.[51]

Seroma in breast reconstruction: Studies of mastectomy without reconstruction showed that seroma can be produced for lymphatic disruption and dead space after mastectomy and exacerbated for axillary dissection.[55] The incidence of seroma after implant-based breast Reconstruction (IBBR) varies from 0.2 to 20 percent.[56] Obesity, ADM-assisted, and its association with radiotherapy have been implicated in increasing the risk factors.[57,58] Prolonged seroma duration increases the risk of infection and implant loss.[59,60]

Seroma can produce several complications, such as infection, wound healing, and implant loss. It requires chemical, cytologic, microbiologic (bacterial or fungal), and anatomo-pathological analysis for diagnosis.

In humans and rats, the liquid collection can be measured by Ultrasound (Figure 2).[49]

In ultrasound imaging, the interaction between sound waves and living tissue creates an image of the tissue. By analyzing these dynamic, real-time images, quantitative structural and functional information can be obtained. This versatile and noninvasive diagnostic tool is used in human and veterinary medicine.[61] Diagnostic ultrasound commonly uses frequencies between 2 and 15 MHz (106 cycles/sec).

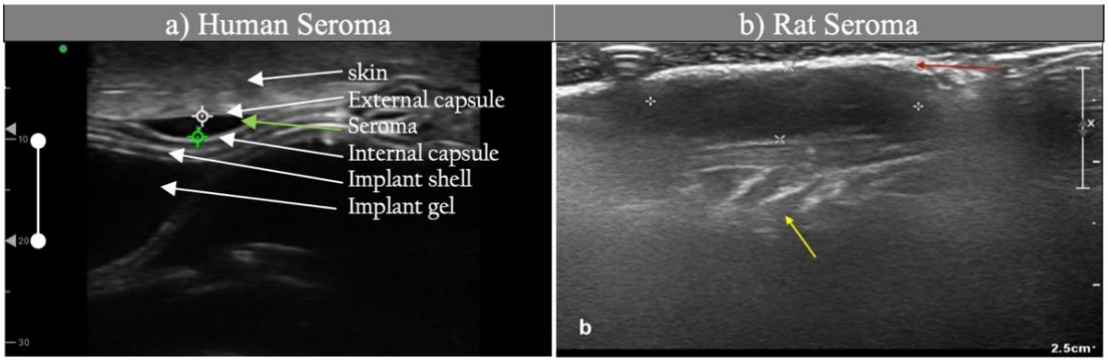

Figure 2: Ultrasound: fluid collection comparison. a) Human seroma delimited between external (white point) and internal capsule (green points). White Barr 10 mm representation. b) Rat fluid cavity (without implant), delineated by red (skin) and yellow arrow (muscle thoracic cavity). The seroma cavity has a length of 1.74 cm and a width of 0.5 cm.

Source: (Left) SF clinical database, (Right) Lese I et al. (2021). doi: 10.1021/acsbiomaterials.1c00283

b) Infection

Breast implant infection, though relatively uncommon, is a serious concern in plastic surgery. When it occurs, it can lead to significant complications for the patient and may need the implant removed. Infections can be caused by various factors, including bacterial contamination during surgery, improper surgical techniques, compromised immune systems, patient comorbidities, or post-operative complications such as hematoma or seroma formation. Mastectomy, radiotherapy, and chemotherapy could increase the risk of developing seroma and infection.[62] Preventive measures play a crucial role in minimizing the risk of breast implant infections. These include meticulous surgical techniques, adherence to sterile protocols during surgery, appropriate antibiotic prophylaxis, and patient education on post-operative care.[63] In cases where infection does occur, treatment typically involves a combination of antibiotics and, in some cases, surgical intervention to remove the infected implant. This can be a challenging and distressing experience for patients, as it may necessitate additional surgeries and delay the desired aesthetic outcome. Incorporating mesh into breast augmentation or reconstruction procedures may increase the risk of infection for several reasons, such as a foreign body reaction (increased for two different materials), complexity of the technique, increased time of surgery, therefore, site contamination.

Given these potential risks, surgeons must carefully assess each patient's risk factors, type of implant, and mesh characteristics. Preoperative optimization, adherence to sterile surgical techniques, appropriate antibiotic prophylaxis, and vigilant post-operative monitoring are crucial for minimizing the risk of infection in patients undergoing procedures involving breast implants and mesh.[63]

c) Capsular Contracture

When performing breast augmentation surgery, the body reacts by wrapping them with a thin, and soft fibrous layer, made of myofibrils and collagen, which normally does not exceed the thickness of 1 to 1.5 mm, known as a periprosthetic capsule.[64,65] This is described as part of the normal internal healing process, and some studies suggested that it might even help maintain the implant in situ.[66,67] Breast implants are encapsulated by fibrotic tissue, which is intended to protect the body from potentially harmful materials but can lead to harmful complications, such as Capsular Contracture (CC).[68]

If this layer becomes thicker and contracts, it compresses the implants, giving the breasts a rounded or spherical appearance and a hard feeling to touch, deforming the appearance of the breast by progressively moving the implant out of its usual location to isolate the foreign body. This condition is described as a CC. It has been reported that between 1.3% and 30% of the patients with implants have developed capsular contractures. Approximately 92% of contractures occur within the first 12 months after surgery. The capsule can compromise only the aesthetic breast appearance; at worst, it is associated with pain, hardening, tightness, deformity, and breast distortion.[69]

The Baker classification is the most practical clinical method to assess the firmness of breasts after augmentation.[70] It uses a four-point scale ranging from grade I (natural) to grade IV (severe contracture).[71]

Textured implants have a lower risk of CC. The contracture risk is fourfold higher with smooth implants in the subfascial plane. The implant surface is not affected by the submuscular plane at 1 or 2 years. It is higher with smooth implants at 1 year postoperatively and similar after 2 years postoperatively. With postoperative complications, CC at 1 year was seven times higher when complications were immediate and eight times higher with smooth implants than with textured implants.[72]

Several factors have been suggested to contribute to CC, while others remain unknown. Some theories have been proposed as the origin of CC regarding bacterial infection, colonization, biofilms, and silicone leakage. Hematomas and blood within the implant pocket are also implicated, increasing the probability of CC.[73] Radiotherapy increases 40 to 50 % the risk of CC in breast reconstruction.[74]

The capsule contains predominantly myofibroblasts, macrophages, fibroblasts, collagen, and several layers of cells.[75,76] The myofibroblasts are associated with wound contraction and correlate with the incidence and severity of CC.[77,78]

The number of macrophages and monocytes in the capsule plays a role in developing fibrosis and inflammation.[79,80]

Histologically, the capsules consist of 3 layers: an inner layer adjacent to the implant consisting of fibrocytes and histiocytes, which forms an epithelial layer identified as a metaplasia-like synovial layer consisting of macrophages and fibroblasts. An intermediate layer of smaller fibrils in a vessel-rich network and an outer collagen-dense layer (Figure 3).[81,82]

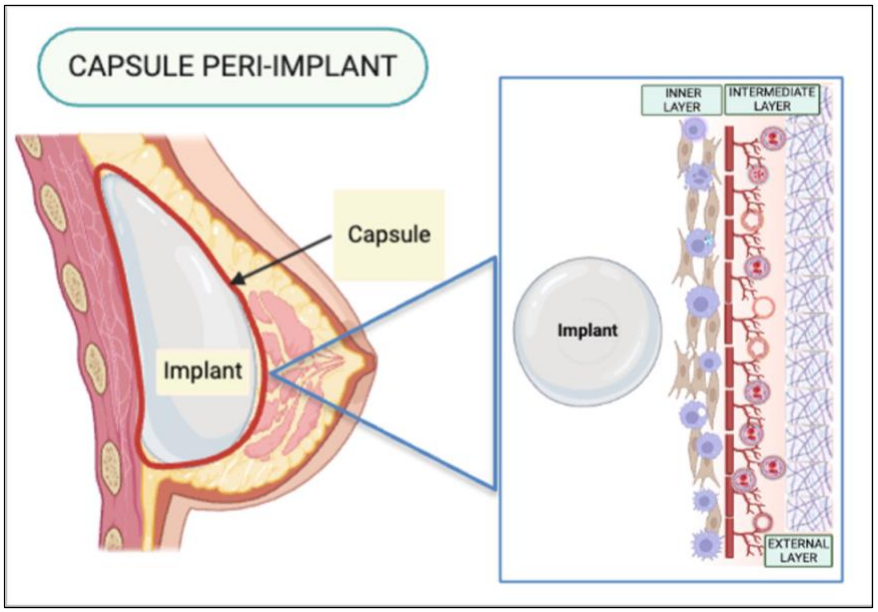

Figure 3: Periprosthetic capsule scheme. The external layer comprises collagen, the intermediate layer with vessels, and the inner layer is integrated by macrophages and fibroblasts.

Source: Own design and execution with BioRender ™ (SF)

The presence of this inner layer is inversely related to higher Baker classification or pathological contracture, and it could, therefore, protect against the formation of CC.[83] Beyond this layer, several studies found organized layers of loose and dense connective tissue containing the capsules' vascular supply. The inflammatory process is angiogenesis, growing new blood vessels.[84]

The disposition and density of collagen fibers determine the characteristics of CC. Parallel fiber disposition with a more uniform alignment was observed in the smooth surface implant and the contracted capsule compared with a more anarchic pattern, multidirectional, and loosely arranged fibers in the uncontracted capsule and micro or macrotexture devices.[85] A main problem in CC is the lack of integration of foreign material into the human body and the absence of biocompatibility.

Chapter II. BREAST RECONSTRUCTION

1. Definition

Breast Reconstruction (BR) is a procedure that aims to recreate the shape, natural appearance, size, and symmetry of the breasts after total or partial removal due to cancer treatment, injury, burn, or other reasons after complications of aesthetic procedures.

In 2022, there were 2.3 million women diagnosed with breast cancer and 670.000 deaths globally. Breast cancer occurs in every country of the world in women at any age after puberty but with increasing rates in later life. Global estimates in countries with a very high Human Development Index, 1 in 12 women will be diagnosed with breast cancer in their lifetime, and 1 in 71 women die of it.[86]

The breast is considered a sign of beauty, femininity, and sexual symbolism and a sustainer of new life. The absence of the breast, whether total or partial, can alter a woman's physical, sexual, and emotional balance.

More than 60% of women who have a mastectomy for breast cancer treatment choose to undergo breast reconstruction.[87] The increased number of women undergoing mastectomy for prophylaxis contributes to expanding the demand for breast reconstruction.[88]

BR has the potential to enhance a patient's quality of life and level of satisfaction, as well as reduce psychological distress associated with mastectomy.[89]

The first BR was attributed to Vincenz Czerny, who attempted to enhance a woman’s breast in 1895 with the implantation of a lumbar lipoma.[3] The first autologous muscle flap for BR was the latissimus dorsi Myocutaneous flap, described in 1896 by Iginio Tansini, Professor of Surgery at the University of Palermo.[90] In 1977, the technique increased its use with implant-base reconstruction.[91]

Several types of reconstructive surgery are available and often require more than one procedure. The main procedures are **IBBR,** which uses silicone or saline implants to recreate the breast shape, and autologous tissue flap reconstruction, which involves transferring tissue from another part of the body, such as the abdomen, back, or buttocks, to create a new breast, and fat grafting, which uses autologous fat cells from another part of the body and injects them into the breast area to add volume.

More recently, the acellular dermal matrix (ADM) or synthetic mesh has gained importance in supporting the implant or scaffold. Many patients also need nipple-areola

reconstruction if these were not preserved during the mastectomy.[92] It depends on the previous procedure, neoadjuvant, or adjuvant therapy, and the patient's desire.

2. Breast Reconstruction

Sometimes, BR includes symmetrization on the contralateral breast so that the two breasts will match in size and shape. It can be performed at the same time as the mastectomy (immediate reconstruction) or later when the breast cancer therapy has been completed (delayed reconstruction).[92]

a) Immediate BR

It could be performed with autologous tissue when the contralateral breast size is big, if the patient received previous radiotherapy, or by surgeon and patient choice. When the gland is removed and the skin alone (skin-sparing mastectomy) or skin and nipple-areolar complex are preserved (nipple-sparing mastectomy), the reconstruction could be made with the pre-pectoral or submuscular breast implant. In some cases, it is necessary to add an ADM or mesh wrapping the implant in the pre-pectoral pocket or supporting the implant in the submuscular place.[93]

b) Delayed BR

It can be performed with autologous tissue or implant in two stages. In the first stage, the tissue expander is introduced in the submuscular or subcutaneous pocket and then is slowly filled with saline solution weekly after surgery. In the second stage, after 2 or 6 months, when the chest tissue has relaxed and healed enough, the expander is removed and replaced with an implant (Figure 4).[93]

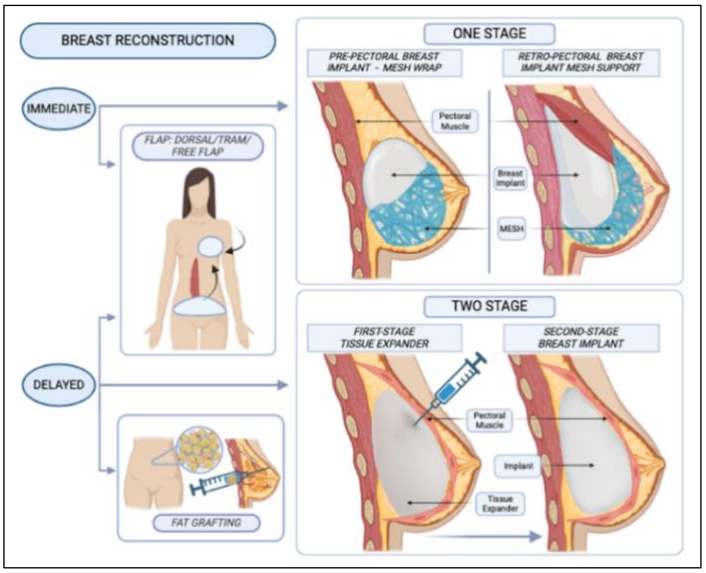

Figure 4: Breast reconstruction stages scheme: Immediate to the mastectomy or delayed. The breast can be replaced with autologous tissue or Implant. Breast implant with or without mesh, pre or retro-pectoral in one stage. In two stages with tissue expander at the first time after 2-month replacement for definitive breast implant. Another option is with autologous tissue flap or fat grafting.

Source: Own design and execution in BioRender ™

3. Breast-implant base reconstruction

a) Immediate breast reconstruction above the pectoral muscle.

This procedure is performed in combination with the mastectomy and results in an immediate breast mound. Preoperative digital mammography can determine if the tissue thickness is enough to cover the implant and avoid rippling.[94] Depending on that, the implant can be wrapped in a biological or synthetic mesh to help the implant maintain the correct anatomic position. This procedure may also require secondary autologous fat transfer to eliminate upper pole wrinkling and rippling over time, which will occur over secondary procedures. As a benefit of this pre-pectoral pocket, the breast implant is not influenced by muscle contraction, and the result is obtained in one stage.[95]

b) Immediate breast reconstruction under the pectoral muscle.

It is performed at the same time as the mastectomy, obtaining the immediate desired shape in one stage. The inferior fibers of the pectoralis major muscle are sectioned and elevated, allowing a superior submuscular pocket to cover the implant. To support the lower pole of the implant, a synthetic mesh or ADM is sutured to the inframammary crease and attached to the muscle (Figure 5).[92]

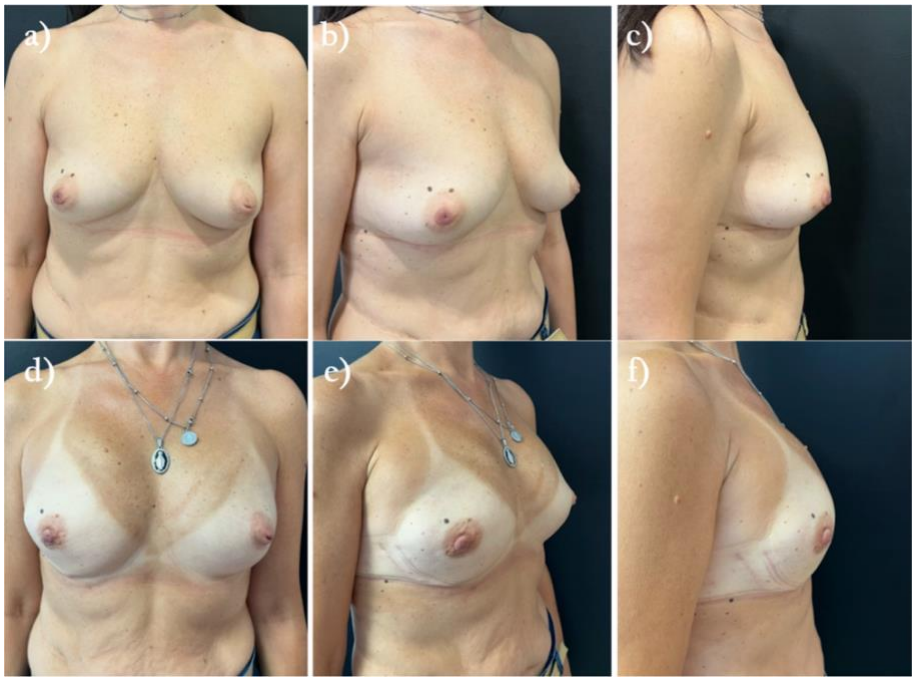

Figure 5**:** Female patient, 43 years old. Bilateral Nipple Skin-Sparing Mastectomy and Immediate Implant-Based Breast Reconstruction and Ultrapro™ mesh inferior support. Preoperative a, b, c): Frontal, lateral, and side view. Postoperative d, e, f): 7 months retro-muscle natural profile breast implant and mesh.

Source: Author's professional photo file (SF) with patient's permission

c) Delayed breast reconstruction utilizing tissue expander.

The tissue expander was designed in 1976 and used in breast reconstruction six years later by Radovan.[10] This procedure is performed in two stages sometime after the mastectomy. The pocket can be pre or retro-pectoral depending on the tissue thickness. Also, a small amount of mesh or ADM can be added to assist in muscle closure. They have a magnetic anterior integrated port or remote port localized subcutaneously far away from the tissue expander to access the expansion weekly with physiological solution. Once the final tissue expansion, or stretching, is completed, there are times of passive expansion where no volume is added. This allows the muscles and skin to stretch and relax. Once this is completed, a second outpatient procedure will be necessary to remove the tissue expander and place the permanent breast prosthesis (Figure 6).[96]

The complications of using a tissue expander or breast implant can be infection, seroma, hematoma, implant extrusion, thrombosis, implant rupture, and some rare immune illnesses. Obesity, diabetes, and smoking may increase the rate of complications.[100]

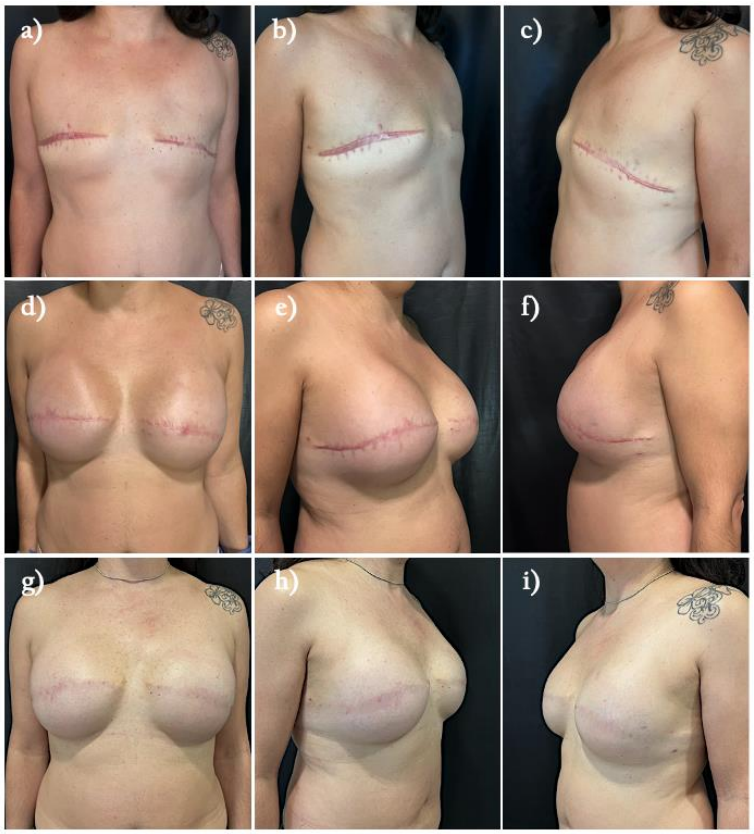

Figure 6: Female patient, 41 years old. Bilateral Mastectomy and delayed two-stage tissue expander BR. a, b, c) Preoperative: 3 years post bilateral mastectomy, frontal, lateral, and side view. d, e, f) Postoperative: 6 months after the first stage autologous fat grafting and pre-pectoral tissue expander (600cc texture integrated valve). g, h, i) Postoperative: 8 months postoperative second stage pre-pectoral 520cc texture high profile breast implant.

Source: Author's professional photo file (SF) with patient's permission.

4. Autologous tissue reconstruction

A flap is a piece of tissue containing skin, fat, blood vessels, and sometimes muscle (flap) from another part of the body that is used to rebuild the breast. Sometimes, a mastectomy or radiation therapy leaves insufficient tissue on the chest wall to cover and support a breast implant, requiring a flap.[97]

Depending on their source, flaps can be pedicled or free. When the tissue and attached blood vessels are moved together from the body to the breast area is a *Pedicled Flap*. The most important are:

TRAM flap (Transverse Rectus Abdominis Myocutaneous). Introduced by Carl Hartrampf in 1982. It involves taking tissue from the lower abdominal area containing skin, blood vessels, fat, and the underneath muscle. The tissue remains attached to its original blood vessels (superior epigastric artery), which are tunneled up to the chest area.[98] Useful in radiotherapy tissue damage, big contralateral breast, or just for a patient choice (Figure 7).

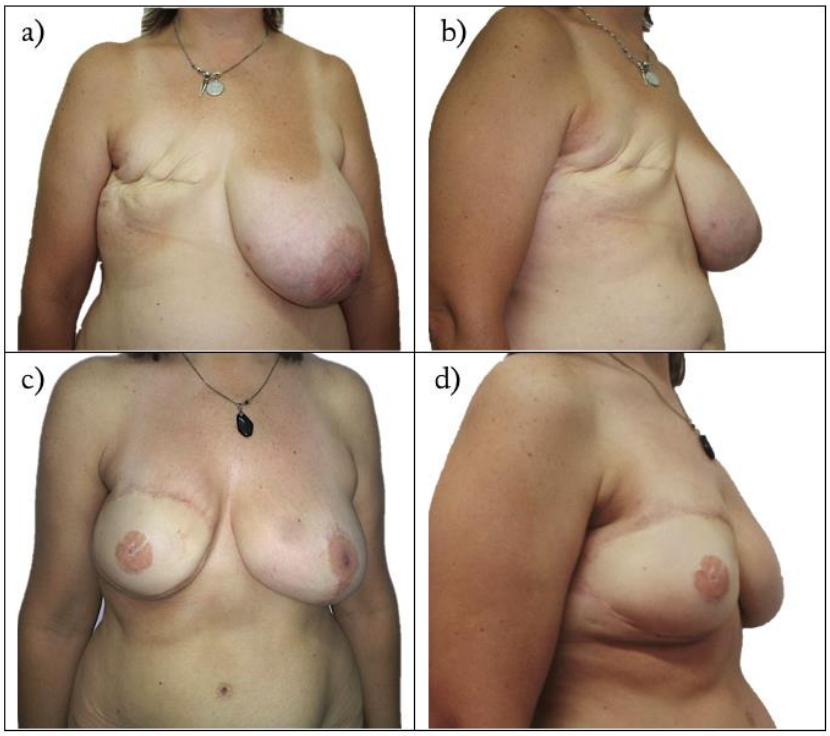

Figure 7: Female patient, 43 years old, right mastectomy after breast cancer. Delayed breast reconstruction TRAM flap. a, b): Preoperative images. c, d): Postoperative 8 months TRAM and Nipple areola complex reconstruction.

Source: Author's professional photo file (SF) with patient's permission

Latissimus Dorsi (LD) flap. The muscle located in the back is used along with its overlying skin and fat to create a flap that is transferred with its blood supply (the thoracodorsal artery) to the chest to reconstruct the breast mound tunneled underneath the

axilla.[99] An implant is then placed behind this flap and in front of the chest. A tissue expander can be utilized to gradually increase the muscle and skin size. It is frequently used when the amount of soft tissue is limited secondary to surgery, the pectoralis muscle is absent, partially removed, or tissue damaged secondary to radiation.[100] The evolution of this flap without muscle was introduced in 1995 by Claudio Angrigiani et al., an Argentinian plastic surgeon.[101]

In the ***free flap,*** the tissue is cut free from its blood supply and attached to new blood vessels in the breast area, using the microsurgery technique. The most common are:

DIEP flap (Deep inferior epigastric perforator). Tissue comes from the abdomen and contains only skin, blood vessels (1 to 3 perforators of the deep inferior epigastric), and fat, without the underlying muscle.[102,103] Since the muscle is preserved, there is a lower risk of abdominal weakness or hernias and less postoperative pain.

SIEA flap (Superficial inferior epigastric artery). Tissue comes from the abdomen as in a DIEP flap but includes different blood vessels. This method doesn't require the incision of the rectus abdominis fascia or muscle, leaving these structures completely untouched, which is superior in terms of donor-site morbidity.[104,105]

In women who have had previous major abdominal surgery or do not have enough abdominal tissue to reconstruct a breast, flaps taken from the thigh or buttocks are utilized.

IGAP flap. Tissue comes from the buttocks and contains only skin, blood vessels, and fat.[106]

PAP flap. Tissue, without muscle, that comes from the upper inner thigh.[107]

SGAP flap. Tissue comes from the buttocks as in an IGAP flap but includes a different set of blood vessels and contains only skin, blood vessels, and fat.[108]

TUG flap. The transverse upper gracilis, including muscle, comes from the upper inner thigh.[109]

In some cases, an implant and autologous tissue are used together. For example, autologous tissue may be used to cover an implant when there isn’t enough skin and muscle left after mastectomy to allow for expansion and use of an implant.[110]

The flap reconstruction has longer surgical procedures than implants. The initial recovery period may be longer than for implants. Free flap reconstruction is a longer, highly technical operation than pedicled flap reconstruction. The possible complications are necrosis of the transferred tissue. Certain flap sources may lead to a higher rate of blood

clots. Pain and weakness at the site from which the donor tissue was taken. Obesity, diabetes, and smoking may increase the rate of complications.

5. Autologous Fat grafting (AFG)

It is the procedure that takes adipocyte tissue from different areas of the body by suctioning and injecting it into the breasts for enlargement.[111] The indications for lipofilling include micromastia, tuberous breasts, Poland syndrome, post-mastectomy deformity, sequelae of radiotherapy, secondary reconstruction after flap or prosthesis reconstruction, or nipple reconstruction.[112,113] It can be performed to replace a total or partial breast volume for aesthetic or reconstructive reasons. AFG is commonly involved in implant placement after tissue expansion or between the expansion over the tissue expander for patients who have received previous radiation treatment or with thin mastectomy flaps.[114] Moreover, AFG has been used in irradiated tissue and scars to improve fibrosis.[115]

Several studies have reported success with primary reconstructions only using AFG with multiple grafting sessions.[116] The number of sessions depends on the quality of the tissue, the main of the reconstruction, and the volume of adsorption per session, which can take 1 to 6 sessions.[117] However, the best volume can be rich with the hybrid BR using lipofilling to improve the outcomes in IBBR in one or two stages.[118]

Although AFG stimulates angiogenesis and tissue regeneration, many studies have suggested that adipocytes, preadipocytes, and their products may play a role in tumorigenesis, tumor progression, and tumor recurrence or metastasis.[119] The meta-analysis of oncological data from the published literature involving 4292 patients demonstrated that autologous fat transfer did not result in an increase of locoregional recurrence in patients with breast cancer.[120]

Therefore, lipofilling following breast cancer treatment results in a very low rate of complications and does not affect the radiologic follow-up after breast-conserving surgery.[121]

6. Comments

Several studies showed a high level of satisfaction and physical and sexual well-being when women performed breast reconstruction after mastectomy.[89,122] Patients who opted for autologous unilateral reconstruction had higher satisfaction (Breast-Q™ score) with their breasts and better breast-related quality of life 2 years after surgery than the patients who underwent IBBR. In the long term, all patients, regardless of reconstruction type,

reported improved psychosocial well-being compared with preoperative scores, highlighting the positive association of postmastectomy BR with breast-related quality of life.[123] Although higher postoperative complications in contralateral prophylactic mastectomy and reconstruction, these procedures were associated with decreased anxiety levels and improved satisfaction with breasts for women who underwent implant reconstructions.[124]

Chapter III. MESH

1. Natural History

The natural history of meshes started at the end of the XIX century when Theodor Billroth suggested using a prosthetic material to cover the hernia defect as the ideal way to repair it in 1890.[125] Although many materials were utilized, they all failed due to infections, rejections, and recurrences. The main issue was the suture material made of multifilament.[126]

Finally, in 1958, Francis Usher, after many material evaluations, published his surgical technique using a knitted polypropylene mesh. These were made of large pores, which facilitated incorporation. Comparing it to previous materials, the main difference was the tissue growing through its interstices. After a few days of surgical integration, it was observed that fibroblast activity increased. More collagen was produced without the presence of giant cells.[127]

30 years later, the Lichtenstein repair (known today as the "tension-free" mesh technique) was popularized for hernia repair.[128] The biocompatibility of the material has been identified as a major factor in the rejection of the prosthetic because of scar tissue caused by the immune system. Currently, more than 50 prosthetic meshes can be used to repair hernias.[129,130]

Mesh implants are medical devices that are used to provide support to damaged or weakened tissue. These meshes have been used in various clinical settings, such as breast reconstruction, abdominal or pelvic hernia, hiatal hernia repair, and cardiovascular purposes like surgical, catheterization, or laparoscopic approaches.[131] More recently, its use increased for breast plastic surgery after mastectomy or cosmetic sequelae.

2. Mesh properties and composition

Meshes can be classified according to their absorption and composition. These have been categorized into single-material mesh, composite with two or more layers, and woven or machine-knit mesh with two kinds of fibers. Depending on the source, they could be synthetic or biological.[132]

Poro size. In addition, it can also be classified into porous characteristics and mesh.[133] Based on their pore size, the most frequently used materials in surgery can be grouped into four types. Type I: Totally macroporous prostheses. It contains pores larger than 75

microns, which is the required pore size to enter macrophages, fibroblasts, blood vessels (angiogenesis), and collagen fibers into the pores.[134,135] Type II: Totally microporous prostheses, pores less than l0 microns. Type III: Macroporous prosthesis with multifilament or microporous components. Type IV: Biomaterial with submicronic pore size.[136]

Large pore Type I meshes, compared to small pore Type 2 meshes, showed relatively less inflammation and less frequent infection or chronic pain as an indication for explantation. A disturbed collagen type I/III ratio was found at the periprosthetic scar tissue in 70% of patients with a recurrence, indicating the presence of a fundamental biochemical reason for the relapse.[137]

Mesh fabrication with open pores leads to tissue ingrowth and mesh–tissue integration.[138] Studies have found that larger pore sizes over 1000 μm (macroporous) result in reduced host inflammatory reactions and less fibrosis.[139]

When interstices or pores are less than l0μm, in each of their three dimensions, bacteria averaging 1 micron cannot be eliminated by macrophages and neutrophilic granulocytes, which are too large to enter a l0μm.[140] This provides a suitable environment for bacteria and promotes the development of infection by admitting bacteria but excluding macrophages. The same situation but with pores larger than 10 μm creates a major challenge for the proliferation of bacteria and thus does not contribute to the development of surgical infection. [141,142]

Seroma formation after surgery is caused by an inflammatory response to the implanted mesh and the dead space it creates between tissue. Type I and III pore sizes have sufficient molecular permeability to allow penetration of host protein material into their pores.[136]

Contraction of the mesh fibers during the scarring process leads to shrinkage of the mesh after implantation.

In the large interfilamentous distances, the pores can be filled with local physiological tissues like fat; in the case of small pores, the gap in between the filaments is usually filled with inflammatory infiltrate or a dense fibrotic scar, a phenomenon called ‘bridging’.[215]

The effective porosity is more important than other characteristics in estimating biocompatibility.[143]

The porosity is measured as the percentage of the mesh area not covered by filaments. The effective porosity represents only the area of “good” pores where bridging of scar tissue is avoided by sufficient interfilamentary distance.[144] Most often, the porosity was

determined as the area not covered by the mesh fibers. Considering the importance of porosity and the unaffectedness of porosity to anisotropy, klost et al. developed a new classification (Table 1). [215]

Table 1: Classification of mesh materials based on porosity.

Class I: Large-pore meshes with a low risk for bridging, defined by textile porosity >50% and effective porosity >0%
1a) monofilament
1b) multifilament
1c) mixed structure or polymer
Class II: Small-pore meshes with a high risk for bridging, defined by textile porosity <50% and effective porosity of 0%
2a) monofilament
2b) multifilament
2c) mixed structure or polymer
Class III: Porous mesh with special features in addition to the pure textile construction, e.g. to prevent adhesions
Class IV: Film-like mesh without porosity, sub-micronic pore size or secondarily excised pores
Class V: Complex textiles difficult to uniformly characterize, either preshaped, preformed or 3-dimensional
Class VI: Tissue-derived biologicals
6a) non-cross-linked
6b) cross-linked
6c) special features

Source: Klinge et al. 'The ideal mesh?'. Pathobiology. 2013;80(4):169-75. doi: 10.1159/000348446.

Absorption. Regarding the time of permanence in the body or absorption, they can be absorbable, non, or partially absorbable. Absorbable mesh degradation time does not always match the ingrowth rate of the new tissue, thus causing a loss of mechanical stability due to implant mechanical failure.

A non-absorbable mesh provides additional mechanical support to the tissue due to its durability and mechanical features. Mechanical strength and relatively long degradation rates are desirable properties.[145] It is often accompanied by an excessive immune reaction that results in a non-constructive remodeling of the tissue, adhesion to the viscera, erosion, infectious complications, and a second surgery for removal.[146]

Partially absorbable mesh decreases the biomaterial's density and subsequent inflammatory response while maintaining the intraoperative handling qualities and long-term wound strength. Currently, available meshes are developed with a fusion of non-absorbable (PP) and absorbable materials, e.g., polyglactin 910 and poliglecaprone 25.[147]

Based on the mesh weight or density, Coda et al. (2012) proposed the classification based on the mesh weight: Ultralight ≤ 35 g/m^2, Light 35-70 g/m^2, Standard 70-140 g/m^2 and Heavy ≥ 140 g/m^2.[132]

Lightweight meshes have been described using a variety of criteria such as reduced density, smaller filament diameters, lower tensile strength, or having a “large pore”

macroporous structure compared with the first-generation of "heavyweight" polypropylene meshes.[148]

Physicomechanical characterization is even more important than the mesh structure. There are huge variations in tensile strength and stretchability. Anisotropic is the structural property of non-uniformity in different directions.[149] The mechanical behavior of an anisotropic mesh in one direction is different than its behavior in another direction. Most of the meshes show considerable anisotropy because of the meshes manufactured. This is caused by the fibers mostly running parallel. When stressed in the direction of these warp fibers, most meshes have limited deformation, but perpendicular strain causes a significant elongation of the mesh device. This capacity to stretch is a consequence of the lengthening of the pores and the consecutive mesh width narrowing.[150] In consequence, understanding the anisotropic behavior of the synthetic mesh and the implant-base reconstruction is the key to choosing the strategic mesh orientation to optimize post-surgical outcomes.

High mechanical strength is crucial to proper tissue sustainment, and moderate degradation rates are needed to give cells time to populate the scaffold and produce new tissue while exerting the same time requested mechanical properties.

a) Synthetic

Synthetic meshes are *non-absorbable* (polypropylene, polyester, expanded polytetrafluoroethylene), *absorbable* (poliglecaprone, Monocryl, polydioxanone, polyglycolide), or *partially absorbable* composite material joins two of any previous components.

Despite the large amount of mesh available in the market, we selected the most common in Argentina for breast reconstruction for this thesis. Synthetic meshes (Ultrapro™, Vycril™, Tiloop™, Tigr™, and Galaflex™) were analyzed to define an ideal mesh (Figure 8) and (Table 2).

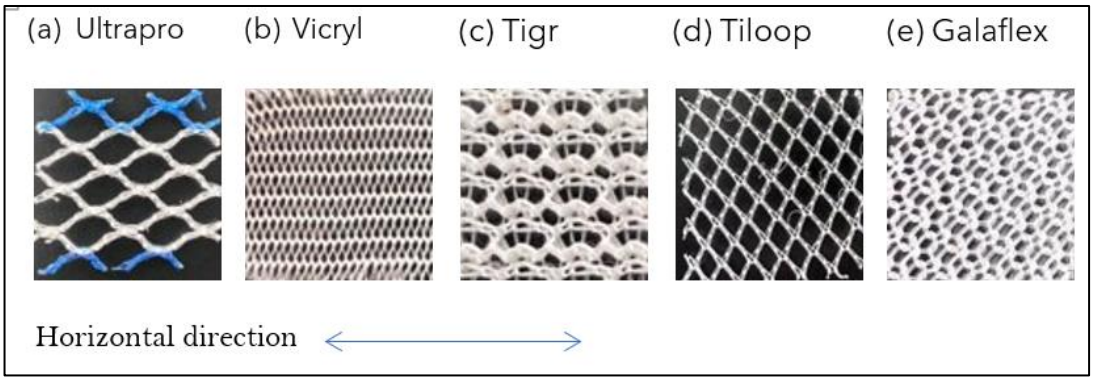

Figure 8: Synthetic meshes and fibers directions (1 x 1 cm)
Source: Picture taken and organized by author (SF)

Table 2: Literature characterization of the Synthetic meshes employed in Implant-Breast breast reconstruction selected for our study.

Commercial/ Synthetic product	Material composition	Physicochemical and biological properties	Density g/m²	Thickness mm	Fiber diameter µm	Porosity mm²	Manufacturer
Ultrapro™	Polypropylene/ Poliglecaprone	Nonabsorbable polypropylene (2/3) and absorbable Poliglecaprone (1/3)	34	0.5	5	4	Ethicon, Inc., Somerville-NJ
Vycril™	Polyglactin 910 (92% glycolide, 8% lactide)	Hydrolytic absorption between 56-70 to 90 days 100%. Multifilament. Woven	50	0.2	N/A	0.16/0.5	Ethicon Inc., Somerville-NJ
Tigr™	Glycolide and trimethylene carbonate; lactide and trimethylene	Absorbable macroporous mesh with two types of filaments (fast and slow degrading). Mechanical support for up to 9 months. Fully degraded after 3 years. Multifilament. Knotted	80	0.51	20	1-1.5	Novus Scientific Uppsala Sweden
Tiloop Bra™	Titanium-coated polypropylene	Permanent monofilament	16-65	0.2-0.45	N/A	1	Pfm medical, Cologne-Germany
Galaflex™	poly-4-hydroxybutyrate (P4HB)	Hydrolytic and enzymatic absorption in 18 to 24 months. Monofilament	182	0.6	154	0.25	Galatea Surgical, Lexington, MA

Ultrapro™: (Ethicon, Inc., Somerville-NJ) is a synthetic macroporous partially absorbable mesh monofilament with low density. It is a combination of nonabsorbable polypropylene (1/3) and absorbable Poliglecaprone (Monocryl) (2/3). Macroporous design (3.2 mm) promotes fluid flow-through, potentially reducing the risk of seromas that could lead to infection. Average filament size 5 mils/monofilament. Different sizes and shapes. Weight 34.0 g/m^2.[148,151] It is indicated for the repair of abdominal wall hernias and abdominal wall deficiencies that require the addition of reinforcing material to obtain the desired surgical result.[152,153]

Vycril™: (Ethicon Inc., Somerville- NJ) is a copolymer of Polyglactin 910 (92% glycolide, 8% lactide. Multifilament and woven. Hydrolytic absorption between 56-70 to 90 days 100%. Porosity 0.16 mm^2/0.5 mm^2. Density 50 g/m^2.[154,155]

Tigr™: (Novus Scientific AB, Uppsala- Sweden) is a synthetic absorbable mesh knitted multifilament and macropores. Dual-stage degradation and full resorption. Fast

degradation at 4 months polymer of polyglycolide polylactide and poly trimethylene carbonate. The slow absorption begins at 9 months to 24-36 months long term, polylactide and poly trimethylene Carbonate Multifilament. Density 80 g/m^2. Thickness 0.51mm and fiber diameter 20 µm.[5,156]

Tiloop™: (Pfm medical, Cologne-Germany) is a titanium-coated polypropylene mesh. Permanent monofilament. Porosity 1 mm^2. Density 16-65 g/m^2. Thickness 0.2-0.45 mm. Long-term duration.[157]

Galaflex™: It is a poly-4-hydroxybutyrate (P4HB) monofilament.[9,158] Porosity 0.25 mm^2 Density 182 g/m^2. Thickness 0.6mm and fiber diameter 154 µm. Hydrolytic and enzymatic absorption in 18 to 24 months.[159] Long-term.[160,161]

b) Biological

Biological meshes are surgical implants derived from biological sources. These materials are processed to remove cells and immunogenic components while preserving the structural integrity and biological properties of the tissue.[162,163]

These groups of biological matrices are obtained from skin donation from the same human species (allografts), animals (xenografts), or plants. Acellular Dermal Matrix (ADM) of synthetic origin are produced by technological processes like polymerization; composite ADMs are biological-synthetic hybrids.[164]

Biological meshes are absorbable and commonly used in various surgical procedures, including hernia repair, abdominal wall reconstruction, and breast reconstruction. The ADM can be derived from human cadaveric skin (Alloderm™), from porcine dermis (Strattice™) and bovine pericardium (XenMatrix™)

The ADM is a type of synthetic skin substitute composed mainly of bovine collagen and chondroitin sulfate. Originally described by Burke et al (1981), the use of ADM for the development of neo-dermis has been extensively studied in coverage deficits in burns at full thickness.[165] Presents a double matrix layer that stimulates fibroblast and endothelial growth through a process of imbibition, neovascularization, and remodeling.[166]

Over time, the indication for using acellular dermal matrix has been expanded, particularly in breast implant surgeries.[167]

ADM was originally used in breast reconstruction as an integrative regenerative tissue matrix to help facilitate and expand the soft tissue envelope of mastectomy. In its first use in breast reconstruction, ADM served as a lower sling attached to the pectoral, thus avoiding the need to raise the rectum and fascia serratus. Benefits found are the use of

direct breast reconstruction to implant in the subpectoral plane with ADM sling, which has a low incidence of CC of 4%.[168]

In pre-pectoral breast reconstruction, a review compared CC data with and without ADM and found that these significantly reduced it. However, studies that did not use ADM were performed with implants from previous generations, thinner mastectomy flaps, and a lack of understanding of CC prevention strategies.[169]

However, it should be noted that ADM increases the risk of seroma, pocket infection, and the cost of the procedure.[170]

3. Uses of meshes. Application in Surgery

There are different mesh characteristics to specific areas and needs. The ideal characteristics that have to fulfill the mesh are biocompatibility, non-immunogenicity, and non-carcinogenicity, resistance to colonization and chronic infection to maintain adequate long-term tensile strength, absence of retraction or expansion after implantation, adequate flexibility to avoid material fatigue, easy sterilization process without alteration of its properties, rapid incorporation to the host tissue, promotion tissue integration, and low cost.[171]

Regarding many different indications, there will never be one ideal mesh for all purposes. The indication for the use of meshes is still expanding.

a) General surgery

Hernia is the main pathology for which mesh is used in general surgery, mainly in abdominal or inguinal areas. It is also useful for other issues, such as diastasis of the abdominal rectus.

Initially, the mesh was used to close complex hernias, usually by placing a large piece of mesh underneath the skin and introducing them by large incision. With the laparoscopic techniques in the 1990s, placement of meshes for the treatment of inguinal hernia became feasible by using laparoscopy, either via the abdominal cavity as TAPP (transabdominal preperitoneal) or pre-peritoneal as a TEP (totally extraperitoneal) procedure. Currently, the Robotic-assisted technique era changed the approaches to inserting the mesh.[172]

b) Plastic surgery

Immediate breast reconstruction with expanders has been performed using total muscle coverage of the prosthesis to protect the implant from exposure. It became apparent that the rigidity of the muscle often restricted inferior pole expansion, resulting in inframammary fold poorly defined and less desirable cosmetic outcomes.[173] Complete muscle coverage is unlike in Immediate IBBR.

Currently, the most conservative breast cancer resection surgeries, preserving better breast flaps in techniques like skin-sparing and nipple-sparing mastectomy, changed the paradigm of BR. This has led to the adoption of surgical devices as a complementary resource. Biologic matrices or synthetic meshes incorporation to cover the breast implant in one stage or the tissue expander in two stages of reconstruction has become essential in BR.

Silicone breast implants or tissue expanders are placed partially under the pectoralis major muscle, providing 40 to 60% coverage of the implants, while the lower pole is covered by the mesh acting as the hammock and lower resistance. This allows for an improved lower pole unfolding and skin expansion in the inferior third of the breast, resulting in a higher projection of a more natural breast appearance and allowing the placement of greater intraoperative volume implants.[174]

The main function is the fixation and maintains the position of the implant in the infra and lateral mammary folds. The superior rim of the matrix is sutured to the inferior muscle edge to hold the contracted and cranially shortened pectoralis major muscle. The lower rim of the mesh is fixed to the inframammary fold. The pectoralis major muscle and the scaffold not only create a complete pocket for the implant but also hold and support the lower pole of the reconstructed breast (Figure 9).

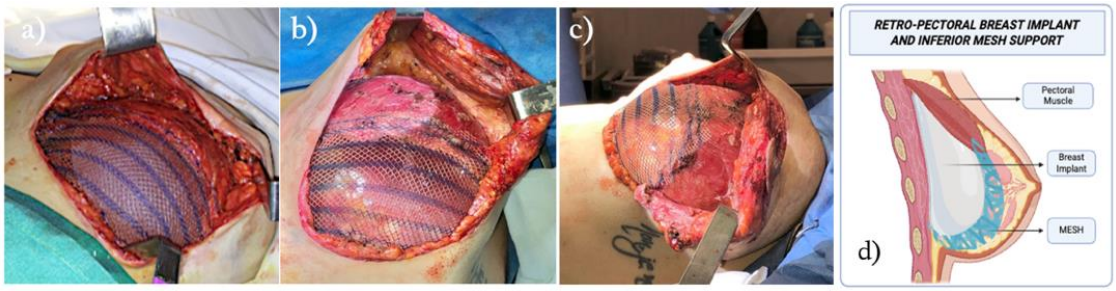

Figure 9: Ultrapro™ Mesh covering the implant lower pole in aesthetic surgery. a) Superior retro-muscle texture breast implant. b) Smooth breast implant covered by pectoral muscle in the upper pole and mesh in the lower pole, frontal view. c) lateral view. d) Scheme of the superior sub-muscular and inferior mesh coverage implant.

Source: Author's professional file (SF)

In 2005, Breuing and Warren first reported the use of ADM in breast reconstruction Surgery.[175] In 2007, was described their use in submuscular implant-based reconstruction.[176,177] Despite the great benefits of implant positioning, better coverage, and the suggestion of a decreased capsular contracture rate, many reports of different problems with the biological matrices including seroma, infection, slow vascularization, disruption, reconstructive failure, expensive cost, and not availability in all

countries.[178,179,180,181] Then, synthetic meshes became an alternative use in breast surgeries.[182,183,184]

Several problems following the aesthetic breast implant complications, such as implant malposition, bottoming-out, symmastia, rippling, and capsular contracture, were difficult to correct in the past.[185,186] Also, in many cases, changing the implant pocket is a challenge with unpredictable results.[187,188]

The use of matrix or mesh in aesthetic breast revisions for sequelae of primary breast implant complications increased their use.[189,190] Surgeries after massive weight loss or recurrent ptosis use the mesh as an important material resource to hold the tissue in position. This allows to maintain the implant in the desired pocket, avoid multiple surgeries, and obtain a permanent or long-lasting aesthetic outcome (Figure 10).[191,192]

Moreover, many reports showed that synthetic meshes have lower infection and seroma rates than ADM.[193,194,195]

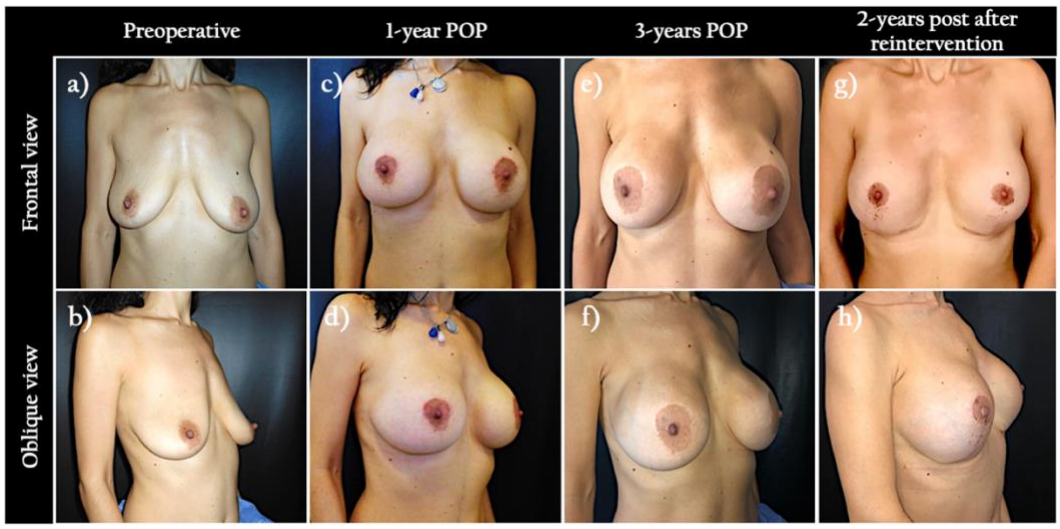

Figure 10: Female patient, 39 years old. Breast ptosis and hypomastia, she refused peri-areolar vertical scar. a, b) *Preoperative*. c, d) *1-year postoperative* of superior peri-areolar mastopexy and 345cc sub-facial texture implant. e, f) *3-year postoperative with recurrent ptosis*. g, h) 2 years post reintervention peri-areolar vertical mastopexy, change pocket and implant for 400cc smooth submuscular breast implant, and mesh as inferior support with a long-lasting result.

Source: Author's professional photo file (SF) with patient's permission

4. Mesh Integration

The immune system constantly checks the body for any tissue damage or invasion by pathogens or foreign materials.[196] To eliminate the risk, the immune system orchestrates a complex cascade of immune modulators. The interaction between an implanted material and host tissue triggers a sequence of events interaction with blood components such as deposition of a protein layer on the biomaterial, formation of a provisional matrix, immune cell recruitment, acute inflammation, chronic inflammation, formation of

granulation tissue, foreign body reaction (FBR), fibrosis and fibrous capsule development.[197]

As a foreign material, the mesh cannot mimic all the properties of the local tissue, disrupting the tissue's physiological regenerative capacity. The body tends to heal by filling the defect with scar tissue. The FBR has the potential to harm both the host and the implanted device.

Firstly, the ***acute inflammatory*** *response* occurs within minutes or hours after the immune system recognizes and responds to foreign material, which envelops and isolates the implanted material necessary for proper wound healing.

In the initial stages, blood and plasma proteins are adsorbed to the surface of the scaffold and form a temporary fibrin-rich matrix. *Neutrophils* act as first responders by phagocytosing cellular debris, secreting digestive enzymes, and initiating scaffold degradation and tissue remodeling processes. Mast cells release histamine, which recruits further phagocytes and causes vasodilation and increased vascular permeability.[198] This step facilitates angiogenesis and promotes cellular infiltration into the scaffolds. Similar chemical signals result from blood clotting and mast cell activation, increasing vascular permeability and attracting monocytes into the site of implantation. Once the *monocytes* reach the implant site, they begin to differentiate into macrophages, which in turn proliferate and fill the lesion. Within two days of implantation, the neutrophils disappear and are replaced with a population of macrophages.[199] By continuously proliferating and releasing chemoattractant, it can sustain itself and attract more macrophages.

Eosinophils are a potential source of pro-fibrotic cytokines, including TFGβ and IL-13, and contain several proteins that contribute to inflammation, tissue damage, and remodeling.[200]

Pro-inflammatory cytokines such as tumor necrosis factor (TNF)-α and interleukin (IL-1β) play an important role in the recruitment of other cell types of the immune system, particularly macrophages, and, thus, are necessary for the initiation of the next phases of the innate immune response.[201,202]

Mononuclear cells like *macrophages* and *mast cells* penetrate a mesh scaffold to begin the process of ingrowth. Grafts with good biocompatibility allow for easy migration of host cells. Moreover, blood vessel formation is a crucial step of the remodeling process as it allows more tissue integration. Mononuclear cells release cytokines and other signaling factors that attract fibroblasts.

Macrophage response is a critical determinant of the host response.[203] The primary function is a phagocyte responding to foreign materials or damaged tissue. Macrophages are capable of phagocytosing very small particles (< 5 μm). Within days of implantation, if a material is too big to be phagocytized, more than (> 10 μm), the macrophage becomes fused with other macrophages and induces the formation of foreign body giant cells (FBGC) on the biomaterial surface seeking to increase their phagocytic ability as part of the FBR.[204,202]

There are two main macrophage subtypes, one of which is pro-inflammatory/M1 macrophages, which are responsible for pathogen killing, dense fibrosis, scar tissue formation, and chronic inflammation. The other is anti-inflammatory/M2 macrophages, which are responsible for immunoregulation, tissue synthesis, repair, remodeling, and production of anti-inflammatory cytokines. It has been suggested that polarizing macrophages towards the M2 phenotype can increase the chance of better healing outcomes with polyurethane biomaterials.[205] If macrophages successfully degrade and phagocytose the implant during this acute phase of FBR, the reaction ends, and the tissue slowly returns to normal. In many cases, however, implants are required to remain implanted indefinitely. When, in these cases, macrophages fail to degrade the implant, FBR transitions into its chronic stage.

Chronic inflammation is defined as an immune response in which inflammation, tissue remodeling, and repair processes occur simultaneously.[206] It is identified by the presence of mononuclear cells, including *lymphocytes* and *plasma cells,* at the implant site. This chronic inflammatory response to biomaterials is usually short-term and confined to the biomaterial interface, where monocytes, macrophages, and foreign body giant cells are present.[203] The implant is covered by a layer of fibrous tissue, which acts as a barrier between the implant and the host tissue, stage over weeks after implantation, and unless the implant is destroyed or removed, it remains active indefinitely.[207]

During the transition to the chronic stage of FBR, macrophages switch from a pro-inflammatory activation phenotype (M1 macrophages) to an anti-inflammatory and tissue generation phenotype (M2 macrophages). It is predicted to result in the deposition of less dense, organized, and site-appropriate connective tissue and is often observed as part of the normal wound healing process, marking the switch from the elimination of foreign threats in an injury to the healing of the tissue. M2 macrophages started to lead the fibrosis process during FBR, decreasing inflammatory activity by releasing anti-inflammatory cytokines such as IL-10 and TGF-β that attract local fibroblast populations and induce

their activation. These activated fibroblasts adhere to the implant's surface and begin depositing layers of extracellular matrix proteins.[204] The pro-fibrotic mediators stimulate fibroblasts to differentiate into α-smooth muscle actin (SMA)-expressing myofibroblasts.[208] Myofibroblasts are responsible for the local extracellular matrix (ECM) protein production and scar formation.[209] A completely new tissue, known as the FBR capsule, is formed when the combination of macrophages, fibroblasts, and myofibroblast differentiation results in ECM production.[210] To supply it with nutrients, new blood vessels must extend into the capsule as it develops into a new tissue compartment. Vascular endothelial growth factor and platelet-derived growth factor, released by the capsule tissue, act as pro-angiogenic factors, drawing in newly forming blood vessels and acting as living tissue.[211]

The inflammation can help the mesh integration through the natural wound-healing mechanisms or cause an excessive inflammatory response. If the reaction is exaggerated, it can result in excessive scarring, graft encapsulation, or degradation. The balance between appropriate wound healing and detrimental effects is mainly controlled by cytokines, growth factors, and other chemical signaling molecules produced by host macrophages at the interface between host tissue and mesh. Many shifts in tissue homeostasis, like infection, bacterial biofilms, high PH, and hypoxia, can lead to fibrotic conditions. [212]

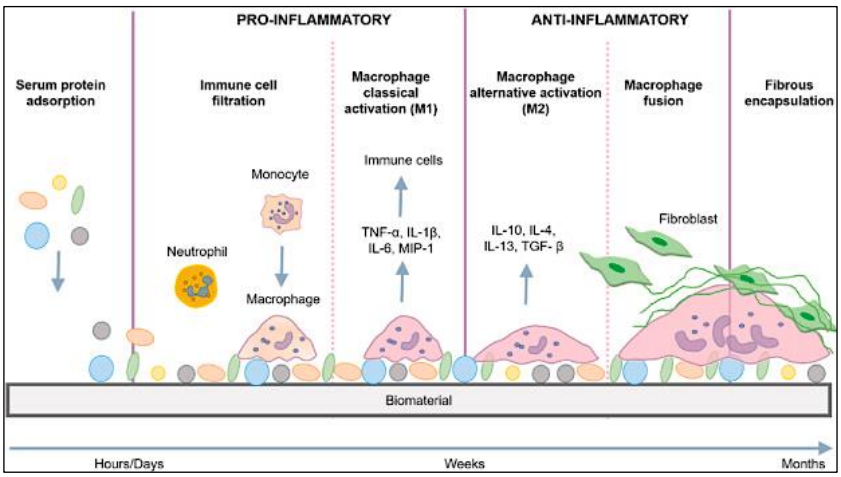

Figure 11: Timeline of the foreign body response. The foreign body reaction begins with the adsorption of proteins onto the biomaterial surface. The adsorbed protein layer favors the attachment of monocytes, which differentiate into classically activated (M1) macrophages that secrete pro-inflammatory cytokines TNF-α, IL-1β, IL-6, and MIP-1. Following a type 2 cytokine (e.g., IL-4 and IL-13) induced phenotype switch, M1 macrophages polarize into alternatively activated (M2) macrophages that release IL-10, IL-4, IL-13, and TGF- β. Sustained release of these cytokines promotes the fusion of macrophages and the formation of FBGCs, fibroblast adhesion/proliferation, collagen deposition, and ultimately forming a largely avascular fibrotic capsule.

Source: Kämmerling, L et al. (2021). Mitigating the foreign body response through 'immune-instructive' biomaterials. Journal of Immunology and Regenerative Medicine, 12, 100040. https://doi.org/10.1016/j.regen.2021.100040

New collagen deposition and tissue regeneration result from graft integration and remodeling, and in the final step, the mesh is often resorbed by the host (Figure 11).[213]

The orientation, type, structure, and amounts of collagen fibrils change with time. The dense parallel bundles of collagen do not have the strength of native tissue. Myofibroblasts' arrival can cause contracture of the wound margins, which is beneficial in normal wound healing; however, around biomaterials can be problematic.[212]

Biomaterial-related complications frequently seen in surgery are excessive scar formation, early or delayed infection by reactivation of biofilm-forming bacteria that were attached to the implant, seroma formation, intestinal adhesion, bowel obstruction, erosion of surrounding tissues, chronic pain due to the entrapment of nerves in a scar-mesh compound, and prosthesis contraction.[214,215]

Synthetic and non-degradable biomaterials induce a pro-inflammatory response, while degradable materials induce a pro-remodeling response.[216]

In biocompatible materials, early resolution of the acute and chronic inflammatory responses occurs within two weeks. Inappropriate tissue response on the material surface often leads to device failure.

In summary, the initial implantation of a device triggers the cellular events leading to FBR, and subsequent trauma around the implant leads to further inflammation and worsens ongoing FBR. Consequently, one of the most effective strategies to reduce FBR is designing implants that minimize tissue trauma. To determine the effect of the material on the tissue response to the foreign body, it is necessary to accurately characterize the device in terms of porosity, pore size, and lightweight. Biomaterial topography may have a significant impact on the foreign body reaction. Porous structures tend to result in a moderate tissue response and enable faster healing processes, with fibrous capsule formation on a porous surface often found to be thinner than that on a dense solid implant surface.[217]

Assuming that the introduction of foreign material into the body is an injury, and the body will want to defend itself, it begins to trigger a cascade of inflammatory events to control the strange body and its potential harm. To minimize that response, it's possible to influence the body by altering fibrotic responses or modifying the characteristics of the mesh to mimic the organism.

To *prevent fibrous* capsule formation around biomaterial, there are anti-fibrotic treatments like a direct injection of collagenase and an anti-fibrotic drug like Pirfenidone that inhibits TGFβ.[218] Immunosuppressive drug treatments include glucocorticoids as

anti-inflammatory, suppress cell proliferation, and modulate the phenotype of infiltrating macrophages and lymphocytes.[219,220] Other general immunosuppressive drugs include colchicine, azathioprine, cyclophosphamide, prednisone, thalidomide, pentoxifylline, and theophylline, which potentially block the action of the inflammatory cytokines and growth factors or deliver anti-fibrotic cytokines.[221] However, they can have undesirable side effects. Many treatments targeting the specific cell response were present in the literature. Serum amyloid P (pentraxin 2) has been shown to inhibit pro-fibrotic macrophage generation.[222] The release of masitinib, a tyrosine kinase inhibitor, has been used in biomaterials to target mast cells, which has led to some reduction in fibrosis.[223] Preventing, interfering, or reversing myofibroblast differentiation can be the designed treatment in pathological fibrosis.[224] The basic cause of fibrosis is an imbalance between ECM production and catabolism. Interfering in these processes seems to be a natural approach for inhibiting fibrous capsule formation. Prolyl-4-hydroxylase enzyme significantly reduced fibrosis.[225] Matrix metalloproteinases MMPs degrade components of the ECM.[212]

We can interfere with *the Biomaterial* before or at the same moment of the implantation to prevent the initiation of pro-fibrotic signals. Moreover, the biomaterial can deliver an anti-fibrotic agent, although it could have a temporary effect. The challenge is to create a material that resembles the body and will not be recognized as foreign to overcome the fibrotic response.[212] The engineering focus must be on minimizing biomaterial surgical damage, mimicking the mechanical properties of local tissue, and altering surface topography (increasing porosity or surface roughness).

Fibrosis is a complex and multifactorial process that is difficult to modify.

Thus, the overall aim of material design is to develop a mesh that can leverage the body's defense and pro-healing abilities to promote healing and integration while minimizing the detrimental effects of FBR and fibrotic capsule formation as appropriate. Electrospun material provides microenvironments such as porosity and interconnectivity that can mimic structural features present in the ECM. In terms of the immune response, the shape of materials can also impact the behavior of immune cells.

Chapter IV. MESH EVOLUTION: PCUU – TECOFLEX™

1. History

In 1983, the concept of scaffolding as a porous matrix or as an implant in which cells can slowly infiltrate and regenerate the local tissue was first introduced.[226]

In tissue engineering and biomaterials, scaffolds for medical applications are defined as tissue substitutes. These substitutes are grafts or porous substrates that interact with cells to promote and maintain their differential state during the time, contributing to forming a precise functional tissue.

The engineered environments could be designed to direct the cells added from exogenous sources or mobilized from the host to regenerate specific tissue structures and functions.

The native extracellular matrix (ECM) is a well-organized nanocomposite that not only supports embedded cells mechanically but also interacts with them. Thus, promotes and regulates cellular functions such as adhesion, migration, proliferation, differentiation, and morphogenesis.[227]

Tissue engineering scaffold fabrication utilizes non-woven biomaterials that can be categorized as synthetic, semisynthetic, or naturally derived. The advantages of natural materials are their proper physiological activities, mechanical properties like natural tissues, and biodegradability.[228,229]

Synthetic materials can be produced in large quantities and converted into exogenous ECM. The microstructure, mechanical properties, and degradation time can be easily controlled and manipulated. To replicate the topological and microstructural characteristics of the ECM, a scaffold must have high porosity, an adequate surface-to-volume ratio, high pore interconnection, proper pore size, and controlled geometry.[230]

A good scaffold should have properties like biocompatibility, adjustable degradation rate with non-toxic degradation products, good porosity for transporting nutrients and wastes, resemblance to the structure of the target tissue, and appropriate mechanical strength.[231]

The term *"biocompatibility"* is the ability of the biomaterial to exist in contact with tissues of the human body without causing an unacceptable degree of harm to that body.[232,233] It means that a polymer composition and its normal degradation in vivo products are cytocompatible, non-toxic, and non-carcinogenic in a patient within useful, practical, and/or acceptable tolerances.[234]

The length of time the scaffold must be present in the body is unknown. Although a short duration improves biocompatibility, it could cause mechanical failure, and excessive exposure could result in inappropriate tissue development or fibrosis.

Depending on the target function, the simulated tissue-engineered construct must be biologically stable, resistant to hydrolysis and enzymes, or biodegradable. The polymers must maintain their shape and mechanical properties for a specified duration. To maintain appropriate stability and function, the biodegradable polymer must be replaced by newly synthesized tissue.[229]

2. Polymer composition and uses

a) PCUU

Polyurethane (PU) has unique physical and mechanical properties, including durability, flexibility, and abrasion resistance. Their use involves producing flexible and rigid foams, adhesives, gaskets, and coatings with high-performance parameters, utilized as biomedical materials because of their biostability and biocompatible properties with certain tissues. PU is biodegraded via hydrolysis of their ester and urethane groups or oxidation of the aliphatic fragments carrying ether bonds.

Poly (carbonate-urethane) urea (PCUU) is a biostable and slow degradable. Synthesized from polyurethane, poly(1,6-hexamethylene carbonate) diol (PHC Mn= 2000, Sigma)) and a hard segment of 1,4-diisocyanatobutane (BDI, Sigma) with chain extension by putrescine (Sigma).[235]

PCUU is an interesting one among PUs.[236] The group of polymers known as aliphatic polycarbonates has a higher resistance to hydrolytic and enzymatic degradation than polyesters. As a result of their environmental resistance and mechanical and thermal properties, PCUU has become a viable competitor to poly(ester-urethane) s and poly(ether-urethane) s in the biomedical field.[237,238]

Tissue engineering scaffolds must be biocompatible with the tissue and maintain the right mechanical properties in the body's complex environment.[239] PCUU was clinically used alone or blended with other materials in humans as vascular or bypass graft, with no cytotoxic effects, infection, or inflammation and allowing antiplatelet and anticoagulant function, allowing endothelial cells to grow.[240,241]

Acting as a matrix permits cell infiltration, proliferation, and integration with the surrounding tissues. They can mimic the structure of the extracellular matrix. They are

produced by electrospinning, the best way to create structures that look like the natural extracellular matrix (Figure 12).[242]

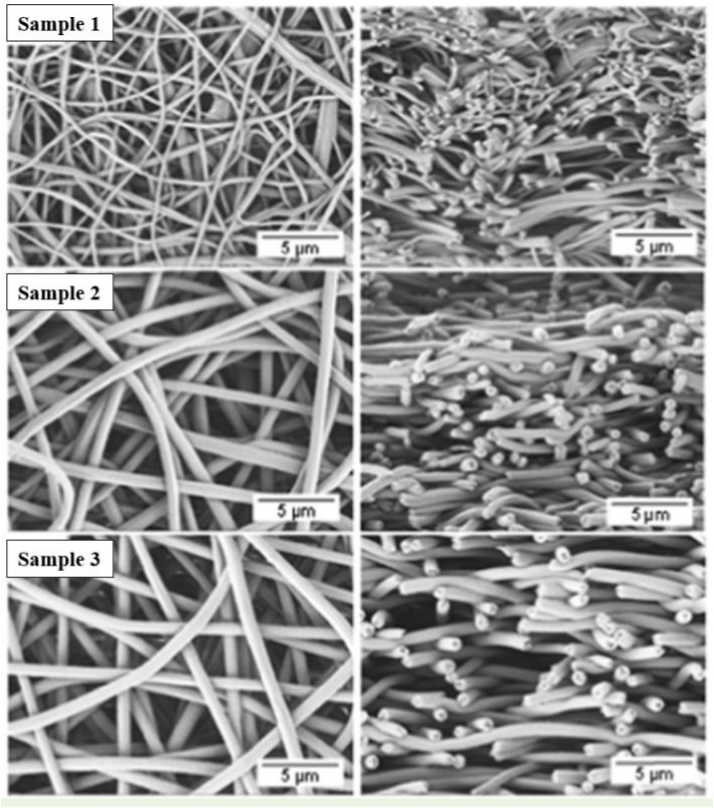

Figure 12: SEM micrographs showing the top (left) and cross-section (right) views of PCUU-based nonwovens obtained on a plate collector.

Source: Rolińska K, Bakhshi H, Balk M, Blocki A, Panwar A, Puchalski M, Wojasiński M, Mazurek-Budzyńska M. Electrospun Poly(carbonate-urea-urethane) s Nonwovens with Shape-Memory Properties as a Potential Biomaterial. ACS biomaterials science & engineering, 2023;9(12), 6683–6697. https://doi.org/10.1021/acsbiomaterials.3c01214

b) Tecoflex™

Thermoplastic polyurethanes (TPUs) are a family of medical-grade, aliphatic, polyether-based TPUs synthesized from methylene bis(cyclohexyl)diisocyanate, poly (tetramethylene ether glycol) and 1,4-butanediol.[243]

In the context of replacing and ingrowing tissue, such as blood vessels, non or slow biodegradability could be beneficial. Despite relatively good cell viability or cytocompatibility, Tecoflex™ surfaces provide poor adhesion and proliferation of endothelial cells (ECs), which have a key role in giving the luminal surface of a blood vessel its anti-thrombogenic properties (Figure 13).[244,245]

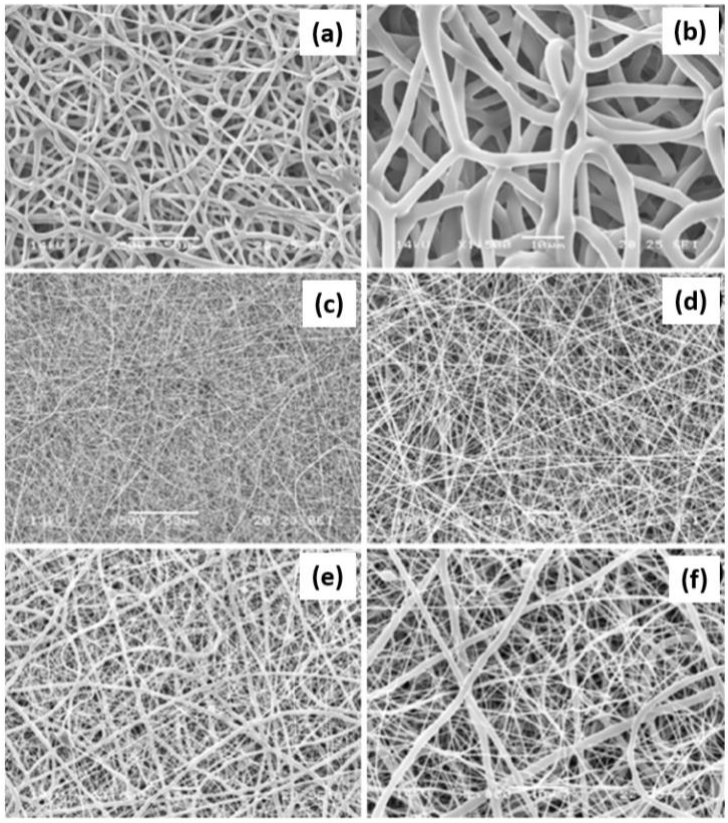

Figure 13: SEM micrographs of Tecoflex™ (a and b), gelatin (c and d), and composite mesh obtained by electrospinning (e and f) at low and high magnifications. In the case of composite, gelatin fibers *(smaller)* are visible together with Tecoflex™ fibers (larger), creating an integrating network.

Source: Detta, N., Errico, C., Dinucci, D., Puppi, D., Clarke, D. A., Reilly, G. C., & Chiellini, F. (2010). Novel electrospun polyurethane/gelatin composite meshes for vascular grafts. Journal of materials science. Materials in medicine, 21(5), 1761–1769. https://doi.org/10.1007/s10856-010-4006-8

3. PCUU-T fabrication: ELECTROSPINNING

a) Definition

Electrospinning (ESP) is a technique for manufacturing materials with polymer solutions, producing and folding fibers into 3D matrices with specific surface area and porous structure. Combining polymers with additional components in the solution makes it possible to produce fibers with different properties, shapes, orientations, and mechanical anisotropic properties.[246]

A prototype of an electrospinning device was described in two patents filed by Morton and Cooley in 1902. Formhals invented and patented an experimental device in 1934 that used electrostatic force to prepare polymer fibers, considered the beginning of the fibers using ESP technology. The number of publications on ESP has increased exponentially since Reneker et al. demonstrated the possibility of producing electrospun nanofibers from various polymers in the 1990s.[247,248]

b) Uses

The dimensions of ESP fibers generally range from nano to microscale. It has been demonstrated that the size and surface texture of the ESP scaffolds can influence the rate and morphology of cell proliferation.[249]

By ESP, nanofibers are obtained with strong plasticity, flexibility, and a large surface area volume ratio, which can improve cell adhesion, proliferation, and differentiation. The method has advantages such as producing fiber with high porosity, adjustable pore size, and small fiber diameter, which facilitates native tissue ingrowth and enhanced cellular infiltration in aligned nanofibers. ESP can be adjusted to create randomly or aligned oriented nanofibers.[250,20]

The ESP is a simple, cost-effective, flexible, and feasible continuous method for preparing micro-nano polymer fibers and synthesizing three-dimensional structures.

The ability to manipulate nanofiber components to achieve the desired properties and functions makes it suitable for different applications and exploring new scaffold constructions.

The ESP has gained popularity in the biomedical field due to its widespread application. There are various applications such as cardiovascular tissue engineering (myocardial, vascular grafts, heart valve), bone, cartilage, neural, and skin.[251] The small diameter and adjustable pore size of electrostatically spun nanofiber films have also been advantaged in the manufacture of wound dressing, cancer diagnosis, and treatment by drug delivery systems.[242,252]

The innovation of a mandrel-less electrodeposition apparatus to fabricate continuous microfiber wires allows controllable microarchitecture and mechanical properties that can be used as suture materials, improving the number of anti-inflammatory macrophages.[253]

The key to tissue engineering is to select the right biomaterials and construct the right scaffolds. A scaffold material must be biocompatible and biodegradable, mimic the features of the natural extracellular matrix, promote cell penetration and tissue growth, provide biomechanical support, have a low price, and be easy to obtain, produce, and handle.[254]

The introduction by D´Amore of the double-component deposition and electrodeposition technique that employs multi-phase electrodes allowed control of scaffold macro-scale morphology, mechanics, and microstructure, enhancing the generation of engineered valves.[255]

More than 200 kinds of natural polymers and composites, such as gelatin, silk fibroin, chitosan, and collagen, as well as many synthetic polymers, such as polycaprolactone. (PCL), Polylactic acid and poly (lactic-co-glycolic acid) have been applied in ESP technology systems.[256]

At the time of writing this thesis, in Italy, Foundation RiMed is using PCUU for valvular construction and is expanding the use of these elements in other areas of surgery.

Yet, there is no published evidence of PCUU-T nanofiber manufacturing to generate a slow and non-biodegradable mesh, using it as a scaffold associated with a breast implant.

c) Basic electrospinning equipment

ESP equipment involves a high-voltage power supply, a flow controller, a syringe pump with a needle, and a grounded collector.[257] At a particular speed, the syringe pump controls and propels the polymer solution for ESP. Surface tension causes the initially extruded liquid to form suspended spheres that change to a conical due to the high voltage. The filament will extend from the tip of the cone when the voltage exceeds a threshold, creating one or more jets of charged polymer solution. The charged jet gradually becomes refined and solidifies while moving, and the resulting solid fibers are attracted, deposited, and collected by an electrically charged grounded collector. By doing this, it is possible to obtain polymer fibers with diameters between nano and submicron. The ESP process is influenced by many adjustable variables, such as the spinning conditions, the polymer solution, and the environmental conditions (temperature and humidity). The intensity of voltage, flow rate controlled by the syringe pump, and tip-to-collector distance are the main spinning conditions. The concentration, conductivity, viscosity, surface tension, and polymer molecular weight of the polymer solution also affect the ESP and play a key role. Specific applications can be achieved by controlling the materials and methods of electrospinning (Figure 14).[242]

Figure 14: Basic electrospinning equipment.
Source: Picture from SF in D' Amore Lab, Rimed

HYPOTHESIS AND OBJECTIVES

Many changes in breast skin elasticity are common occurrences, especially after significant life events like childbirth, breastfeeding, weight loss, sequelae after aesthetic surgeries, or skin-sparing mastectomy for breast cancer.

Breast implants are medical devices used for aesthetic and reconstructive purposes to enhance the size and shape of the breast. Obtaining an aesthetic result is a great challenge. The submuscular breast implant technique is a good option to give volume and provide upper pole implant coverage. However, in many cases, the lateral and inferior pole could be covered only by the thin skin, predisposing to ptosis, bottoming out, and implant malposition.

Using biological or synthetic meshes for coverage and lower implant support is an essential technique to achieve better results in aesthetic and breast reconstruction. The mesh is placed underneath the skin, in the lower pole, helping to create a more natural-looking breast shape and providing additional support to the implant to rebuild the breast. However, meshes have different structures, morphologic, mechanical characteristics, thickness, and weight; there are some potential drawbacks to using mesh in implant base-breast surgery. One concern is the risk of mesh infection or rejection, which can lead to complications and additional surgeries. Mesh degradation can be problematic since rapid absorption can cause the implant to fall out, and malposition altering the natural-looking breast or long-lasting durability can produce a continued foreign body reaction.

To produce a new “optimal” mesh, it is necessary to evaluate and analyze the available meshes in the market for breast reconstruction after compared with the literature. The safety and effectiveness of surgical mesh in breast surgery, including augmentation or reconstruction, have not been determined by the FDA.[1]

Biological or synthetic meshes are fabricated to induce tissue integration, or they may be developed to house or attract cells, which, in turn, assist in inducing tissue integration. Several key characteristics make a current biomaterial suitable for tissue engineering applications. Biomaterials could be absorbable or degradable and, therefore, facilitate new tissue integration with native tissue over time. The shape and texture of the material do not have to resemble that of natural tissue, but it should induce the growth of new tissue resembling native tissue. Cellular affinity is another important aspect of a biomaterial. Biomaterial must interact favorably with cellular components without negative impacts such as tumorigenicity or toxicity. Some elements of porosity or surface

texture are helpful and potentially allow cellular ingrowth into the material, transfer nutrients and waste products, stimulate vascular network into the scaffold, and induce the differentiation of multipotent cells.[2]

Many surgical mesh products are cleared for the repair and reinforcement of soft tissue where weakness exists.

This thesis presents experimental in vivo model research about a novel non-woven mesh fabrication. Different concentrations of biodegradable Poly(carbonate-urethane) urea (PCUU) and Tecoflex™ (a non-degradable medical grade polyurethane), named PCUU-T, were used. Each different blend was evaluated with specific tests (thickness, weight, degradation, mechanical, and porosity tests) to achieve the optimal mesh and compared with five synthetic meshes used in breast reconstruction. Experimental surgery was performed in 18 Wistar rats. The Ultrapro™ chosen commercial mesh and PCUU-T were located in their respective subdermal dorsal pockets, covering smooth and textured mini-breast implants. Rats were clinically examined for 9 weeks, and explantation was performed by removing in block skin, mesh, capsule, and implant after euthanasia (day 63). That material was intensively examined using histology and bacteriology.

Hypothesis

We hypothesize that a PCUU-Tecoflex™ (PCUU-T) nanofiber mesh could provide mechanical support in breast implant procedures, stimulate tissue ingrowth, and reduce scar formation compared to these other synthetic meshes.

General Objective

The general objective of this work is to evaluate the use of electrospun biodegradable Poly(carbonate urethane) urea (PCUU) plus non-degradable Tecoflex™ (PCUU-T) non-woven mesh as a scaffold in association with a breast implant and its behavior in a small animal in comparison with commercial mesh Ultrapro™.

Specific Objectives

To evaluate the “properties” of 5 synthetic meshes in terms of thickness, density, mechanical, and porosity to identify the optimal mesh of them.

To elaborate biodegradable mesh using different blends of PCUU and Tecoflex™. Achieve mechanically relevant support for the breast implant compared to the commercial meshes.

Achieve host tissue integration and regeneration, which helps to maintain a lasting successful repair, sufficient support, and position of the breast implant.

Obtain good revascularization, cell repopulation, and collagen deposition with minimal foreign body reaction.

Decrease the rates of complications such as explantation, reoperation, infections, bacterial contamination, and capsular contracture in comparison with other materials.

MATERIAL AND METHODS

1. Study type

This project was carried out by the Universidad Abierta Interamericana (Argentine) in collaboration with the University of Palermo and Fondazione Ri.MED (Italy) is already working with the PCUU in cardiovascular tissue repair.

This study was experimental research using an *in vivo* model. It involved blending PCUU and Tecoflex™ to design and create an optimal mesh for use in plastic and reconstructive breast implant surgeries.

2. Research Workflow

This experimental research included several steps schematized in (Figure 1).

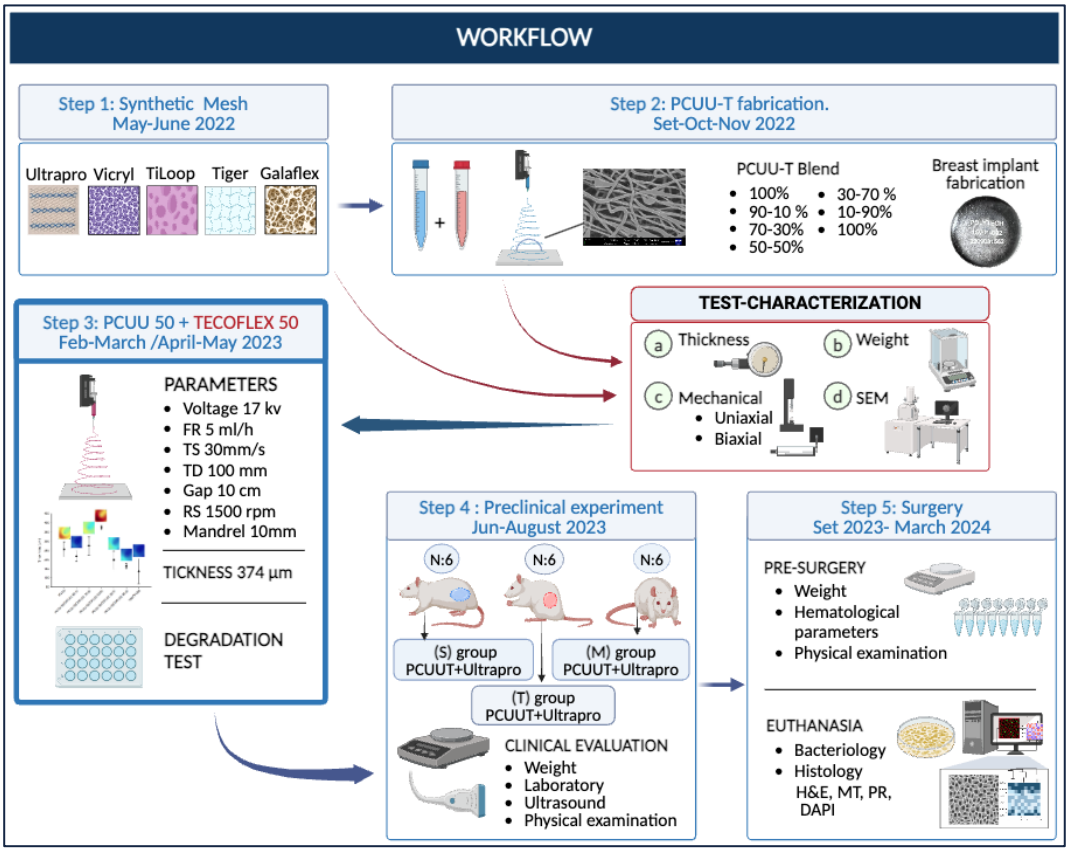

Figure 1: Research Workflow. Step 1: Five synthetic mesh analyzed. Step 2: Blend PCUU and Tecoflex™ in different blends. Test and characterization of the different blends. Polytech™ mini breast implant fabrication**.** Step 3: Parameters used to obtain the blend of PCUU 50 and Tecoflex™ 50. Step 4: Preclinical research on 18 rats, one group received Smooth, second textured implant, and the third without implant as a control group. Everyone had PCUU-T mesh on the left side and Ultrapro™ mesh on the right side. Step 5: Post mesh + implant explantation analysis.

Source: Self-made scheme (SF)

Five *synthetic commercial* meshes were examined in terms of thickness, density, porosity, and mechanical test to understand the properties and arrive at the optimal characterization. Different *blends of PCUU and Tecoflex™* **(PCUU-T)** were fabricated by Electrospun and evaluated in terms of thickness, density, porosity, mechanical properties, and biodegradation profiles to determine the most appropriate blend to prepare a novel mesh (PCUU-T). The mini breast implants (smooth and texture surface) were fabricated by Polytech™ (Health and Aesthetic, Dieburg, Germany) and specifically customized for this research to be incorporated under the mesh in the dorsal subcutis on the rat model.

Preclinical Experiment: The experimental procedure was carried out on 18 healthy rats randomly assigned to three groups. Group S: (n=6) rats received a smooth implant surface covered by the PCUU-T on the left side and Ultrapro™ mesh on the right side of the dorsum. Group T: (n=6) rats received a textured implant surface covered by PCUU-T on the left side and by Ultrapro™ mesh on the right side of the dorsum. Group M: (n=6) rats without implants but received PCUU-T on the left and Ultrapro™ mesh on the right side as a Control Group.

The groups were clinically evaluated and examined by ultrasound every week. The weight was recorded on the first day (pre and postoperative) and before euthanasia.

After euthanasia, the mesh + implant was explanted and analyzed through histology, and bacteriology (Figure 2)

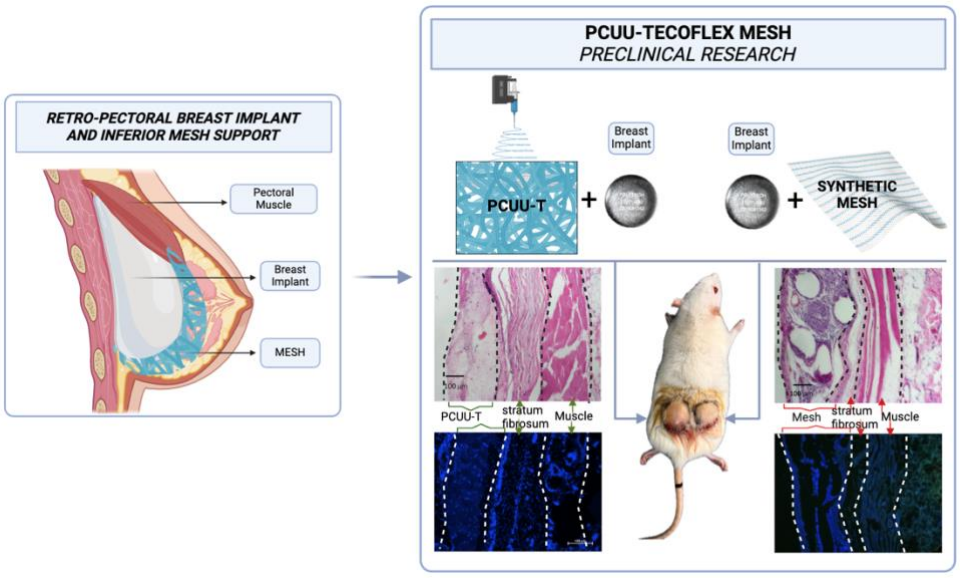

Figure 2: On the left: Schematic Submuscular Breast implant reconstruction covered by a mesh in the lower pole; this encouraged the idea of a new mesh. Preclinical research scheme since the mesh fabrication to the histological analysis H&E and DAPI.

Source: Self-made scheme (SF)

3. Material

a) Meshes

The partial and totally degradable synthetic meshes selected were Ultrapro™, Vycril™, Tigr™, Tiloop™, and Galaflex™.

Since the very beginning of the project, the biostable and degradable mesh composed of poly (carbonate-urethane) urea (PCUU) has been selected as the most elastic and least biodegradable polyurethane available. Synthesized from polyurethane, polycaprolactone diol (PCL, Mn ¼ 2000, Sigma), poly (1,6-hexamethylene carbonate) diol (PHC Mn= 2000, Sigma), and hard segment of 1,4-diisocyanatobutane (BDI, Sigma) with chain extension by putrescine (Sigma).

To increase PCUU (Y modulus 2MPa) mechanics, we have prepared different blends with Tecoflex™ 85a (Y modulus 9MPa). PCUU-Tecoflex™ ratio 100:0, 90:10, 70:30, 50:50, 30:70, 90:10, 0:100.

The biostable Tecoflex™ 85A is an aliphatic polyether urethane that is combined with PCUU 12%[236], 50/50, which was named PCUU-T in this experience.

The PCUU-T fabrication was made through electrospinning (ESP) (Figure 3).

Figure 3: PCUU-T mesh fabrication. a) PCUU synthesis. b) Tecoflex™ weight. c) PCUU and Tecoflex™ dissolved under mechanical stirring. d) mesh thickness measure.

PCUU: Polycaprolactone diol (PCL) and poly (1,6-hexamethylene carbonate) diol (PHC) were dried under vacuum at 50° C to remove the residual water before synthesis. A hard segment of 1,4-diisocyanatobutane (BDI) with chain extension by putrescine was distilled before usage. Dimethyl sulfoxide (DMSO), N, N-dimethylformamide (DMF), 1,1,1,3,3,3-hexafluoroisopropanol (HFIP) and phosphate-buffered saline (PBS) were used as received. Stannous octoate (Sn (Oct)2) was dried using molecular sieves.[235]

The PCUU polymer was dissolved in 20 mL of HFIP hexafluoroisopropanol (12% volume/V) under mechanical stirring at 24 hs at room temperature. Tecoflex™ 85A. Tecoflex™ was dissolved in HFIP at 12 % (w/V).

PCUU-T. PCUU and Tecoflex™ were weighed and dissolved on a plate with a magnetic stir bar. They were blended and placed in a 12ml syringe to produce the new scaffold. For PCUU-T manufacturing, an electrospinning device ESP high voltage (NF-500, MECC Co, Ltd., Japan) was used (Figure 4)

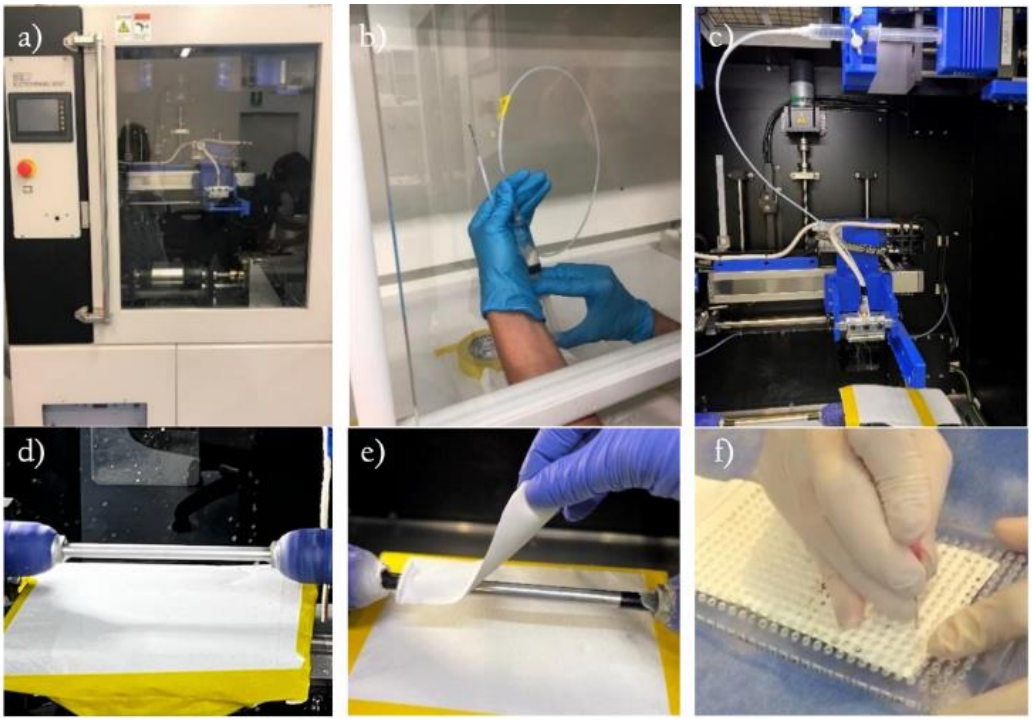

Figure 4: PCUU-T mesh manufacturing. a) Electrospinning machine. b) Syringe luer lock 12 cc, tube, and needle 16G connected. c) Syringe pump and system preparation. d) Mandrel 10 mm. e) Rectangular flat mesh design 10 x 6 cm. f) Acrylic laser customed mesh, the holes were 1mm and 10 mm separation between each with needle 18G.

The general process for every mesh was performed in the laboratory spinning unit in the Lab for biomaterial fabrication (ATEN center, building 18 UNIPA). The mandrel

collector diameter of 10 mm with a speed controller was used. The gap distance between the drum collector and the nozzle was 10 cm, and the speed rotation was 1500 RPM.

Each solution was placed in a 12 ml Luer lock syringe with the plunger, stainless-steel needle 16 G, and copper wire.

The power supply was set up for a positive stream voltage of 17 kV. The flow rate of the solution was set up on the syringe pump at 5 ml/hr, rastering 3 mm/sec, transverse speed 30 mm/sec. Transverse distance 100 mm. The deposition time depended on the PCUU and Tecoflex™ concentration; in our model mesh was 45 min. The flat single-layer mesh was fabricated via wet ESP (Figure 5).

The mesh was removed from the mandrel after being in a pure ethanol bath, frozen (-80) for 60 min, and left under the hood to complete the solvent evaporation. After all, the horizontal section was performed over the mesh with surgical blade N° 23 to obtain a flat mesh. The process resulted in a 10 x 6 cm patch.

To obtain a 1mm porous, many incisions were made on the mesh with an 18 G needle, split up each other 10 mm, using an acrylic laser customed hole puncher (Figure 4 f)

The size to cover the outer surface of the implants was 2,5 cm in diameter, cutting with scissors.

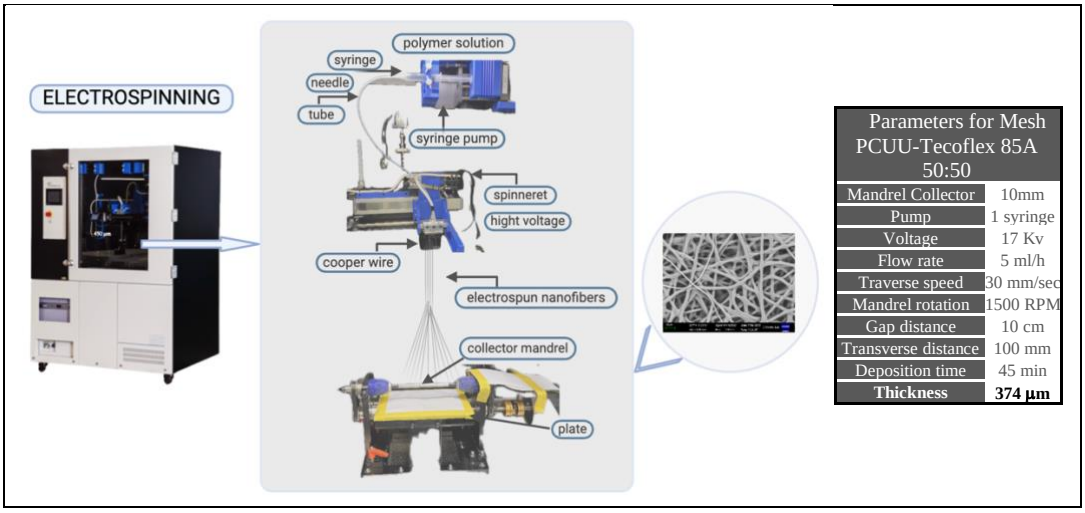

Figure 5: ES device (NF-500 MEC Co). The major components. Basic setup for aligned nanofiber PCUU-T 50/50 fabrication.

Source: Self-made scheme (SF)

b) Mini-breast implant fabrication

Customized 40 mini silicone breast implants filled with cohesive silicone gel were fabricated. They were round-based, 25 mm in diameter, and 5mm in projection. The silicone volume was 2 ml. Twenty mini-implants had textured surfaces (MESMO™) and

twenty smooth surfaces. All were produced and donated by the company POLYTECH™ (Health and Aesthetic, Dieburg, Germany).

MESMO™ is a CE-marked, class III, sterile, surgically implantable medical device manufactured by POLYTECH Health & Aesthetics GmbH. It is a round silicone breast implant with a fine microtextured shell surface. MESMO™ fine microtextured shell combines the benefits of both smooth and textured surfaces.

POLYTECH™ implants have a chemically and mechanically resistant, soft silicone elastomer shell comprising several Polydimethylsiloxane layers. The shell of gel-filled implants is additionally equipped with a special barrier layer.[258]

Wall thicknesses of the shells for micro-textured MESMO™ implants are 0.35–1.0mm, and the average surface roughness of textured implants is approx. 25µm.

POLYsmooth™ POLYTECH smooth shell surface has an advanced shell construction with a smooth surface. 2,5 ml smooth and texture round silicone implants (Polytech™, German). (Figure 6). Before surgery, the implants were autoclaved.

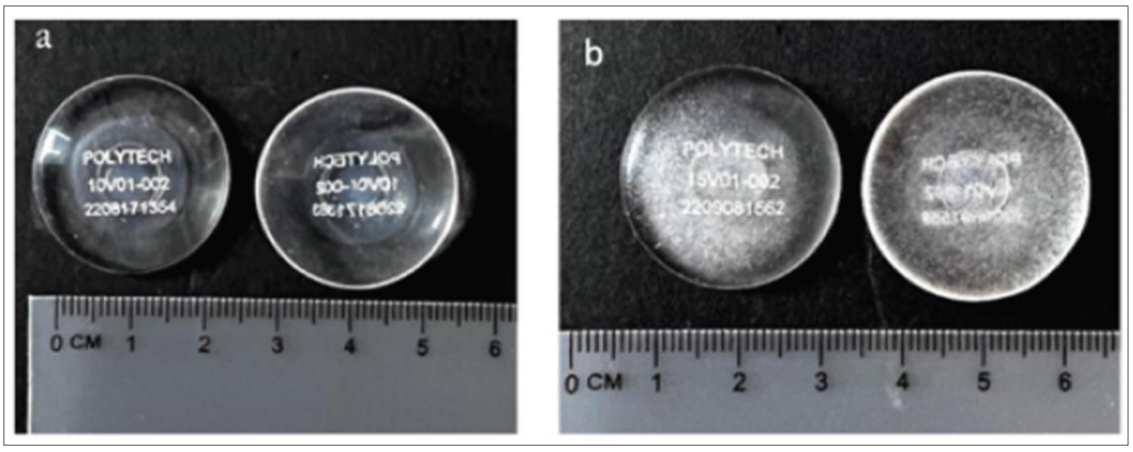

Figure 6: Mini breast implant Polytech™. a) Smooth surface. b) Texture surface.

c) Experimental animal

For experimental purposes, n=18 adult female Wistar rats, 70 days old and weighing an average of 231 gr (range: 213 - 250 g), were studied. They were maintained for two weeks in a room at constant temperature with a 12 h light-dark cycle, with food and water supplied ad libitum.

Experimental protocols were performed according to the NIH "Guide for the Care and Use of Laboratory Animals" (Publication no. 25-28, revised 1996)[259], and approved by the local animal care and use of Universidad Abierta Interamericana (UAI) and the National University of Rosario (UNR) Committees.

4. Methods

a) Thickness test

The thickness of each mesh was measured with a micrometer pocket dial gauge 1010 M (Starrett Co, Athol, MA USA).

The five synthetic meshes and PCUU-T were cut in 10 mm2, obtaining 5 samples of each one. The thickness was assessed 13 times and reported as mean.

b) Density test. Weight

The five synthetic meshes and PCUU-T blend were cut in 10 mm^2, obtaining 5 samples of each. The mass was obtained using an Orma™ Scientific electric digital weight scale (Max 160g Min 0.01g). Density (g/m2) was calculated by dividing the mass (g) by the specimen's area (m^2). The outcome was registered.

c) Mechanical test

UNIAXIAL

The uniaxial tensile strength was tested in 6 samples for each synthetic mesh in two main directions (horizontal and vertical). The test was carried out by the Instron™ device (Figure 7)

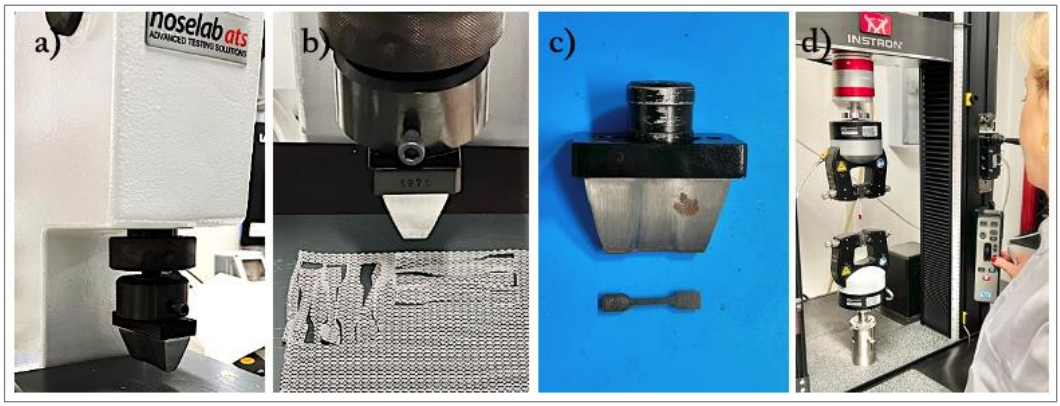

Figure 7: Uniaxial test. a) Noselab ats ™ punching machine to prepare standardized samples. b) Process of cutting Galaflex ™ mesh in the horizontal and vertical direction with the dog bone shape. c) Die cutter with dog bone shape. d) Instron™ uniaxial machine in the process of testing Galaflex™ mesh. Author processing (SF).

The manual die cutter Noselab ats ™ (Italy) was used to obtain standardized strips cutting with shaped blades (Force exerted 5kN).[260] The samples were cut out in 10 mm wide and 50 mm long with a dog-bone shape (5 mm wide and 25 mm long in the middle part) (Figure 8).

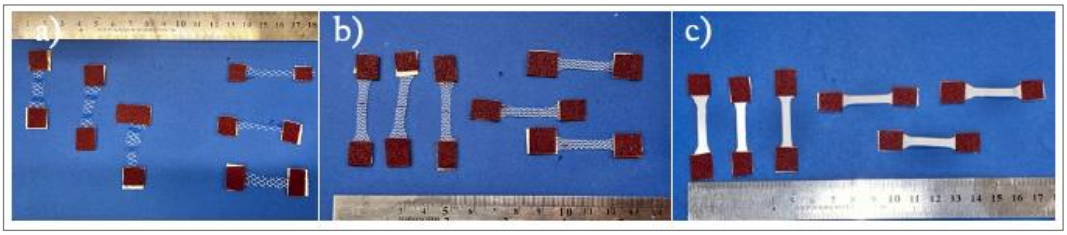

Figure 8: Preparation mesh for the mechanical uniaxial test, sandpaper glued on the ends to avoid sample slippage. a) Ultrapro ™ mesh. b) Galaflex ™ mesh. C) PCUU-T mesh.

The specimen´s thickness was determined with a caliper before the test. To prevent mesh slippage, the strips were glued with sandpaper strips used as layers between specimens and pneumatic grips.

The strain rate was 0,4 mm/s. Each test ended after the sample failure. The ultimate tensile stress of each mesh was calculated using the maximum load sustained by the mesh and the cross-sectional area of the central region of the mesh specimen.

The ultimate tensile stress of each mesh was reported in units of megapascals (MPa) as mean ± standard error of the mean (SEM).

BIAXIAL

The biaxial tensile properties of the PCUU-T blend scaffolds processed at different concentrations were evaluated using an equi-stress biaxial test.[261] Five 10 mm x 10 mm samples were obtained from each group. After the sample thickness was measured using a caliper, five marker dots ~1 mm in diameter positioned in the sample at the corners and in the center of a 6 mm × 6 mm square were utilized to calculate the deformation gradient tensor.

Samples mounted on the device were anchored by sutures on each edge using four equidistantly placed small surgical hooks. To maintain the stress and strain states uniform in the central region, the hooks were located away from the outer edges to avoid the effects of specimen anchoring. Sutures were attached to the four electromagnetic motors of the biaxial system, aligning longitudinal edges with the direction of stretching. Samples were loaded into a custom-made biaxial testing device and tested in PBS at room temperature for 10 cycles with an unloading and loading time of 30 s/cycle (Figure 9).

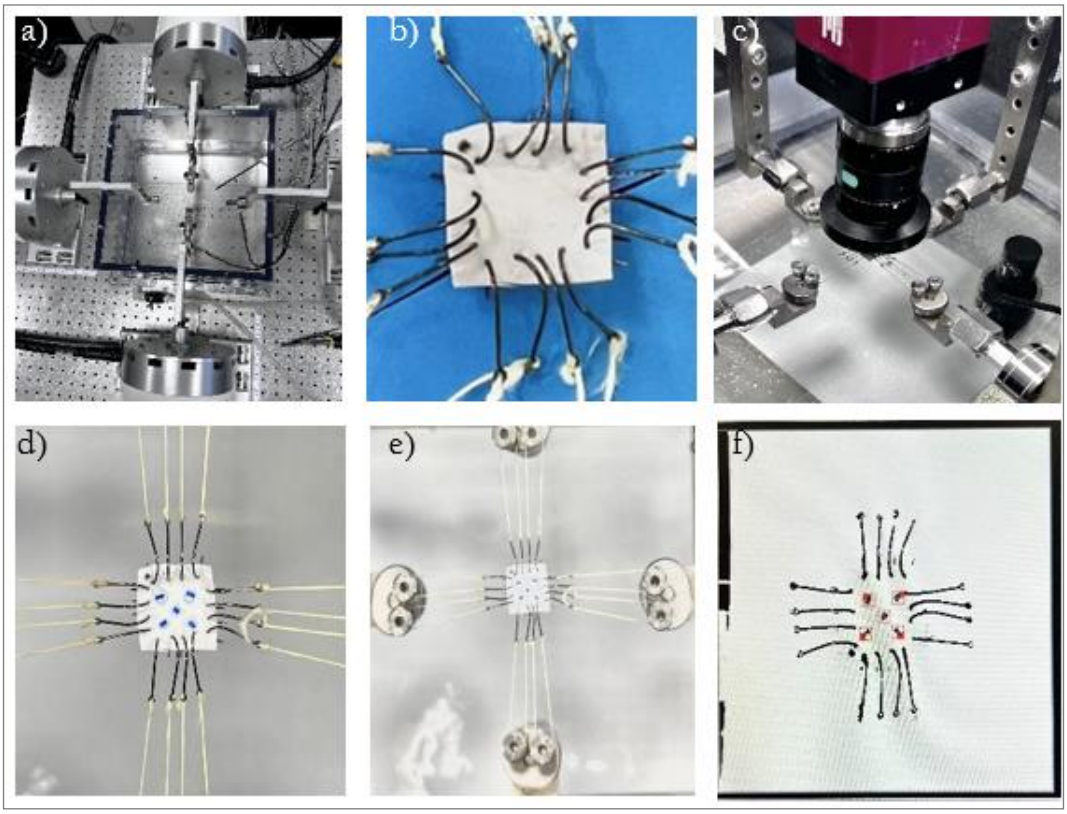

Figure 9: Biaxial test PCUU-T. a) Four electromagnetic motors of the biaxial system. b) PCUU-T 10 mm square with four equidistantly small surgical fishhooks. c) Setup. d) Five marker dots ~1 mm. e) Sample mounted on the device, anchored by sutures on each side.

Every sample (n=5/group) was preconditioned and then tested in Lagrangian equi-stress control to peak stress of 400 kPa. Two 200 N load cells were used to record the force along material directions. From marker positions, the in-plane Green strain tensor was calculated as:

$$E = \frac{1}{2}(F^T F - 1)$$

Where *(E)* is the elastic modulus, *(F)* is the gradient deformation tensor.

For in-plane biaxial stretching, the in-plane Green strains are:

$$E_{H=}\frac{1}{2}(\lambda_H^2 - 1)$$

$$E_V = \frac{1}{2}(\lambda_V^2 - 1)$$

Where *(λ)*, λ_H, and λ_V are the *(H)* horizontal and *(V)* vertical stretches in the deformed equilibrium configuration, respectively.

The first Piola–Kirchhoff stress tensor P was calculated from measured loads and initial specimen dimensions so that nonzero components of P are:

$$P_{HH} = \frac{F_H}{H\,X_V} \text{ and } P_{VV} = \frac{F_V}{H\,X_H}$$

where F_H and F_V are the measured loads along each direction, X_H and X_V are the unloaded specimen dimensions along each direction, and H is the average specimen thickness in the unloaded reference configuration. The anisotropy ratio (AR) was selected to study the impact of the different processing variables on the in-plane behavior of the electrospun mats. AR was defined as the ratio of the Lagrangian's stretches during equi-stress biaxial testing using the equation:[262]

$$AR = \frac{\lambda_V}{\lambda_H}$$

where λ_V and λ_H are the stretches in the vertical and horizontal directions, respectively.

d) Porosity test

The synthetic mesh and PCUU-T scaffold were observed under scanning electron microscopy (SEM) (EVO 10™, Zeiss, Deutschland) for topological analysis.

Scaffold samples of 3 mm × 6 mm were sputter-coated with 4.5 nm of Pd/Au. and stuck on specific holders with conductive adhesive.

Images (n=5/sample/group) were captured at 1000 × magnification with a desktop SEM. Pore size was measured using ImageJ software (National Institutes of Health, Bethesda, Md). Digital image analysis (number, spatial position, and density of the fiber intersections, connectivity distribution, fiber orientation angle, and diameter distribution) was utilized to fully characterize the microstructure of the scaffolds.[269]

A different algorithm was used to quantify the main angle of fiber orientation and the corresponding level of fiber alignment.

e) Degradation test

Six samples of each blend of PCUU-T were cut into 5 x 5 mm^2 pieces and stored in the 24-wall plate at -80°C overnight. The following day, the samples were freeze-dried at -110°C under vacuum for 48 hours. The weight (Wi) of each sample was recorded using a precision scale before and after the procedure. Degradation was evaluated through an accelerated hydrolysis test. All meshes were hydrolyzed in Chlorohydric acid HCl 3 Molar 3 ml at 37 °C for 24 hours on the tilting plate (80 rpm).

At each time point (0, 1, 2 days), the samples were washed using water three times and lyophilized overnight before recording the weight (Figure 10).

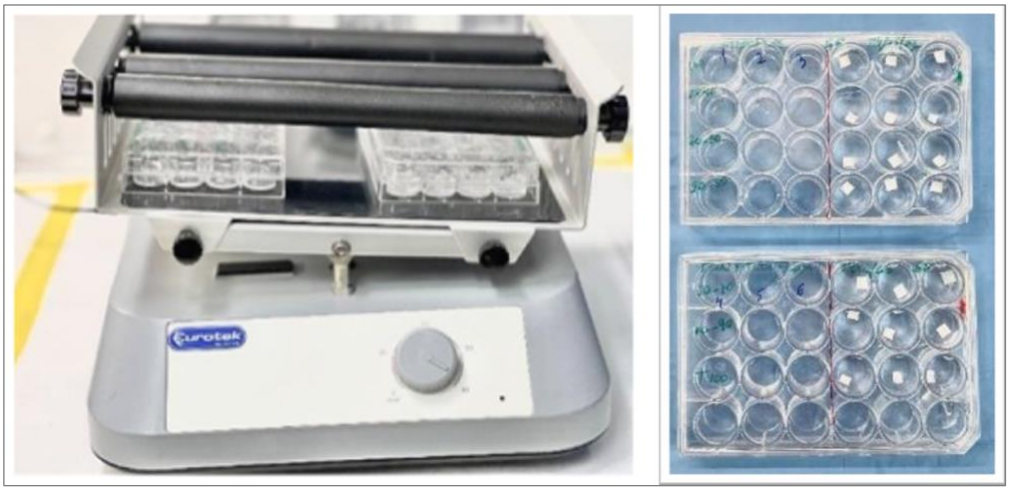

Figure 10: Degradation test. Plate 24 with samples inside.

Weight loss was calculated from the formula:

$$(Wf - Wi) \times 100 / Wi.$$ [263]

Where *Wf* stands for final weight and *Wi* for initial weight.

5. Preclinical Research. *In-vivo rat model*

a) Protocol

At the end of the two-week acclimatization period, rats were divided randomly into three groups of six rats each. They were fasted overnight (16 h) and subjected to general anesthesia with a mixture of ketamine and xylazine (70 mg/kg body weight and 2.1 mg/kg body weight, respectively).

b) Surgical Procedure

Surgery protocol: The experimental procedure was carried out on 18 healthy rats randomly assigned to three groups:

Group S: n=6 rats received smooth surface implants, covered by the PCUU-T on the left side and by Ultrapro™ mesh on the right side of the dorsum.

Group T: n= 6 rats received textured surface implants, covered by PCUU-T on the left side and by Ultrapro™ mesh on the right side of the dorsum.

Group M: n=6 rats without implants but received PCUU-T on the left and Ultrapro™ mesh on the right side -Control Group- (Figure 11) (Table 1)

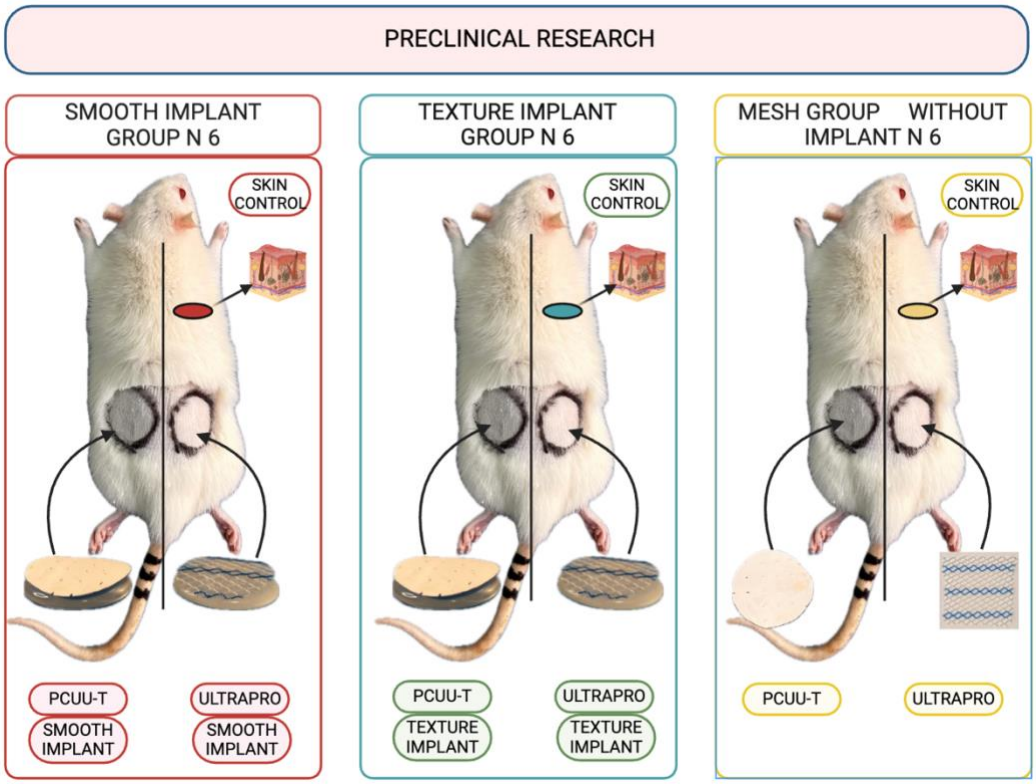

Figure 11: Scheme of the research in vivo experiment.
Source: Self-made scheme (SF)

Table 1: Group studied.

	Samples n=18 rats		
	Group S: Smooth breast implant n = 6	**Group T: Textured breast implant n = 6**	**Group M: Mesh Only n = 6**
PCUU-T left side	6	6	6
Ultrapro™ right side	6	6	6
Skin control	2	2	2

Each rat was anesthetized and maintained on a surgical plane[1]. After shaving and cleaning the dorsum with a povidone-iodine solution, sterile drapes were used to prepare the operative site. Bilateral paramedian 2,5 cm skin incisions were made on the dorsal area with N° 15 blade and scissor. The horizontal incision began 2 cm from the vertebral area,

[1] The skin rat is composed of different stratus from external to skeletal muscle: epidermis, dermis, and stratum adipose as the human, but the difference is the panniculus carnosus (vestigial in humans). It is a thin striated muscle layer intimately attached to the skin of most mammals, where it provides skin twitching and contraction functions, facilitating wound contraction and collagen formation. It is considered a functional part of the skin shaking off foreign bodies or stimuli and even plays a potential role in contractile-mediated shivering thermogenesis. The fibrous layer (stratum fibrosum) also absent in human skin, forms the lower boundary of subcutaneous tissue *(Note from the author SF)*.

between the middle and distal thirds of the animal's back. A 2.5 cm per 2.5 cm soft tissue was dissected, creating a subdermal pocket underneath the panniculus carnosus, taking care not to communicate them (Figure 12) (Figure 13).

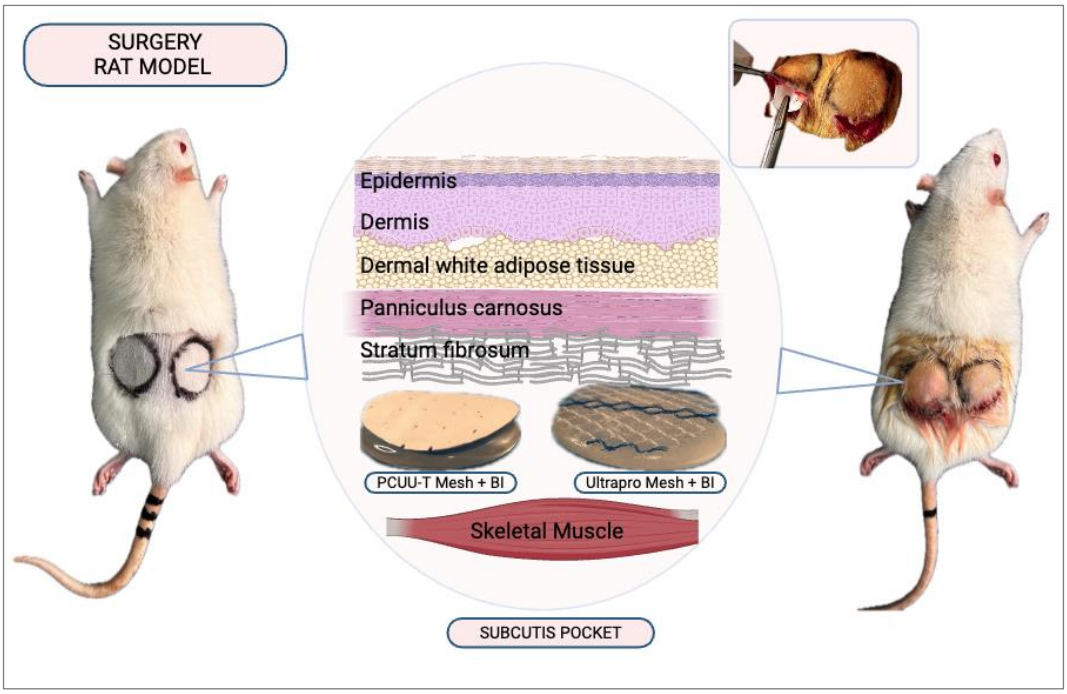

Figure 12: Graphic representation of the rat skin stratus that differs from human.
Source: Self-made scheme (SF)

Figure 13: Surgical Procedure. a) Rat with covered eyes for protection and dorsal shaving. b) Antisepsis surgical area c) Introducing implant and PCUUT mesh on the left and Ultrapro on the right side.

The mini-implants covered by PCUUT mesh were positioned on the left side, and the implants covered by Ultrapro™ mesh on the right side. The skin was closed, ensuring the incision was not over the prosthesis, using non-absorbable 5–0 Nylon monofilament sutures (Covidien, Dublin, Republic of Ireland) in a continuous fashion suture (Figure 14).

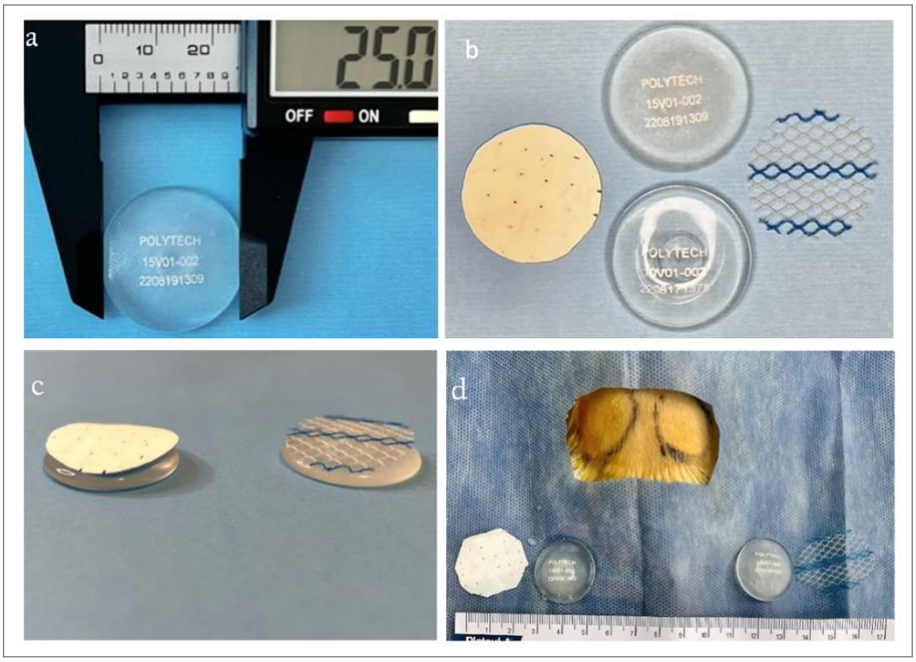

Figure 14: Breast Implant. a) Mini-breast implant Polytech™ 25 mm. b) Texture and smooth implant, PCUU-T and Ultrapro™ mesh. c) Mesh over the implant in the same position as into the pocket. d) Different implants and meshes in a sterile fashion.

Each rat was marked with a different color (blue, black, pink, and green) and line (1, 2, and 3) to differentiate each other. *In cage 1*, Smooth implant group, Rat Smooth (RS) (1, 2, and 3 black lines on RS1, RS2, and RS3, respectively, and 1, 2 pink lines on RS4, RS5). *In cage 2* Textured implant group, Rat texture (RT) (1, 2, 3 black lines on RT1, RT2, RT3 respectively and 1, 2 pink lines on RT4, RT5). *In cage 3* Mesh group without implant, Rat Mesh (RM) (1, 2, 3 black lines on RM1, RM2, RM3 respectively and 1, 2 pink lines on RM 4, RM5). *In cage 4*, we meet RS6 with one green line, RT6 with one blue line, and RM6 with one purple line.

The animals recovered from anesthesia under a heating lamp until normal activity was observed in each rat. During this period, animals had free access to food and drink. To compare the effects of the procedure on body weight, animals were weighed before and after the surgery (Figure 15).

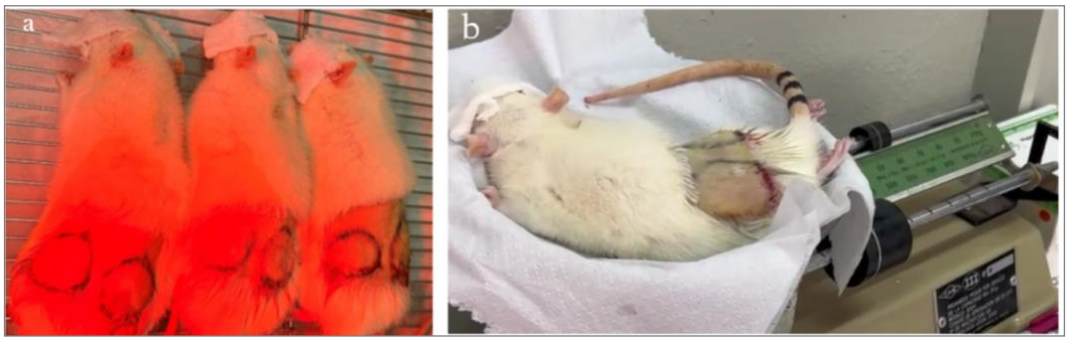

Figure 15: Immediate postoperative. a) Rats under red heater light. b) Rat weight measure after surgery.

Before the surgery, blood from the tail vein was collected, and serum was separated by decantation. Samples were centrifuged at 3.500 g for 10 min, and serum was prepared and frozen until further analysis.

The animals were allowed to eat a regular diet for the entire experiment, and antibiotic prophylaxis was not used (Figure 16).

Figure 16: a) Blood collection. b) Healthy rat group after surgery.

The animals were examined weekly for any evidence of hematoma, seroma, mesh or prosthesis extrusion, abscess, implant infection, or wound dehiscence.

After 63 days post-implantation and follow-up, animals were humanely euthanized with an excess of ketamine/xylazine, followed by exsanguination and chest opening.

c) Biopsy

The implant and surrounding tissue were removed in a block under sterile conditions. During explantation, macroscopic evaluation and photographic documentation of visible findings were recorded. After removing the implant, to have access and section quality by cutting the specimen, the excised tissue was sectioned into thirds and each of them in two to perform for histological studies in Argentina and Italy. The cut measure was 25 x 7 mm, parallel to the longest axis of the animal.

Not treated skin (control skin) was biopsied from the right scapular area, divided into thirds, and each in two.

One portion of each sterile capsule of all groups was sent to culture.

Samples were routinely collected and processed for histology. Three sections of each block (A: internal, B: medial, C: external) for each side from all animals were fixed in 10% paraformaldehyde buffered into the cassette for 24 hours, washed in 0,1 M phosphate buffer, dehydrated with ethanol solution at 50-75-90 and 100% following the histological

protocol overnight. Then, the samples were embedded in paraffin for histological analysis (Figure 17).

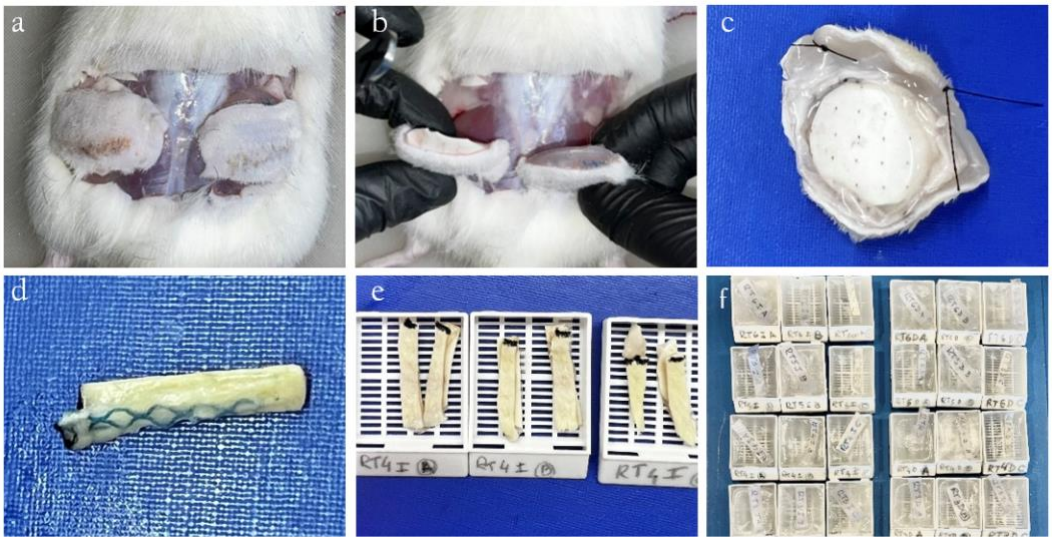

Figure 17: Biopsy procedure. a) Block surgical section (up cranial and down caudal). b) Immediate block section containing implant wrapped by capsule, mesh, and skin on both rat sides. c) View from the internal side. d) Biopsy section. e) Two sections per cassette and three for each side (internal, medial, external). f) All specimens in paraffin.

On the following day, samples were soaked in xylene for 45 min before embedding in paraffin for histological analysis (Figure 18).

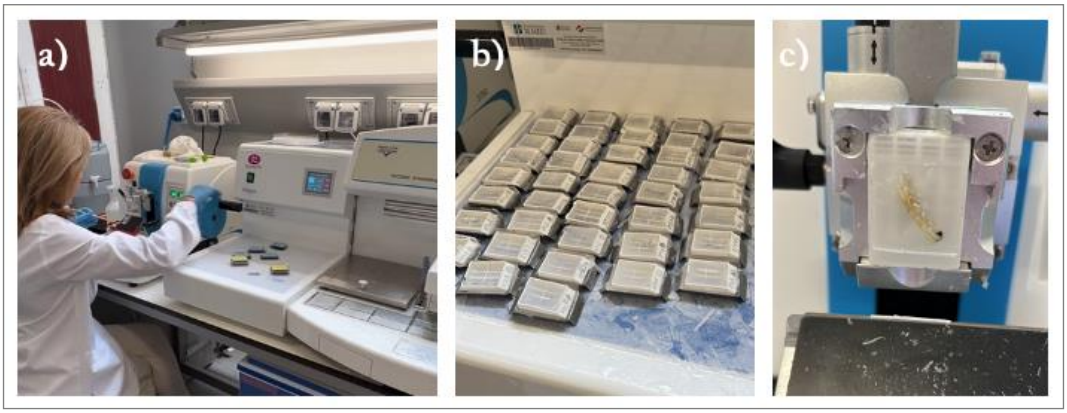

Figure 18: Histological process. a) Paraffin Station b) The cassette into the metal tray in the freezing station. c) Paraffin block cutting with the microtome.

d) Hematological parameters

To determine whether PCUU-T or Ultrapro™ mesh and implant had side effects, hematological and serum parameters were analyzed after 63 days compared with preimplantation parameters.

Blood was collected into EDTA-containing tubes, and plasma was prepared. Aliquoted plasma was stored at −80 °C.

Hematological investigation included blood glucose level (Glycemia), aspartate aminotransferase (AST/TGO), and alanine aminotransferase (ALT/ TGP) enzyme levels to determine liver function. Lipidic profile triglycerides (TG) and total cholesterol were analyzed. The results were compared with normal values in 77-day female Wistar rats. [264,265]

e) Ultrasound

Throughout the study, the animals were clinically checked and visually inspected by portable linear high-resolution color ultrasound Wireless, eco Doppler 7,5-10 MHz, depth evaluation 20 to 100mm (Gen 4 C10 CX, Beijing Konted Medical Technology Co., Ltd). All the ultrasonographic evaluations were performed by a single experimented examiner. Conventional transmission gel (Delva Laboratories, Argentina) was applied to the shaved skin above the implant, and a picture was taken longitudinally across the implant and parallel to the spine. Observations were performed of the outer margin of the implant at 15, 30, 45, and 60 days after implant insertion for signs of seroma formation (Figure 19).

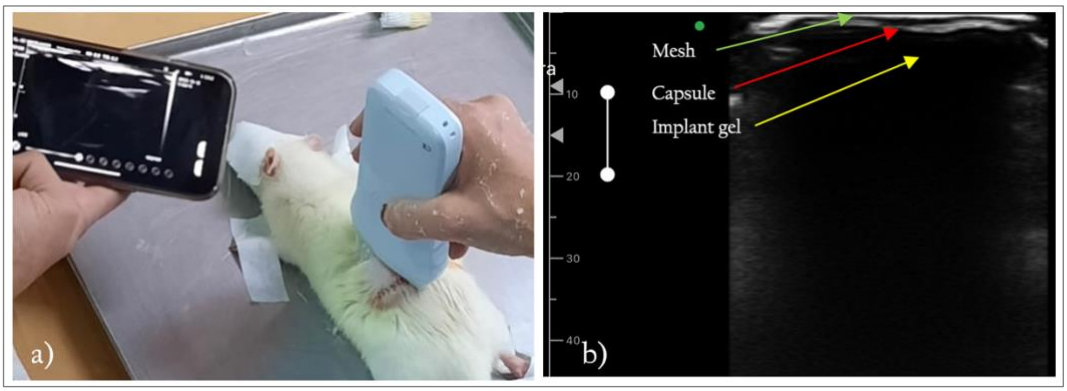

Figure 19: Ultrasound 10 MHz, clinical observation. a) Ultrasound immediate postoperative and weekly control. b) Normal postoperative ultrasound without liquid and normal capsule. Rat Smooth implant and PCUU-T mesh without seroma: red (capsule), green (mesh), and yellow arrow (implant gel).

f) Histology

The *inflammatory response* was graded with cellular counts of Lymphocytes, Plasmacytes, Eosinophils, Mast cells, multinucleated giant cells (MNG), and nucleus. *Vascularity* was evaluated by the number of capillaries per high-power field with hematoxylin and eosin (H&E) within the stratus fibrosum (subcutis) and the graft itself. Cellularity was counted manually and using ImageJ software. The results were compared between the 3 groups and control skin.[266]

(DAPI) 4′,6-diamidino-2-phenylindole, is a fluorescent stain that binds strongly to adenine–thymine-rich regions in DNA. In this experience, we used it to support the general nuclei results.

The *collagen organization* was graded by the presence of collagen tissue at the subcutis, and the graft site was examined by Masson and Gomori trichrome and Picrosirius Red stains (Figure 20).

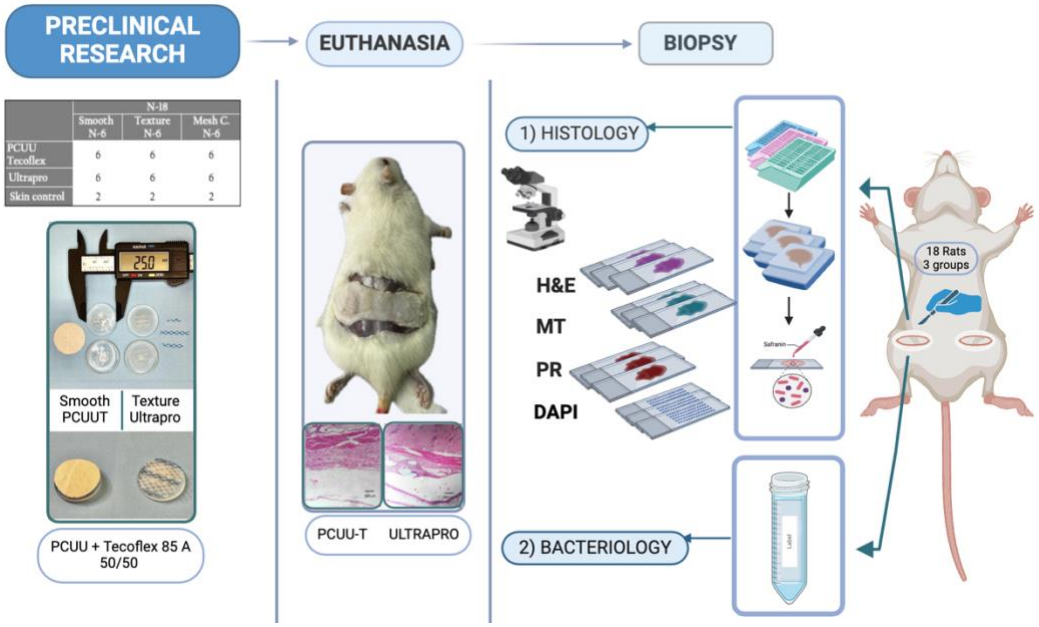

Figure 20: Diagram histology and Bacteriology. Left side PCUU T histologic preparation and process for general staining and Immunofluorescence. Sample for bacteriologic study. The same process is for the right Ultrapro™ side.

Source: Self-made scheme (SF)

The paraffin blocks were trimmed in 4 to 12 μm with the microtome (ARM3750 Histo-line Laboratories) mounted onto glass slides and prepared for different staining.

For each block, three slides were prepared, with two sections for hematoxylin and eosin for general morphological analysis, the same for Masson's trichrome and gomori, and Picrosirius red for collagen organization analysis. A total of 1404 slides were prepared in Italy and 432 in Argentina.

Sections were imaged at 4, 10, 20, and 40X magnifications and analyzed using Nikon Eclipse Ts2R NIS Advance Modulation Inverted Research Software Epifluorescence (Nikon, Tokyo, Japan) in Italy. The Olympus BX 40 adapter U-SPT (Japan) was used in Argentina at 5, 10, 20, and 40X magnifications.

Hematoxylin and eosin staining. The specimens were deparaffinized at 37°C overnight and then hydrated by a scale of alcohols (100%, 95%, 75%, 50%). Sections were stained with H&E (Biognost Ltd, Croatia. EU) Italy and Hematoxylin (Biopur diagnostic, Rosario, Argentina) and for Eosin (BioPak, Buenos Aires, Argentina) used in Argentina, following manufacturer instructions and RiMed protocol. Stained slides were dehydrated using a graded series of ethanol solutions (50, 75%, 95%, 100%) before

coverslipping. A total of 405 slides were evaluated at (4x, 10x, 20x, and 40x) magnification in each H&E section in Italy and 126 in Argentina. For quantification, sections were photographed.

The criteria used to quantitatively evaluate the histomorphology of the specimens included *Cellular infiltration* graded with cellular counts of chronic inflammatory cells to include plasma cells, lymphocytes, mast cells, eosinophils, and multinucleate giant cells (MNGC).[266] Those elements (lymphocytes, plasmacytes, etc.) that constituted the granuloma were assessed collectively and not individually counted. *Vascularity* was evaluated by the number of capillaries identified per high-power field (HPF).

The histological evaluation did not include animals with complications such as implant extrusion, wound dehiscence, or contamination.

The total number of each cell and vessel per field of view (FOV) was manually quantified at 40X magnification by the pathologist. The grid was added to the light microscope to count the cells. Every slide was counted in 19 fields. The standard criteria were used to include and exclude cells. For nuclei that fall on the grid boundary, exclude those that lie on the left and bottom boundary, but include those that lie on the top and right boundary. The general nucleus into the stratus fibrosum and mesh was also counted in ImageJ software to register the increasing general cellular number and compare it between the groups. Image J software (National Institute of Health)[267] was used to analyze the total number of slides for the three groups and the control skin at 20x magnification, using the Plugins Color Deconvolution2[268] and Threshold Toolbox to analyze particles. Two slides from PCUU-T and Ultrapro™ side from each rat were measured, including 98 images in H&E. The average and standard deviation were registered.

Masson Trichrome (MT) and Gomori Trichrome (GT). They were performed to assess the collagen. A collagenous layer was defined between the muscular layer (panniculus carnosus) and the mesh (included in the observation). The collagen intensity was measured in terms of percentage.

After deparaffinization and hydration, the sections were stained with Masson trichrome in Italy (Histo-Line Laboratories SRL, Milan, Italy). Gomori Trichrome one-step fast green, used to distinguish between collagen fibers in green and muscle in tissue sections (BioPak, Buenos Aires, Argentina), was used in Rosario, Argentina.

Picrosirius Red (PR). To assess the quantitative percentage of collagen, a picrosirius staining was also performed in the Morphologic Laboratory of the National University of Rosario. A collagenous layer was defined between the muscular layer

(panniculus carnosus) and the mesh. 81 glasses of 4µm slides were prepared. After deparaffinization and hydrating, the specimens were stained with a Picrosirius Red kit (Direct Red 80 Fluka) in Argentina, following the protocol.

The sections were examined under an optical microscope (Olympus, Japan), and images were captured with an Olympus U-SPT camera (Olympus, Japan) at a magnification of 10 times, for a total of 162 photos.

The slides were analyzed by Image J (National Institute of Health) using the Plugins Threshold color IHC Toolbox for color segmentation to measure the collagen (Figure 15).[269,270]

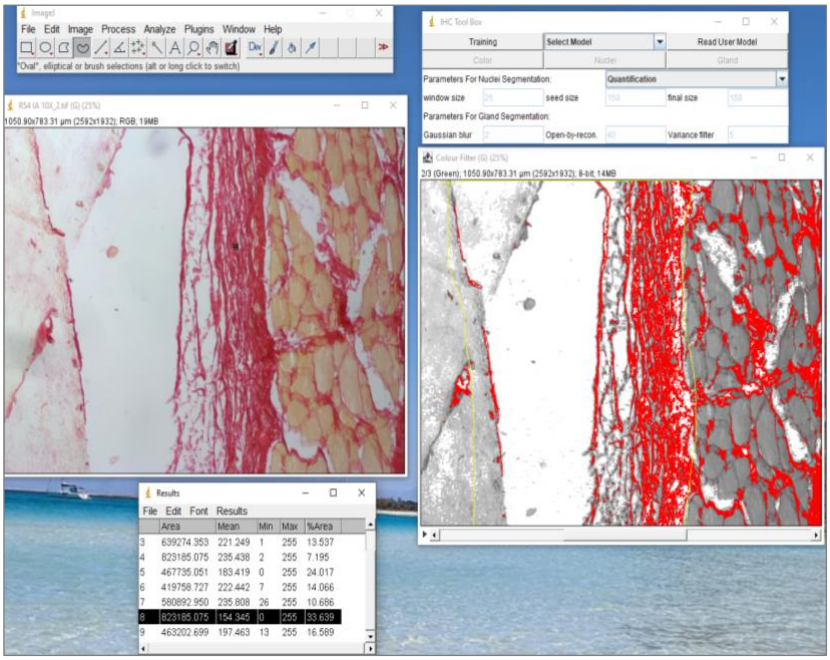

Figure 15: Image J software Using Plugin Threshold color IHC toolbox to acquire and select images to count. Picrosirius Red staining at 10x.

DAPI was utilized to provide nuclear staining (5 mL/section, DAPI H-1200; Vectashield).[271,272] To analyze cellularity, the nucleus between the end of the panniculus carnosus, including the mesh, was evaluated in 18 slides (Figure 16). DAPI immunofluorescence images were compared with H&E. Also, it was counted in ImageJ software to register the general cellular number increase between the subcutis and mesh.

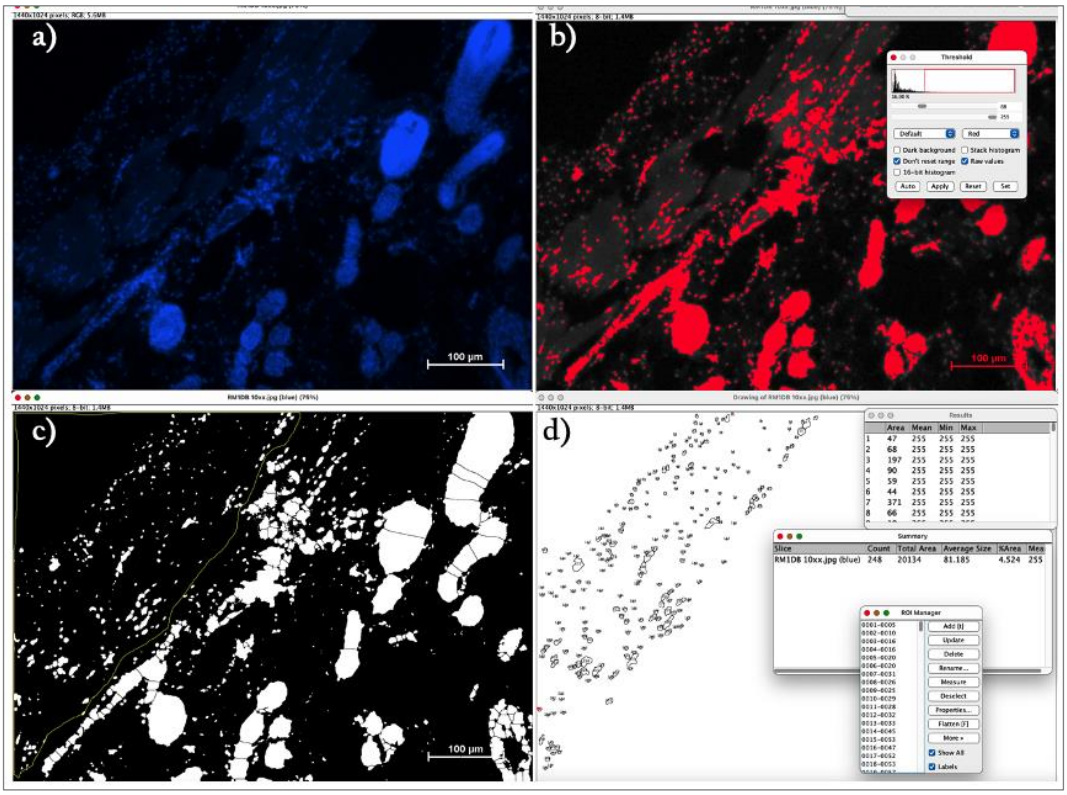

Figure 16: Representative process of nuclei counting by ImageJ in DAPI staining at 10x. a) First step: Split channel to obtain 3 images (blue, red, and green). b) Adjusting thresholding to fill the nucleus in red and then in white. c) Splitting big images (watershed) and selecting the area to count the nucleus (yellow) after the muscle to the mesh. d) Analyze particles, obtaining the results and summary of the nucleus number.

g) Bacteriology

One block of skin and mesh from each animal was cut into small pieces under sterile conditions and placed in 5.0 mL of saline solution. They were agitated on a vortex mixer for five minutes. A portion of the specimen was prepared on the slide for Gram-Nicolle staining and microscopic observation. Another was incubated for aerobic culture in 5% blood agar and Brain Heart infusion Broth for 24 hours. The third was placed on an agar plate of anaerobiosis for 48 hours. The last portion of the processed material was placed in Agar Sabouraud dextrose Britannia to perform Mycological Culture.

6. Statistical analysis

Statistical analysis was conducted using Sigma-Plot™. A one-way analysis of variance (ANOVA) was applied to compare different samples. Data were considered statistically significant with a value of p below 0.05, and differences between groups were compared using the Tuckey t-test. Each test was developed in triplicate. In all tests, a P-value <0.05 was considered statistically significant.

RESULTS

1. Synthetic Mesh Characterization

a) Thickness

The measurement was done in 13 points using 5 samples of each synthetic mesh; the result was Ultrapro™ 556.8 µm, Vycril™ 186.5µm, Tigr™ 620.9 µm, Tiloop™ 221.8 µm, and Galaflex™ 663.6 µm. The average was 449,95 ± 196,62 µm (± SEM). The thickness distribution is shown in the plot graph (Figure 1). The different colors represent a homogeneity map, where the colors are more homogenous. This means that the sample has the same thickness in the whole surface tested, where the color changes, meaning they are not homogenous in thickness.

An ANOVA test determined a significant difference between them (P<0.001): Galaflex™, Ultrapro™ , and Tiger™ meshes (with similar mean between them) had significantly higher thickness than Vycril™ and Tiloop™ (similar between mean) (P<0.001 of Tuckey test).

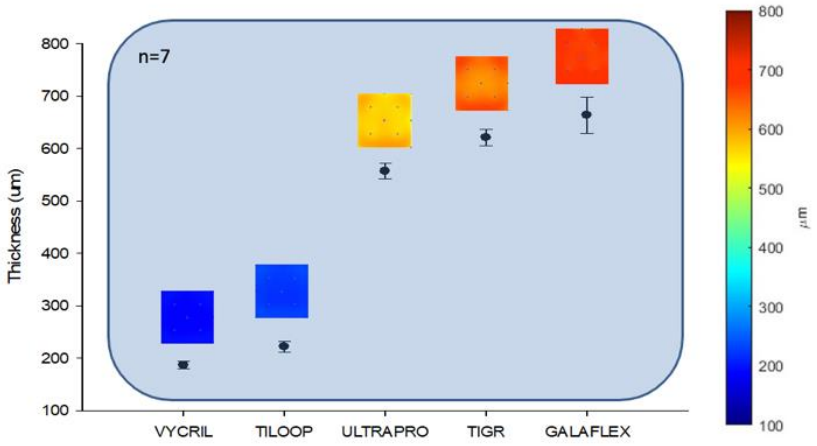

Figure 1: Plot graph of thickness (µm) in five synthetic meshes. The uniformity of the color represents the thickness homogeneity.

When we compared our outcome (black bars) with those we searched in the previously published literature (gray bars), the results were quite similar (Figure 2).

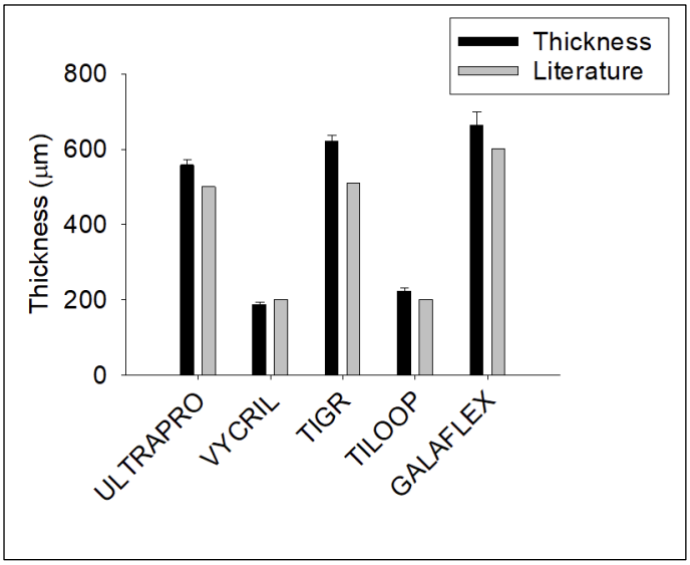

Figure 2: Synthetic mesh thickness comparison between the present study and published literature.

b) Density

The measurement was made in 5 samples of each synthetic mesh. The result was Ultrapro™ 54,6 g/m^2, Vycril™ 50 g/m^2, Tigr™ 165 g/m^2, Tiloop™16,4 g/m^2, and Galaflex™153 g/m^2. The average was 87,76 ± 62,84 g/cm^2, as shown in the plot graph, compared with our finding in the literature reference (Figure 3). Comparing the lightweight distribution, an ANOVA test determined a significant difference between them (P<0.001): It was identified three groups of similar density each: Galaflex™ and Tigr™ meshes, Ultrapro™ and Vycril™ meshes, and the last, Tiloop™, with significantly lower density than the other groups; P<0.001 of Tuckey test.

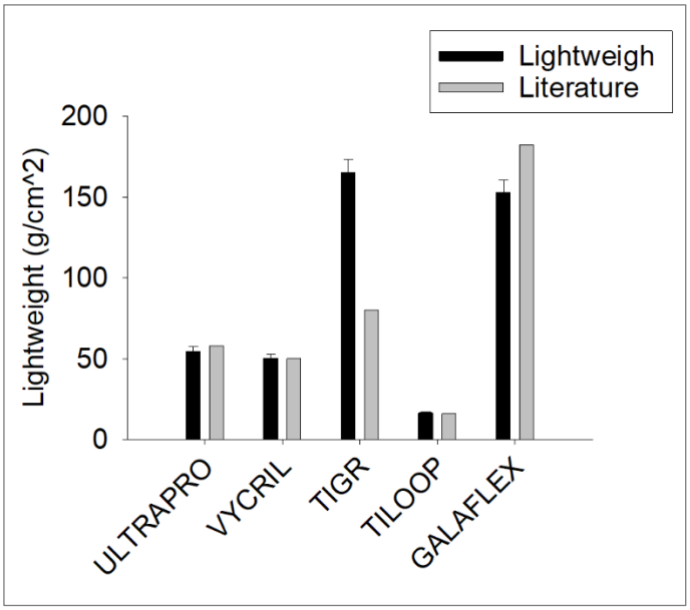

Figure 3: Density synthetic meshes comparison. Outcomes of the present study and the published experiences.

c) Mechanical

A uniaxial tensile test was performed on the commercial synthetic meshes in horizontal and vertical directions (6 samples of each brand) and averaged to obtain the measure of Young Modulus (MPa). In the vertical direction, the Vicryl™ was statistically stiffer compared to the other materials, with no statistical differences among groups. In the horizontal direction, Ultrapro™ was statistically stiffer compared to other materials. Tiloop™ was statistically stiffer than Vicryl™, TIGR™, and Galaflex™ while less stiff than Ultrapro™. Vicryl™ was statistically equivalent to TIGR™ and Galaflex™. TIGR™ was statistically stiffer compared to Galaflex (Figure 4).

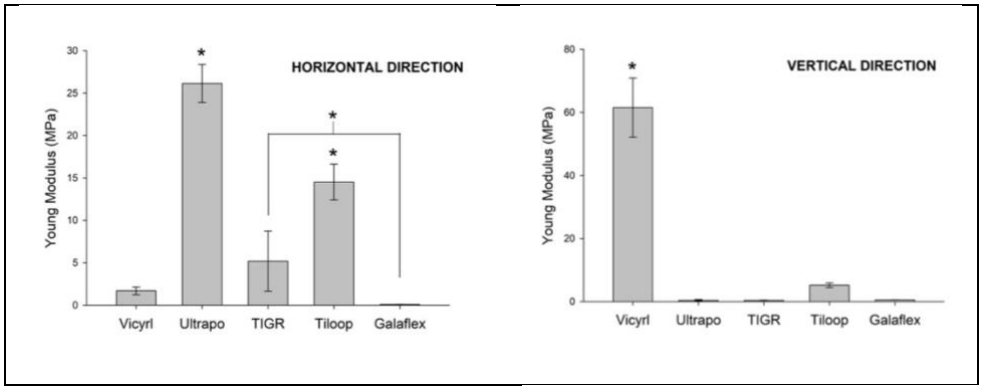

Figure 4: Young Modulus (MPa) of the synthetic meshes. Tensile test.

d) Porosity

Twelve samples of each synthetic mesh were measured in SEM. The distribution of porosity (in μm²) in each mesh is shown in the plot graph (Figure 5). Comparing the pore distribution, an ANOVA test determined a significant difference between them (P<0.001): It was identified that Ultrapro™ had a porous area significantly higher than the rest of the synthetic mesh (P<0.001; P<0.001) on the Tuckey test.

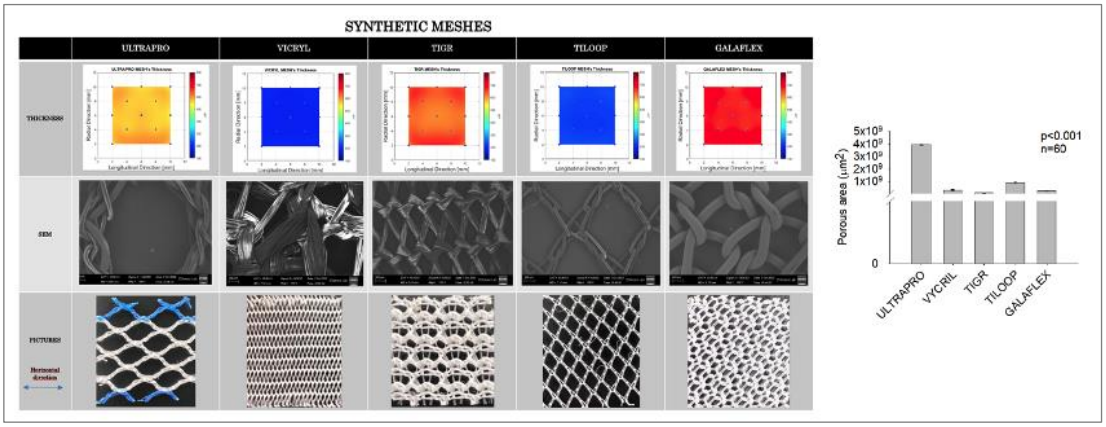

Figure 5: Commercial mesh comparison. The superior file shows the thickness. The middle file shows the pore size observed at the SEM**.** The last file shows the pics of each synthetic mesh. Graphic of pores area (en μm²) in five synthetic meshes.

2. PCUU and PCUU-Tecoflex™ fabrication

Poly (carbonate-urethane) urea (PCUU) is a biostable and degradable mesh. To increase PCUU's (Y modulus 2MPa) mechanics, we have prepared different blends with Tecoflex™ 85a non-degradable (Y modulus 9MPa).

Therefore, the present research has evaluated PCUU blended with Tecoflex™ in different percentages; the PCUU-TecoflexTM ratio (PCUU-T) was 100:0, 90:10, 70:30, 50:50, 30:70, 10:90, and 0:100.

To determine the optimal blend of PCUU-T, the mechanical characteristics of different blends were evaluated in terms of thickness, density, mechanical, porosity, and degradation tests. Table 1 shows the fabrication of a PCUU-T blend at different percentages of its components and parameters. The optimal blend to obtain the highest thickness is written in red.

Table 1: Parameters of PCUU and Tecoflex blend fabrication.

Name fabrication	Flow rate (ml/h)	Voltage (kV)	Gap Distance (cm)	RPM	Mandrel size (cm)	Volume (ml)	Transverse speed (mm/s)	Transverse Distance (mm)	Deposition time (min)	Thickness (μm)
PCUU 100%	5	17	10	500	1	5	30	100	45	257
PCUU-T 90-10%	5	17	10	1500	1	4	30	100	45	219
PCUU-T 70-30%	5	17	10	1500	1	5	30	100	45	275
PCUU-T 50-50%	**5**	**17**	**10**	**1500**	**1**	**5**	**30**	**100**	**45**	**374**
PCUU-T 30-70%	5	17	10	1500	1	4	30	100	45	198
PCUU-T 10-90%	5	17	13	750	1	5	30	100	45	165
Tecoflex 100%	10	20	20	1500	1	8	8	70	45	136

a) Thickness

The thickness distribution of different concentrations of PCUU-T is represented in the plot graph in Figure 6. The best thickness of 374 μm was obtained with a blend of PCUU/Tecoflex 50:50.

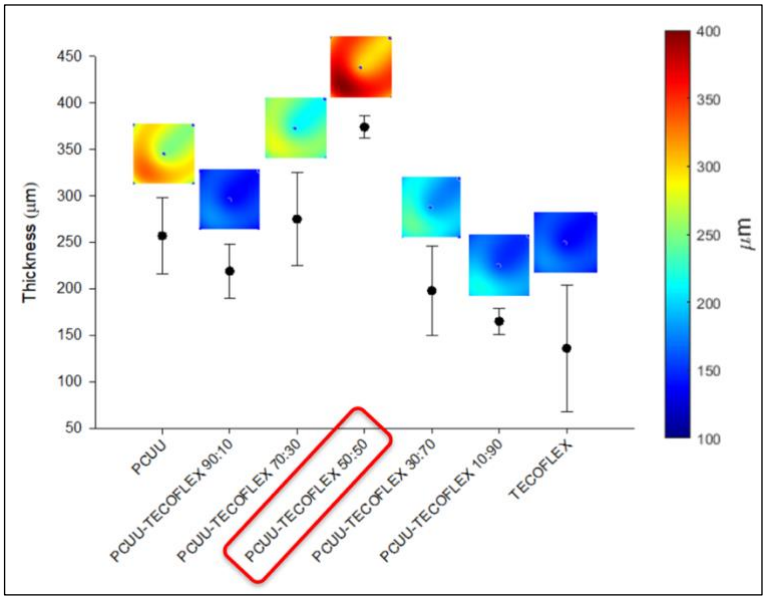

Figure 6: Thickness (µm) plot graph of PCUU-T at different concentrations. The uniformity of the color shows the thickness homogeneity.

b) Density

The PCUU-T weight was 46,33 mg ± 3,78 mg, and the media of weight loss after the accelerated hydrolysis test at 3 days was 24,5%.

c) Mechanical characterization

Blends were analyzed in terms of anisotropy ratio through biaxial testing.[130] The Anisotropic Ratio of PCUU-T 50/50 was 2,14. Comparing the anisotropic ratios for the different blends, PCUU 100% has a higher statistical anisotropic ratio, while other groups did not exhibit significant differences. The stiffness in vertical and horizontal directions was analyzed, but there were no statistically significant differences among the blends (Figure 7).

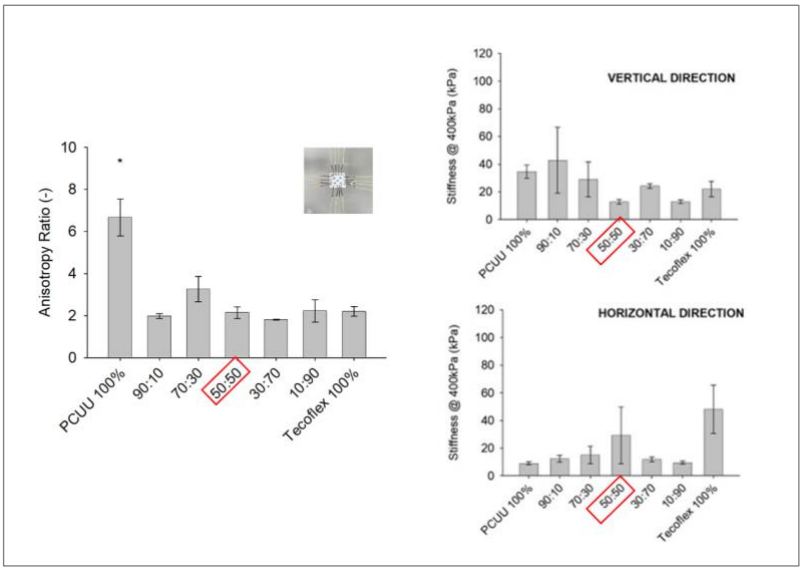

Figure 7: Biaxial properties of PCUU and Tecoflex different blends. Anisotropy ratio and stiffness in vertical and horizontal directions were reported.

d) Porosity

The fiber morphology of each blend was analyzed via SEM (Figure 8). The porosity area on the PCUU-T 50/50 was 4.708 ± 1.919 μm, microfiber 8,29 ± 1.94 μm. It was possible to observe alignment fibers in all blend concentrations. It was qualitatively assessed that increasing Tecoflex™ content to the formulation increases fiber diameter size (Figure 9).

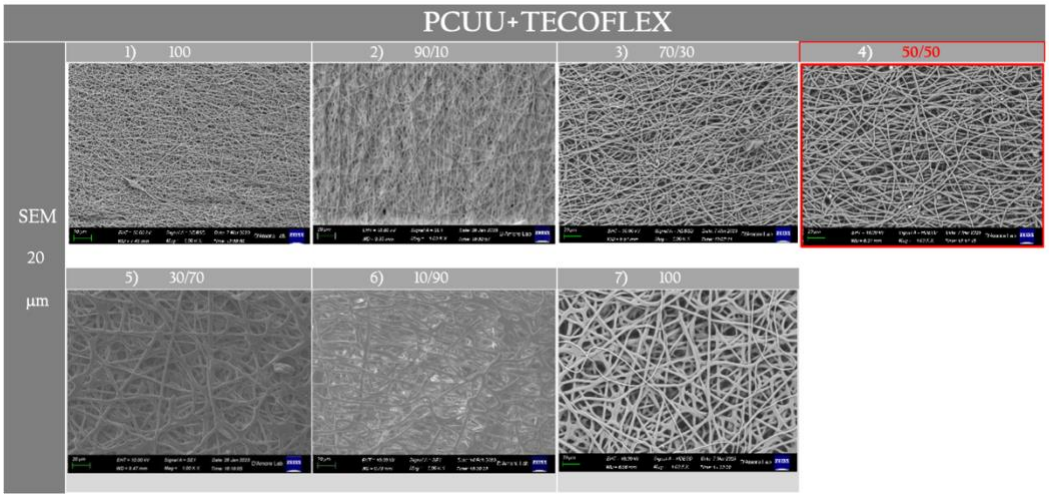

Figure 8: SEM images PCUU-Tecoflex™ at different concentrations and 20 μm. The red rectangle shows the image of the most optimal PCUU-Tecoflex™ blend.

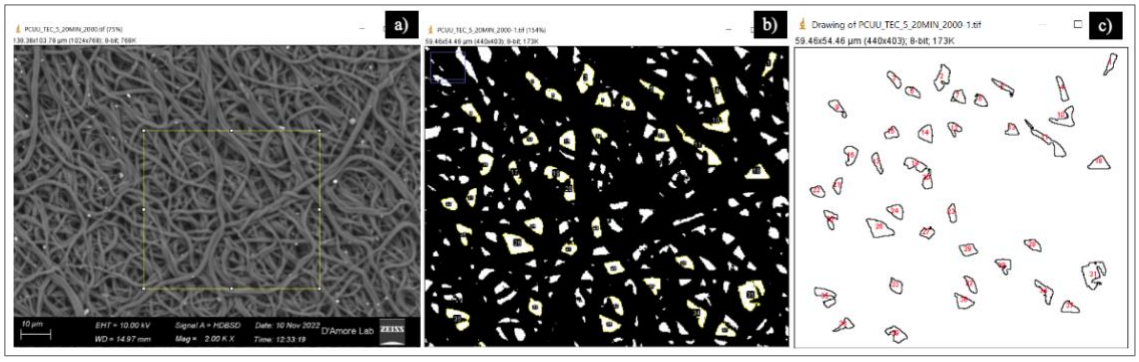

Figure 9: PCUU-T measures pore size using ImageJ software. **a)** Squared selection in yellow to measure on SEM. **b)** Threshold pores selection. **c)** Image in black and white to count the number and pore size.

e) Degradation test

The degradation rate was used as one of the main features to identify the blend with less degradation. Specifically, it was observed that weight decreased significantly in all blended concentrations during the initial 1 day and 3 days ($P<0.05$). The *PCUU and Tecoflex™ 50/50* evidenced less percentage of degradation in comparison with the other concentrations without statistical differences ($P>0.05$) and therefore it was selected as the *ideal blend* for preclinical purposes and will be mentioned in the next paragraphs of this thesis as PCUU-T (Figure 10).

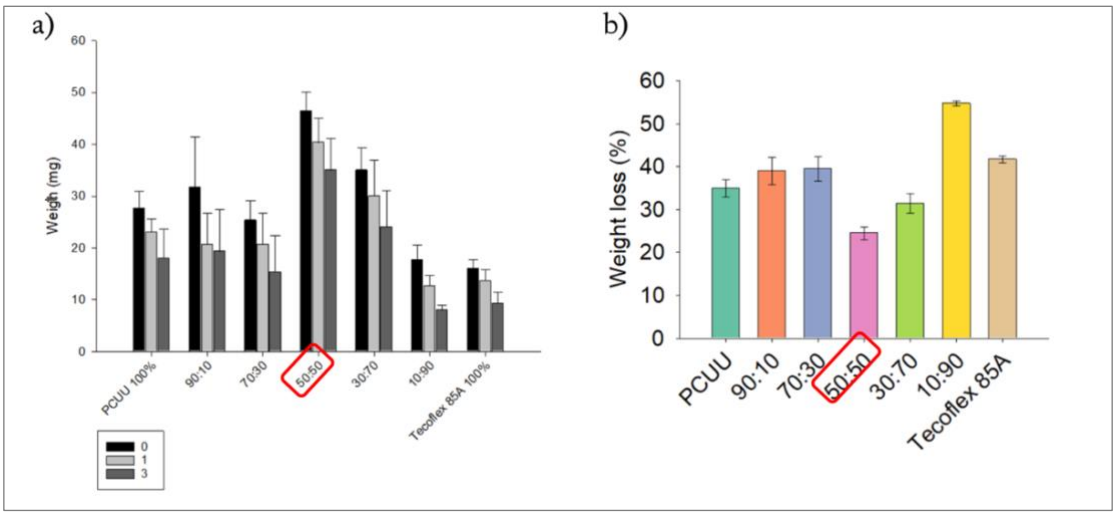

Figure 10: Degradation test. a) Different blend concentrations; weigh at 0, 1, and 3 days. b) Weight loss in % on different blend concentrations.

3. Characteristics of PCUU-T designed mesh

After evaluating the mechanical characteristics of different blends of PCUU and Tecoflex™, it was concluded that the most optimal blend of PCUU-T is the one with equal amounts of both components (Table 2).

Table 2: Parameters of 50/50 PCUU-T designed mesh.

Properties 50/50PCUU-T	
Thickness	374 μm
Anisotropic ratio	2,14
Tensil Peak tension	3.61 N/cm^2
Tensil Peak strain	0.03%
Microfiber (SEM)	8.29 μm
Porosity	4.71 μm
Weight	46.33 mg
Weight loss	24.46 %

4. Preclinical experimentation

The experimental procedure was carried out at the Universidad Abierta Interamericana (UAI) and the Universidad Nacional de Rosario (UNR), both in Argentina, with n=18 adult female rats.

Two subdermal pockets in the dorsum rats were performed. The experiment was divided into three (3) groups that included 6 rats in each one. Each group received PCUU-T mesh on the left and Ultrapro™ mesh on the right. In the first group, Smooth **(S)**, the rats received smooth mini-breast implants per side. In the second group, Texture **(T),** rats received textured implants per side, and in the third group, Control mesh **(M),** rats

received mesh but not implants. Also, we removed the skin without treatment from the other area as a control skin, 2 biopsies for each group.

a) Weight

On a presurgical day, n=18 Wistar rats (70 days old) weighed an average of 231.39 ± 9.29 g (± SD) (range: 213-250g), increasing on the same day after surgery up to 233.44 ± 9.02 g (range: 215-253g), without statistical differences (P>0,05). But on day 63rd, before euthanizing, they weighed an average of 281.89 ± 14.75 g (range: 255-310 gr), a difference of 48,45 g (21%) significantly higher than postoperative day weight. This result shows healthy rats. (P<0.05) (Figure 11).

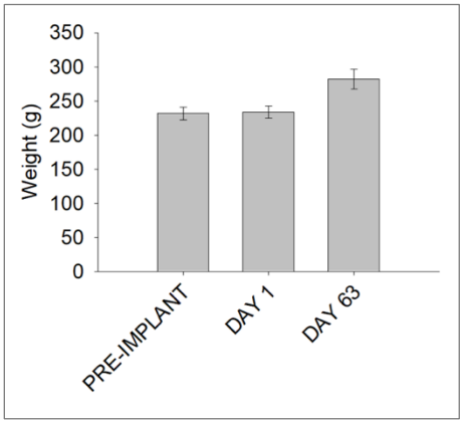

Figure 11: Measurement of weight of rats (in grams) at day 1 (pre and postoperative) and at day 63 before euthanasia.

b) Ultrasound

Ultrasound and clinical evaluation were performed at 15, 30, 45, and 60 days to evaluate seroma formation as an inflammatory reaction. There was no liquid accumulation below the skin or peri-implant on both sides of rats from the Smooth, Texture, and Control M groups (Figure 12).

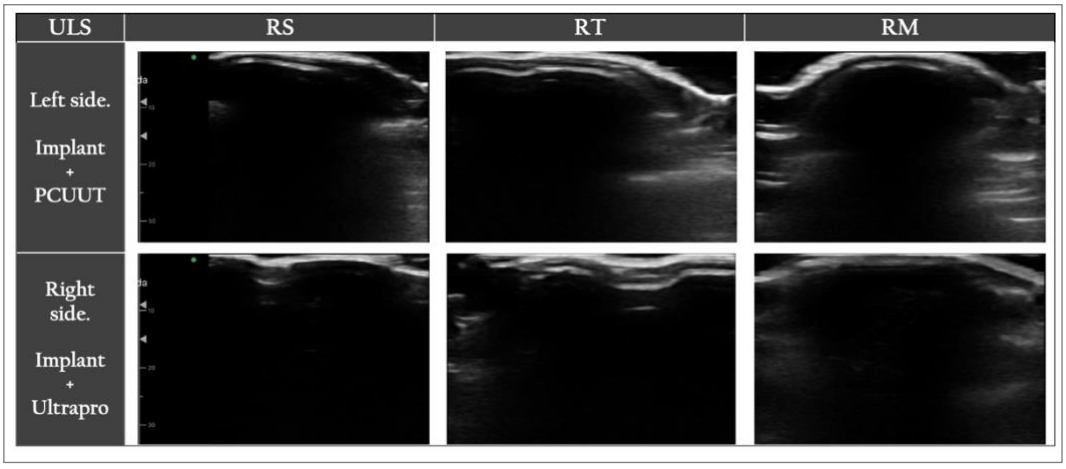

Figure 12: Ultrasound at 60 days. Dorsal images of Smooth, Texture, and Mesh control groups on the left (PCUUT mesh) and right side (Ultrapro mesh).

c) Hematological results

To determine whether mesh and implant had side effects, hematological and serum parameters were analyzed after preoperative and at the postsurgical 63rd day.

Considering that Wistar female rats were obtained under the same housing conditions, sex, and age.[273] Group S showed slight differences in some hematological parameters (cholesterol, aspartate transaminase, and alanine transaminase) compared with reference values. However, there was no difference between pre- and post-values in all those parameters; Group T and M remained statistically unchanged (Figure 13).

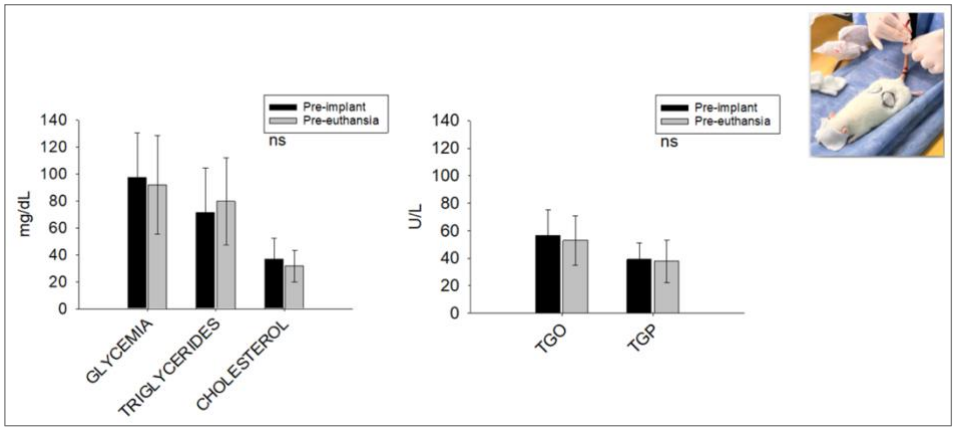

Figure 13: Hematological level analyzed on the three groups in the pre and postoperative 63 days.

d) Clinical examination

At all-time points (15, 30, 45, and 63 days) macroscopic evaluations showed 32 (89%) rats with no complication, 3 (8%) wound dehiscence on the PCUU-T side (2 in the S group with implant loss, and 1 in the T group). One rat in the T group had wound dehiscence on the Ultrapro side (3%) (P=0.61 between PCUU-T and Ultrapro™, without statistical significance). None of them were in the M group (Figure 14). There were no other local adverse effects for each group and no biologically significant differences in the postoperative course.

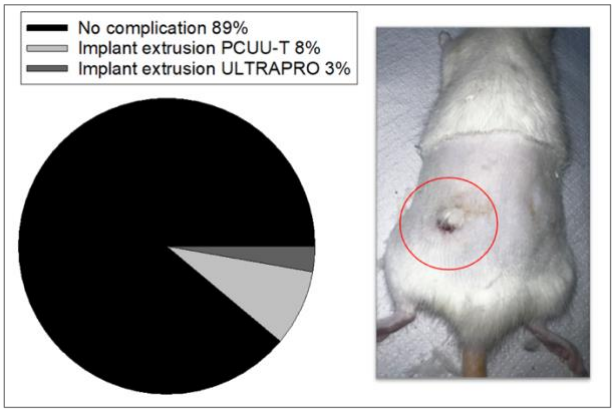

Figure 14: Postoperative extrusion implant complication in PCUU-T and Ultrapro side.

e) Histology

After euthanasia, a general evaluation by microscopy was initially performed, comparing the skin and subcutis structure of PCUU-T (left side) and Ultrapro™ (right side) meshes with the control skin after 63 days of the implantation (Figure 15).

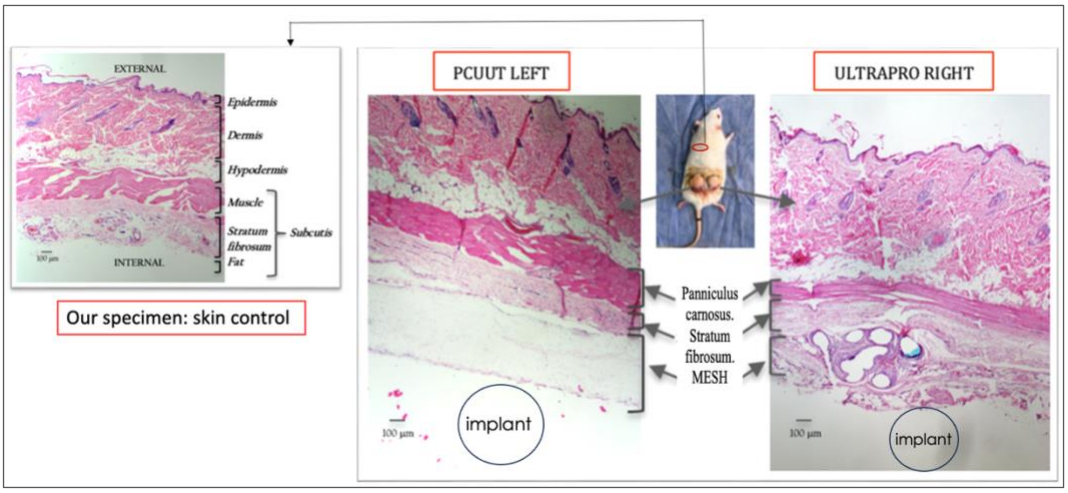

Figure 15: Hematoxylin-eosin staining of the skin. Layers: Epidermis, dermis, hypodermis, and subcutis (panniculus carnosus or muscle and stratum fibrosum). Structure comparison of normal skin, PCUU-T (left side), and Ultrapro™ (right side) showing tissue incorporation (cross-section) in the mesh. The prosthetic filaments (blue polypropylene) are surrounded by scar tissue.

Morphometric analysis.

On the *PCUU-T side*, the findings were similar to those observed in control skin. Despite having observed plasmacytes and lymphocytes on the observation, the foreign body-type giant cell reaction associated with the mesh was not observed. No important apparent inflammatory process was identified. Only eosinophils and mast cells were identified, which in some cases appeared to be increased in number and are normal in the rat skin. The vascular component had characteristics similar to those of the control group (multiple vessels, mostly small caliber), showing congestion in some samples. Variable low fibrosis was observed on the periphery, surrounding the implanted material. PCUU-T mesh maintains structural integrity in vivo after 63 days.

On the *Ultrapro ™ side,* below the panniculus carnosus, there was an evident foreign body-type giant cell reaction to odd material (mesh), forming granulomas associated with central polymorphonuclear infiltration surrounding the prosthetic filaments. Chronic inflammatory infiltration of lymphoplasmacytic type in mild/moderate grade and a regular number of eosinophils cells was evidenced. Vascular congestion and hemosiderin deposits were observed. Mild fibrosis was recognized on the periphery, surrounding the implanted material (Figure 16).

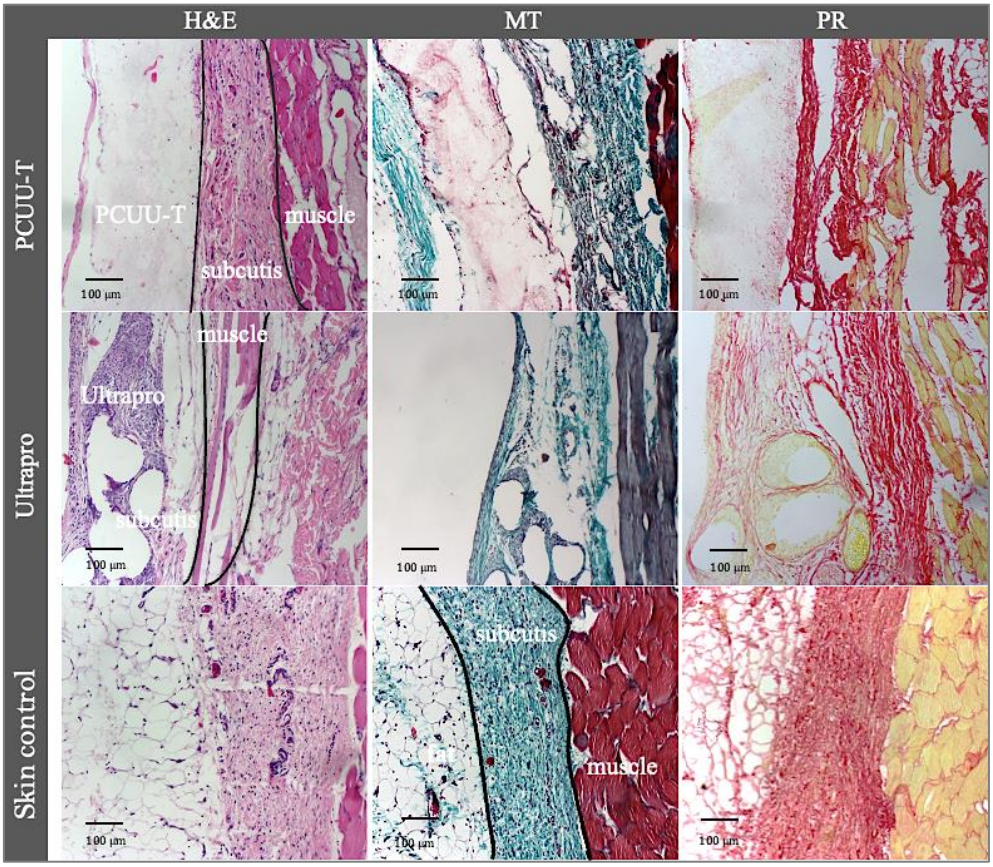

Figure 16: Representative cross-section, 63 days of PCUU-T, Ultrapro™, and skin control samples on the same animal. Microscopic evaluation of Hematoxylin & Eosin, Gomori trichrome, and Picrosirius red staining. Magnification 10x scale bar indicating 100 µm. PCUU-T mesh maintains structural integrity.

Tissue Integration and Angiogenesis.

The Pathologist was responsible for observing, analyzing, and manually counting. Nineteen (19) high-power fields 40x in H&E staining were analyzed in every slide. Previously, the fields were selected for panoramic magnification, focusing on the highest inflammatory process spot (selection of hot spots) (Table 3) and (Figure 17).

Table 3: Comparison and representation of cellular infiltration on each group in HPF (40x) per mm².

number/mm²	Control skin	PCUU-T mesh mean ± SD	Ultrapro™ mesh mean ± SD
Giant cells			
Group S		0	51.3 ±1 1.7
Group T	0	0	42.0 ± 3.2
Group M		0	34.3 ± 4.8
Plasmacytes			
Group S		17.0 ± 4.3	82.0 ± 17.5
Group T	1	96.7 ± 35.2	161.3 ± 28.1
Group M		193.3 ± 108.7	61.3 ± 17.7
Lymphocytes			
Group S		17.3 ± 8.6	463.3 ± 21.3
Group T	15.3	83.0 ± 35.0	285.0 ± 68.0
Group M		48.3 ± 20.4	179.0 ± 9.0
Eosinophils			
Group S		84.0 ± 17.9	104.0 ± 19.5
Group T	340.0	147.3 ± 20.0	121.0 ± 5.4
Group M		198.0 ± 18.6	65.0 ± 4.1
Mastocytes			
Group S		28.0 ± 6.4	5 ± 1.5
Group T	43.0	19.3 ± 4.9	5 ±2.6
Group M		45.0 ± 8.3	21.7 ± 5.6
Vessels			
Group S		321.0 ± 33.9	334.7 ± 3.1
Group T	241.0	328.7 ± 13.2	245.3 ± 24.9
Group M		304.3 ± 23.7	425.7 ± 51.5

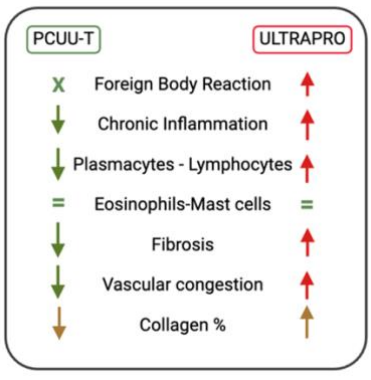

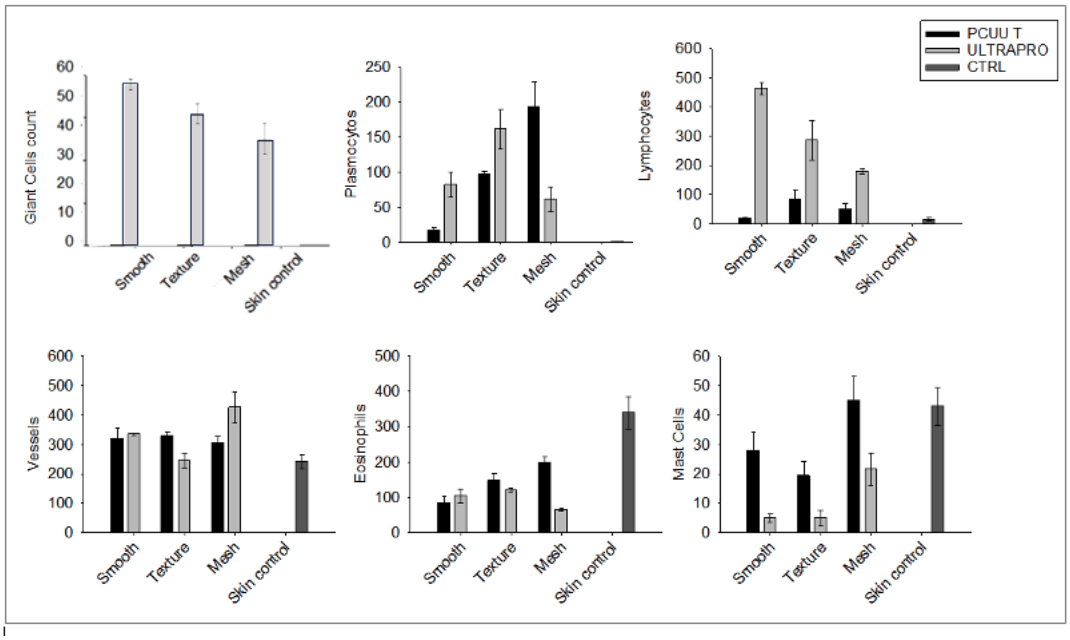

Figure 17: The chart plot shows *giant cell response* only on the Ultrapro side more in Smooth implant. There is a higher level of *plasmacytes* (Plasma cells) in all groups treated than in the skin control group, and the highest level of *lymphocytes* is found in the Ultrapro mesh with smooth implant. There is a high level of *eosinophils* in the control skin. There is a high level of *mast cells* in PCUU-T, like the control skin. There is a similar quantity of *vessels* in the three groups and the control skin, although it appears Ultrapro without implant presents more vessels.

Foreign Body Reaction. Giant cells. No giant cells were found on either the PCUU-T side or in all groups (S, T, M) or the control skin samples. These types of cells were observed only on the Ultrapro™ mesh side. Ultrapro™ meshes placed over smooth implants (Group S) had significantly more giant cells than those placed over textured implants (Group T) ($P<0.05$) (Table 3) (Figures 17 and 18).

Plasma Cells/ Plasmacytes. As a normal population, one (1) plasma cell per mm² was quantified in the skin control without any treatment. The mesh group without implants (Group M) showed a significantly higher amount of plasmacytes than the skin without treatment ($P<0.05$). The tissues from the PCUU-T mesh side showed significantly fewer plasmacytes than those from the Ultrapro side, both in those placed on smooth implants (Group S) and textured implants (Group T) ($P<0.05$) (Table 3), (Figures 17 and 18).

Lymphocytes. A total of 15.3 lymphocytes per mm² were quantified in the skin control. The number was significantly lower than the mesh group without implants (Group M) ($P<0.05$). The tissues from the PCUU-T mesh side showed a significantly lower average of lymphocytes than the Ultrapro meshes, both in smooth (Group S) and textured surface implants (Group T) ($P<0.05$) (Table 3), (Figures 17 and 18).

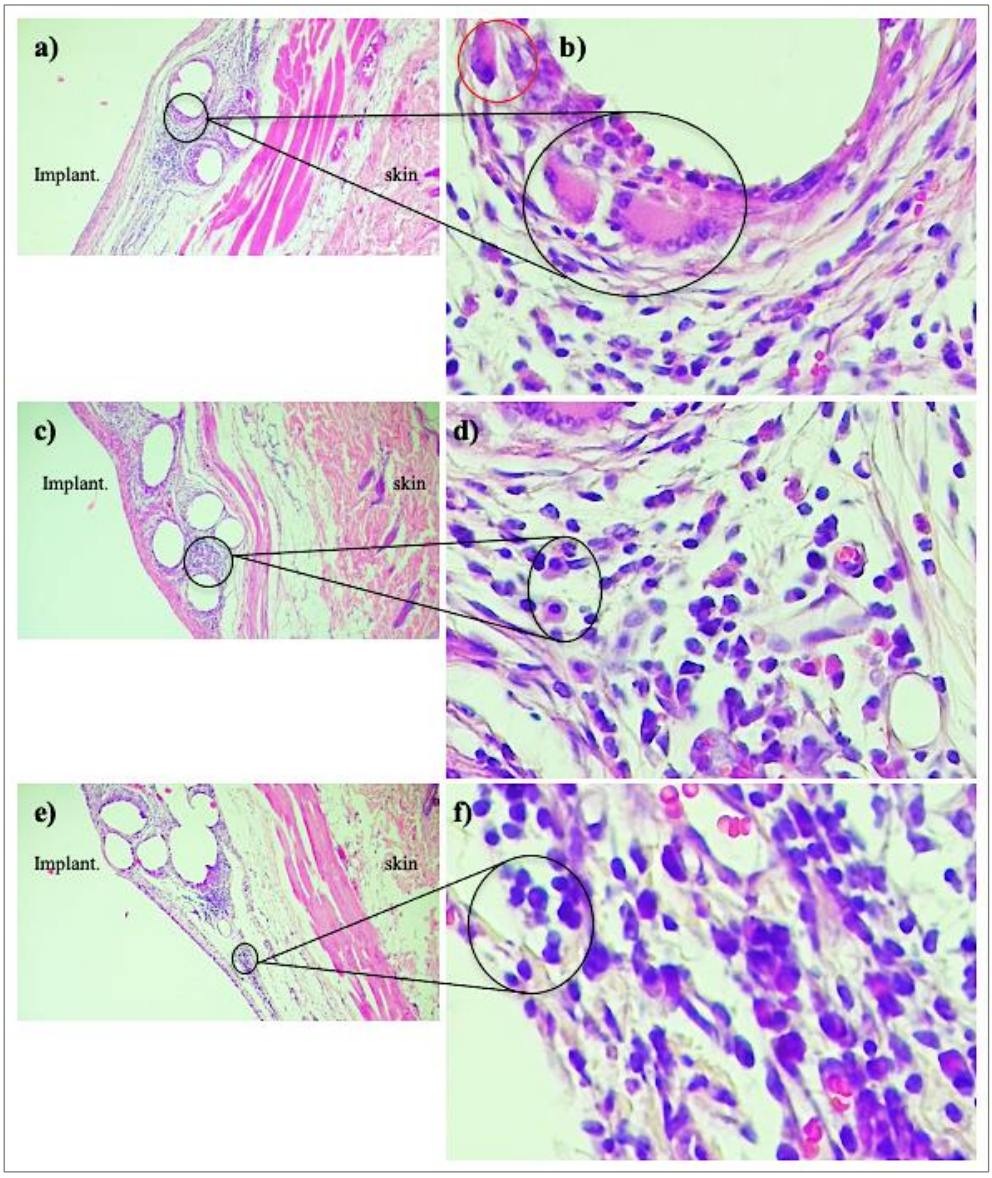

Figure 18: H&E staining, 63 days postoperative, Ultrapro™ mesh side, all cells show **Chronic Inflammation**. On the left, space for the implant and the skin on the right. a) Image at 10x magnification shows two Multinucleate Giant Cells **MGC** (black circle) as a foreign body reaction around the big white space (empty mesh threat) b) Image at 40x magnification big MGC, eccentric multinucleate, and pink cytoplasm (black circle) around the thread (white area). The macrophage (red circle). c) Image at 10x, group of **Plasma Cells** (black circle) in the mesh and subcutis intersection d) Image at 40x two small cells with an eccentric nucleus and pink cytoplasm (black circle). e) Group of **lymphocytes** at 10x magnification (black circle). f) Image at 40x round lymphocyte with big nuclei, poor cytoplasm (black circle).

Eosinophils and Mast cell. A total of 340 eosinophils per mm² were quantified in the skin control, a significantly higher amount than in the mesh group without implants (Group M) ($P<0.05$). In textured surface implants (Group T), it was observed that a significantly higher number of eosinophils in the tissues coming from the PCUU-T mesh side ($P<0.05$), but there were no differences between meshes in the group of implants with smooth surfaces (Group S) (P=NS) (Table 3), (Figures 17 and 19).

A total of 43 *mast cells* per mm² were quantified in the skin control. In group M, a similar number was found in the tissue from the PCUU-T mesh side (P=NS); on the Ultrapro™ mesh side, the average of this type of cells was significantly lower (P<0.05). The average mast cell count was significantly higher in the tissues on the PCUU-T than the Ultrapro™ mesh side, regardless of the implant surface placed (P<0.05) (Table 3) (Figures 17, 19).

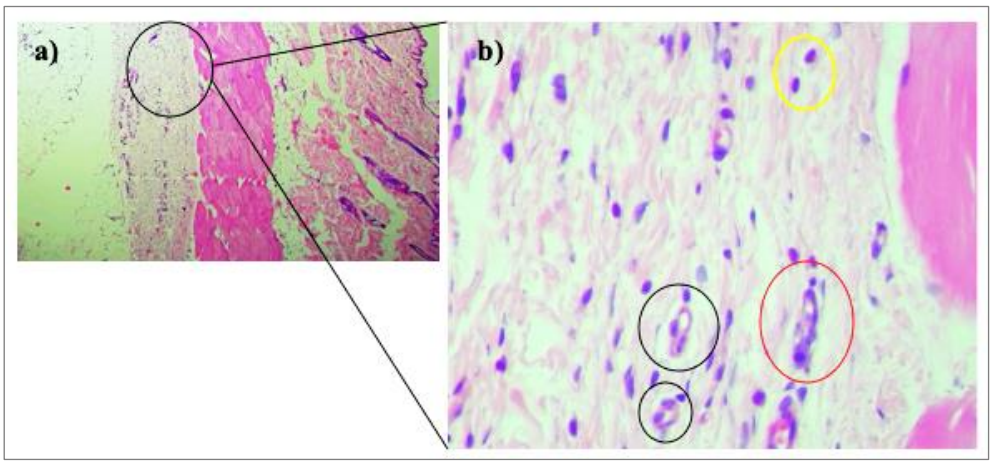

Figure 19: H&E staining on the control rat skin. a) Image at 5x magnification eosinophils, mast cells, and vessels in the connective tissue (black circle). b) Image at 40x magnification **Eosinophils**: showing pinky-reddish cytoplasm and multilobular nuclei (yellow circle). **Mast cells** are central and not lobulated nuclei; they are amphophilic and granulated cytoplasm (red circle). Round vessels with nucleus and media in pink (black circle).

Vessels. A total of 241 vessels per mm² were quantified in the skin control, a number significantly lower than the average recorded in the mesh group without an implant (Group M) (P<0.05). Only in the textured surface implants the average was significantly higher in the tissues on the PCUU-T mesh side than on the Ultrapro™ mesh side (P<0.05); in smooth-surfaced implants, both averages were similar (P=NS) (Table 3) (Figure 17 and 20).

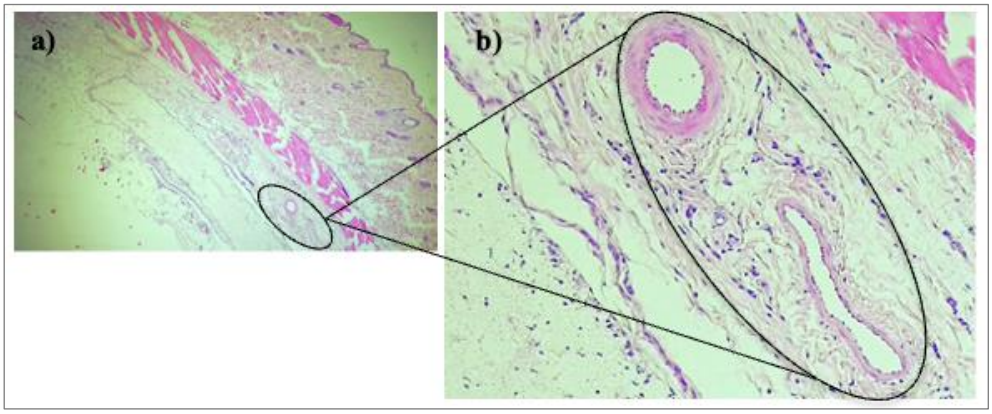

Figure 20: H&E staining, PCUU-T mesh 63 days postoperative. **a)** Image at 5x magnification showing 2 **vessels** (black circle) above the mesh. **b)** Image at 10x. Large and round vessels notable media (circular muscle) and intima (nucleus) (black circle).

*Cellularity***.** The nuclei were counted by ImageJ software (Figure 21). A total of 294,13 nuclei were quantified in the skin control, a similar number observed in the tissue of group M from the PCUU-T mesh side, but significantly lower than the average recorded in the Ultrapro™ group (P<0.05). In tissues from mesh over implants placed, the average number of cores was significantly lower in those on the PCUU-T mesh side than in those on the Ultrapro™ mesh side, regardless of the surface of the implant placed (P<0.05) and (Figure 22)

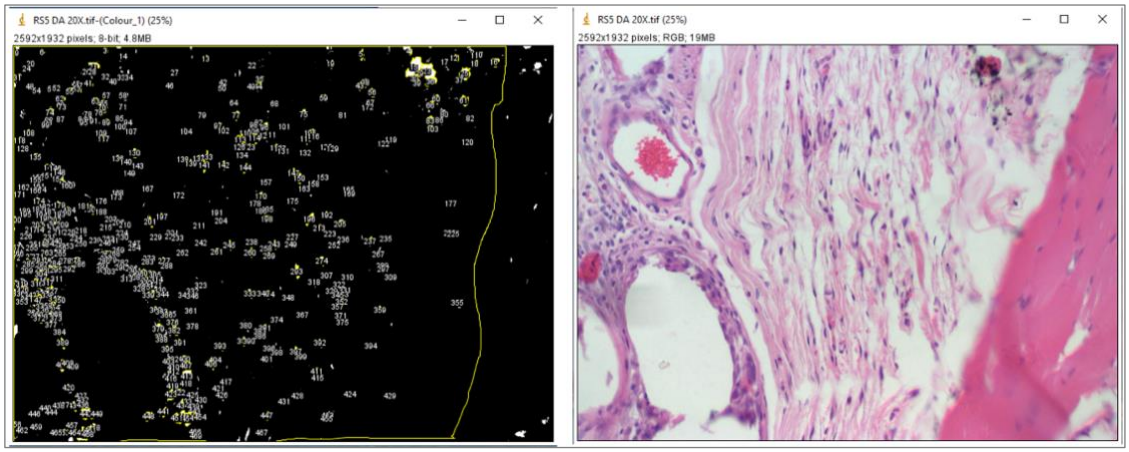

Figure 21: Sample image processing by ImageJ software and color deconvolution2 plugin to count nucleus. The area analyzed was between the end of the panniculus carnosus (yellow line), including the mesh at 20x magnification. The black image shows the nucleus bounded in yellow after the program analyzed the particle. H&E image used as a pattern.

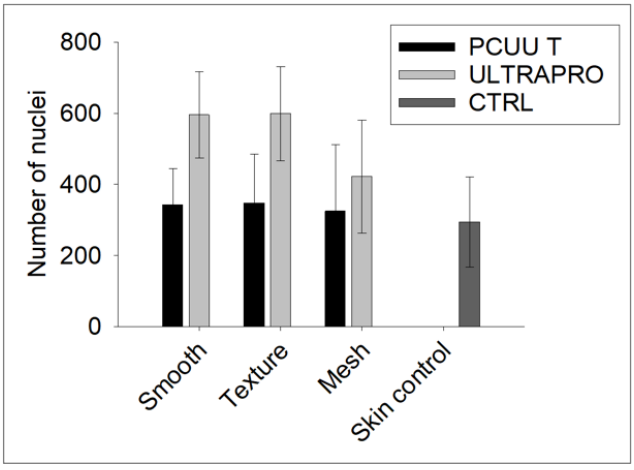

Figure 22: Number of cells in the study groups measured from the end of the panniculus carnosus, including the mesh. ImageJ software and deconvolution color.

Cell infiltrations were also assessed via *DAPI*, showing the nucleus into the PCUU-T mesh, indicating cell infiltration throughout the scaffold. On the Ultrapro™ side, the mesh is wrapped and incorporated by the cells (Figures 23 and 24).

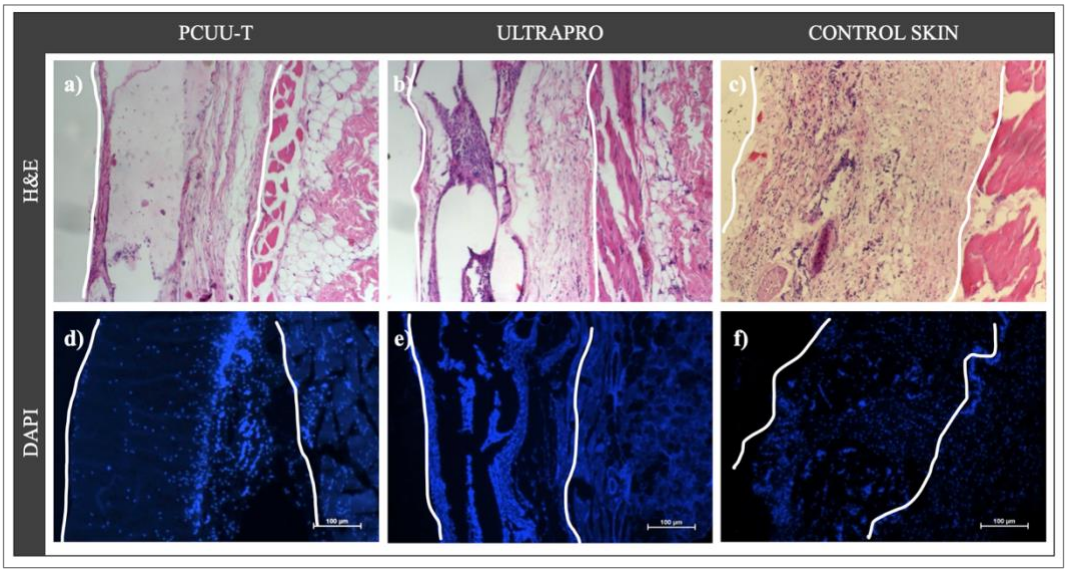

Figure 23: Nuclei were stained by DAPI (blue) to assess the number of general cells comparing both sides and control skin. a, b, c) H&E staining in PCUU-T, Ultrapro™ , and skin control. d, e, f) DAPI staining in PCUU-T (showing nucleus inside the mesh), Ultrapro™, and skin control, respectively, compared with H&E. Black lines represent the limited counting space.

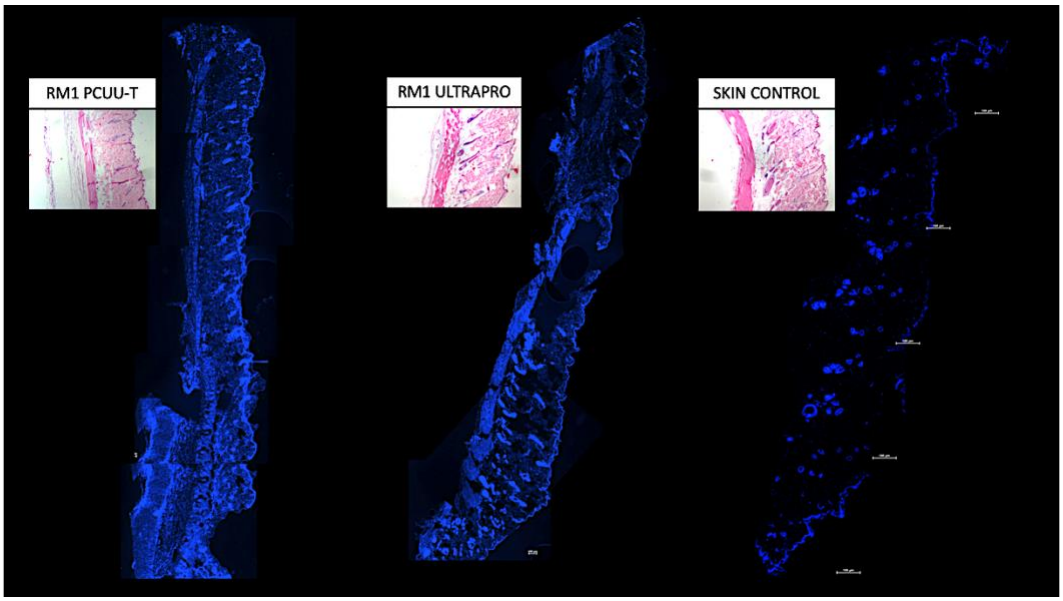

Figure 24: Representative images of the sample reconstruction 4x magnification. Nuclei were stained by DAPI (blue) PCUU-T and Ultrapro mesh side compared to skin without treatment. Small images in H&E at 4X next to each reconstruction. All the images were taken on the same rat.

Collagen. The collagen concentration test showed that PCUU-T led to significantly less collagen formation than Ultrapro™ ($P<0.05$), whatever the implant surface, suggesting less fibrosis. Picrosirius Red and Gomori Trichrome staining showed the formation of aligned and organized fibers, compared with the PCUU-T, which was more disorganized. The control skin that received any treatment showed the most disorganized and in-ball collagen fibers (Figures 25 and 26).

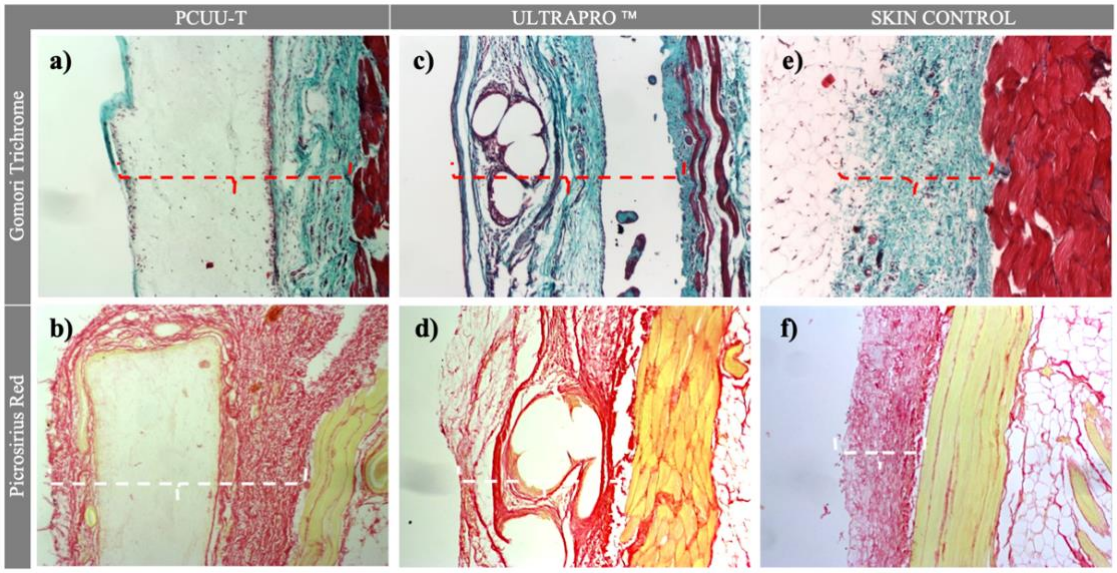

Figure 25: Histological analysis of collagen at 10x. On the top are Gomori Trichome (GT) staining in PCUU-T, Ultrapro™, skin control, and collagen measurement (red line). Below the Picrosirius red (PR) staining in PCUU-T, Ultrapro™, and skin control, collagen measurement (white line). a, b) GT and PR in PCUU-T showed newly formed collagen tissue surrounding the mesh; the collagen appears slightly disorganized. c, d) GT and PR in the Ultrapro™ side showed tissue ingrowing, incorporating the mesh and the aligned collagen fibers. e, f) GT and PR in the skin without treatment showing the normal disorganized and in balls collagen.

f) Bacteriology

The tissue analyzed after euthanasia showed 30 samples (88%) negative for bacteria. Two (6%) *Staphylococcus epidermidis* (one in the S group on the Ultrapro™ side and the other in the M group on the PCUU-T side). Two (6%) meshes were positive for *Corynebacterium sp* (both in the S and T group on the Ultrapro™ side); it is important to remark that both germs are hosts in the skin rats. No rats who tested positive for bacteriology showed extrusion or wound dehiscence, and analyzing which mesh had contamination, PCUU-T presented 1 and Ultrapro™ 3 positive samples. All tests were without statistical significance (P=NS) (Figure 27).

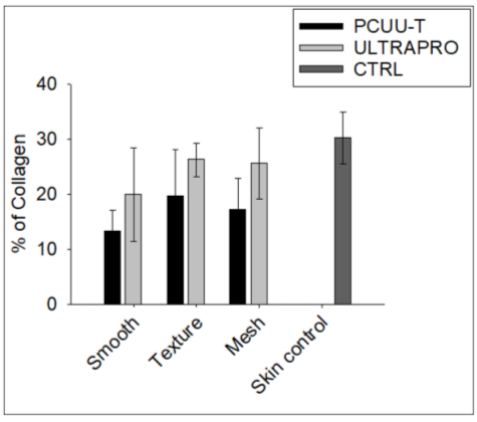

Figure 26: Chart plot: collagen concentration according to study groups and type of mesh.

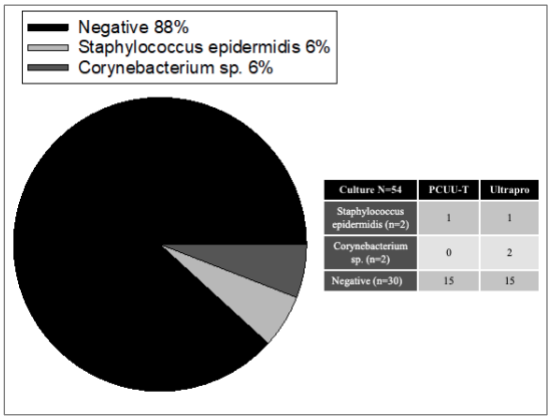

Figure 27: Bacteriological analysis after mesh explantation.

DISCUSSION

According to statistics from the American Society of Plastic Surgeons (ASPS) 2022, Breast reconstruction (BR) post-mastectomy appears for the first time in the Top 5 reconstructive procedures. It has been shown to improve self-esteem and aid in positive body image after undergoing breast cancer diagnosis, treatments, or other medical conditions. Over the past decade, single-stage direct-to-implant (DTI) BR has become an accepted way of treating breast cancer.[274]

Scaffolds were designed for rebuilding or replacing lost tissue. Using biological ADM or synthetic mesh in the inframammary pole is mandatory for a stable implant position, complete coverage, and support. Different materials are available in the market to use in breast reconstruction as breast implant support.[183] When a foreign material is introduced into the body, the immune system protects against injury. It triggers a cascade of inflammatory events to control the strange material and its potential harm.[197] The inflammation can either help to integrate the foreign material through the natural wound-healing mechanisms or cause an excessive inflammatory response, leaving several complications that the surgeons and patients must face and solve. If the reaction is exaggerated, it can result in excessive scarring, graft encapsulation, or degradation. Seroma formation due to the excessive inflammatory reaction is a significant problem for the surgeon and patient, causing anxiety and discomfort. It is followed by frequent outpatient visits, follow-up treatment, increased costs, possibly impeded aesthetic outcomes, and implant failure.

This study analyzed five well-known synthetic meshes used in BR to define their specific features in mechanical properties, porosity, and thickness. Additionally, we studied and analyzed electrospun PCUU and Tecoflex™ in different blends (PCUU-T), and the best-blended mesh obtained was compared with the optimal synthetical mesh selected (Ultrapro™) in a rat model.

Mesh

As we study in Chapter IV, the *Synthetic meshes* have different properties that can improve host tissue integration. The *weight* of synthetic meshes can affect the intensity of the inflammatory reaction and, consequently, the result of the surgery. Lightweight meshes have allowed for less foreign material to be incorporated into the tissue, and they are less prone to shrinkage than heavyweight mesh.[275,276] Nevertheless, studies comparing heavyweight and lightweight meshes implanted found no difference in the inflammatory

response, mesh shrinkage, adherences, or other complications.[277] *Macroporous* meshes greater than 75 μm have been shown to produce less infection when compared to microporous counterparts. Multifilament meshes with pores smaller than 10 μm allow bacteria infiltration while preventing macrophages from entering to combat the infection.[304] Due to host penetration, meshes constructed using large pores appear to promote increased vascularization and collagen deposition.[278] In summary, lightweight meshes generally contain larger pore sizes (>1 mm), thinner filaments, improved elasticity (25–35%), smaller surface areas, a decreased foreign material, and shrink less in physiological conditions, suggesting that the biological response is significantly more favorable compared to heavyweight.[279] *Absorbable materials* are fully degraded over time, and they do not maintain a chronic inflammation. The ideal material should be replaced with the host tissue with functional properties like the lost one.[280] However, incorporating the breast implant in the tissue loss adds an extra load to be supported for a long period. For this reason, the idea of incorporating a blended mesh with non-absorbable parts would fit this requirement.

Biological absorbable meshes are surgical implants derived from human or animal sources used in breast implant reconstruction as an integrative regenerative tissue to help facilitate and expand the soft tissue envelope of mastectomy and support the breast implant. ADM can become highly vascularized over time, promoting host collagen deposition and tissue ingrowth as they slowly degrade. providing strength and integrity.[155] However, at the same time, the major limitation is the rapid enzymatic and hydrolytic degradation because of the immunogenic response. So, current research is looking for a synthetic engineered scaffold.[281] Also, despite the great benefits, there are many reports of different complications.[177,178]

In the literature, Ultrapro™ has an 18.3% overall complication rate (seroma formation 5.1% and infection 4.5%). Complications increase by 50% in patients with previous radiotherapy (RT), and these are seven-fold higher than in cases without these factors.[183] Fluke et al. showed in their preclinical research that Vicryl mesh has substantial degradation at 2 weeks, resulting in denser scarring. PLCL poly (propylene) caprolactone nanofiber scaffolds provide a longer period of healing and strengthening surrounding tissue before the absorption of the mesh. The long mesh absorption time could improve the healing and remodeling of surrounding tissue.[266] Many publications show similar rates of complications with or without mesh. Comparing synthetic meshes with titanium coating, the complications are 17.7 to 29%; in biological matrices, 0 to 32%; and in

reconstructions without meshes, 15%.[282] The metanalysis comparing mesh-assisted BR to no-mesh before and after 2006 showed a higher seroma rate in contemporary no-mesh patients compared to mesh-assisted patients, which is contrary to previous reports regarding seroma rates with the use of ADM. However, the average complication rates of infection, hematoma, explantation, and capsular contracture appeared to differ slightly, and almost all these differences were not statistically significant.[283] Current approaches involve meshes and biomaterials to promote the integration of native tissue. *Nanofibrous scaffolds* began to be used as a solution to many issues to address the complexities of wound healing and inadequate tissue strength.[284]

Biocompatibility

Biomaterials used for mesh prostheses can lead to adverse inflammatory FBR, including fibrosis, calcification, thrombosis, infection, granuloma, fistula, and seroma formation.[216] In contrast, meshes that are derived from biological sources can show a decrease in FBR, particularly in the long term, thanks to their improved integration with neo-tissue and the presence of bioactive signals and growth factors in the bio-derived materials.[155] Meshes with larger pores have been found to have significantly less FBR and fibrosis of localized tissues than meshes with small pores.[285] To minimize FBR, it's possible to influence the body by altering fibrotic responses or modifying the characteristics of the mesh to mimic the organism.

The ECM plays a key role in controlling cell adhesion, proliferation, migration, and differentiation. Nanofibrous scaffolds used in tissue engineering meet these criteria by having a topography of the ECM that could provide this special microenvironment suitable for cell adhesion, proliferation, and angiogenesis, thus facilitating the formation of a mechanically reliable scar.[286]

What are the requirements for meshes to be an optimal scaffold? These materials must interact favorably with the host tissue without negative impacts such as tumorigenicity or toxicity and have well-maintained mechanical strength and good structural integrity. An optimal scaffold should consist of pores that allow cells to interconnect and adhere to one another and vascular ingrowth. The pore size necessary to promote Angiogenesis is about (30–40 μm).[287,288] Scaffold porosity and packing density can be produced by introducing a porogen such as salt crystals, laser ablation following fabrication, or electrospraying an aqueous medium to loosen interactions between polymer layers.[289,290] Furthermore, tissue-engineered scaffolds should be *biodegradable* depending on their role. This means

that the scaffold should be able to break down safely, without cytotoxicity, within the body once the cells have formed into their intended shape. Also, it should prevent the occurrence of a long-term immune reaction and be a more biocompatible tissue scaffold. One of the most important factors is to provide mechanical support during regeneration until it is mature enough to support itself. An "ideal" scaffold must meet similar physical and biochemical properties as the tissue it replaces.

Electrospinning

The electrospinning (ES) technique is a novel, feasible, cost-effective, and flexible fabrication method to obtain a nanofiber mesh with a customizable thickness, mechanical properties, and degradation profile. ES technique has been extensively used in tissue engineering applications due to its ability to create very thin fibers and fibrous architectures that have been proven to mimic extracellular matrix properly.[291] Electrospun can be modified during fabrication to introduce functionality or modify the microstructure and mechanical response.[292] Also, it allows the use of different blend products and the direct inclusion of medications during the spinning process.[293,294] Furthermore, as reported by Takanari et al., it allows the combination of electrospinning with electrospraying to simultaneously deposit wet-electrospun PEUU fiber and dermal ECM gel hybrid layer (sandwich scaffold technique).[295]

The new paradigm of biotechnologies is incorporating 3D printing to create artificial biosystems from the nano to macro-scales, mimicking biological networks, tissues, organs, and complex 3D shapes.[296] 3D printing can incorporate multiple biological and synthetic materials and porosities into a single scaffold designed with varying pore structures, fiber orientations, and mechanical anisotropy.[297]

Anisotropic mechanical properties of the biomaterial are important for mimicking the ligament and skin breast behavior to support the breast implant. Anisotropic has been achieved by utilizing ES with multiple fiber alignments. The fascial system and the suspension ligaments create a natural support matrix for the breast, allowing sliding and limiting the movement over the chest wall. When they are totally or partially removed for breast cancer, the implant replaces the volume in breast reconstruction. To support the implant, the mesh must meet the properties and mechanical behavior of the suspensory ligament. To reproduce the function of the breast suspensory ligament, it is crucial to understand how a biomaterial scaffold responds to physiologic loading. Mira et al. described a biomechanical breast model using tissue deformation measurements from MR

images and Young's moduli. The findings were 120kPa for the fascia and ligaments, respectively, and the skin 4 KPa.[298] It supposes our mesh must meet the mechanical properties mentioned above. However, our requirements are not only for supporting the breast but also for the breast implant, which imposes additional weight and stress on the tissues. Therefore, the scaffold should have high strength to withstand the pressure of the breast implant. There is a lack of information in the literature about these requirements in reconstructive or aesthetic conditions. To analyze the mechanical properties of organs that exhibit large deformation, Sivaraman et al. used a biaxial test to assess PCUU mesh properties in the urinary bladder, an efficient method to mimic the physiological loading.[299] We characterized our PCUU-T mesh with the same tests; nevertheless, we need mechanical studies to understand the physiology of the breast tissue to perform custom, suitable, and mechanically supportive scaffolds.

PCUU and Tecoflex™ (PCUU-T) designed mesh.

Polyurethane, which combines properties of thermoplastics and rubbers, has also gained attention, especially in the cardiovascular system, in the treatment of pelvic dysfunction and breast implants, mainly because of its biocompatibility, flexibility, hemocompatibility, non-cytotoxic and easy processability. Thanks to its properties, it could be a good choice to potentially reduce mesh-related complications.[300]

PCUU is a synthetic electrospun polymer with low degradation and mechanical properties that can be tailored by optimizing the fabrication parameters with optimal cellular ingrowth, new tissue formation, remodeling, and good incorporation.[235] ES process develops PCUU scaffolds with greater pore sizes and porosity. Polycarbonate urethanes are used to make biostable implantable medical devices.[301] Several uses, such as the valvule heart and vascular grafts, were published in the literature.[302,238] The effectiveness of PCUU mesh in improving mechanical properties for bladder disorders has been demonstrated.[299]

The group of polycarbonate polymers has a high resistance to hydrolytic and enzymatic degradation and environmental resistance. The carbonate molecule selection in the PUU was to have slow degradation in the body. Despite having long-lasting materials, the histology assessed no foreign body reaction (FBR) with a more natural incorporation in our scaffold.

We hypothesize that despite slow PCUU degradation, the ability to maintain mechanical strength at longer implantation times could fail in the face of breast implant pressure. In

addition, the biaxial test outcome showed anisotropic behavior with high stretch in one direction. In the context of replacing tissues, holding breast implants, and the need to support over time, non or slow-biodegradability fiber like a Tecoflex™ was studied as beneficial for our mesh. These thermoplastic polyurethanes (TPUs) have relatively good cell viability or cytocompatibility, Tecoflex™ surfaces provide poor adhesion and proliferation of endothelial cells (ECs). The addition of the Tecoflex™ low or non-degradable polymer could ensure long-lasting support. The concern of having a part of a non-degradable component in the body could be the same as having a breast implant for at least 20 years.

Selected blend

In this work, we have prepared different concentrations of PCUU-T. To select the best blend, we looked focused on the best anisotropic behavior and the most suitable degradation profile to allow cell integration and tissue regeneration.[303] Mechanics did not change significantly in the different blends, so we looked at the degradation. Specifically, it was shown that PCUU-T 50:50 provided the least degradability, and that blend was therefore used for the subsequent part of the study. Whether the pores size of our mesh, we performed artificial macropores with a customized acrylic laser mesher to allow easy drainage of possible fluids. Thus, with some modifications to PCUU material, we could eventually increase the porosity of the PCUU-T scaffolds to promote angiogenesis. Our findings have shown the presence of PCUU-T integrity after 9 weeks of implantation, with cell integration.

Preclinical experimentation

Ultrasound. Diagnostic ultrasound commonly uses frequencies between 2 and 15 MHz (10^6 cycles/sec). Low frequencies have deep penetration.[49] Linear Doppler high-frequency ultrasound is appropriate for detailed skin diagnosis as it provides adequate resolution and depth to discriminate skin structures. In our study, although conventional high-frequency ultrasound (10 MHz) may not give enough structural detail, we used high-resolution Doppler ultrasound with 100 mm of penetration, which was sufficient for controlling serum formation.

Histology.

Cellularity. On the PCUU-T side, the findings were similar to those observed in control skin. No giant cells were found on the PCUU-T side in all groups and the control skin samples; it was presented only in the Ultrapro™ mesh and had a significant association

with smooth breast implants. Also, PCUU-T mesh showed significantly fewer plasmatocytes and lymphocytes than Ultrapro™ mesh. Mild fibrosis was recognized on the periphery of Ultrapro™, surrounding the implanted material. Eosinophils are resident cells in the normal rat skin. Instead of a higher number on the control skin, the texture implant group on the PCUU-T side showed more quantity of eosinophils than the Ultrapro™ side; we cannot determine the meaning of that difference. Mast cells were significantly lower in the tissues of the PCUU-T side than in Ultrapro™. It's worth mentioning that the Ultrapro™ mesh had more inflammatory cells, assuming more reaction to the foreign body.

The strength of this research in the histological evaluation was the intervention of the experimented physician specialized in pathology. He examined cells microscopically, regardless of any specialized technique; personal cell counting and identifying each cell line were a great advantage.

Angiogenesis. The formation of new vessels is considered positive and indicates a good integration of implanted mesh with surrounding tissue, likely favoring the production of non-fibrotic dermal tissue.[304] Group M with mesh without implant showed significantly more vessels than the control skin. Vascular congestion and hemosiderin deposits were observed in the Ultrapro™ mesh. The vascular component on the PCUU-T had very similar characteristics to the control group M (multiple vessels, mostly small caliber), showing congestion in some samples. The result identified a good integration in the PCUU-T mesh.

In our study, the number of cells (counted by their nuclei) between the end of the panniculus carnosus and subcutis, including the mesh, represented the mesh integration. Furthermore, using two staining (H&E and DAPI) and analyzing by ImageJ software, evidence showed an increased accuracy.

We could find a small number of nuclei inside the PCUU-T mesh, but it was not possible to identify by optical microscopy which kind of cells were. These cells could enter by imbibition.

At the time of the study, there was a minimal inflammatory reaction without giant cells, resembling the biocompatible material requirement. Also, we opted not to use suture materials on the mesh to avoid a host reaction with other materials and give real results.

Collagen. In our experience, the collagen concentration test showed that PCUU-T led to less collagen formation than Ultrapro™, regardless of the implant surface. Fischer et al.

compared capsule on texture and smooth implant in rats by histology, MRI, and ultrasound and found that texture surface led to thicker but less dense fibrotic capsules, leading to the question of total collagen deposition differs among both implant types, assuming that smooth surface produces a higher incidence of capsular contracture.[305] Therefore, we thought less collagen concentration could influence good tissue integration and less mesh contracture. Further studies will be necessary to identify collagen subtypes (1 and 3). The literature affirms that the collagen fibers aligning in parallel were observed in capsules formed on the smooth breast implant surface. Stimulated myofibroblasts can contract along continuously parallel fibers, which could result in a stronger contracture force in smooth than textured breast implant surfaces.[306] We also visually observed on GT and PR the orientation of collagen on the PCUU-T side was slightly not aligned; this outcome could suggest that the PCUU-T side has better incorporation on the tissue with less contracture on the mesh. It should be noted that we did not use ultrasound or any software like ImageJ collagen orientation, as presented by Huang in his publication.[306] Therefore, a more feasible approach is needed to analyze the orientation of the collagen on the mesh.

Complications

Although there were wound dehiscence complications on 4 rat sides (11%), all of them were related to breast implants; there were no complications in the Mesh group without implants. The extrusions may have been caused by the implant rather than the meshes themselves, and there was no statistical significance between PCUU-T and Ultrapro™. There were no other local adverse effects for each group and no biologically significant differences in the postoperative course.

ES does allow the entrance of very small cells to infiltrate because of the porous size. Therefore, in our study, the small cells infiltrated our scaffold, which could be because of the incisions we performed on it. They were done to create pores within the scaffold and allow the transfer of possible liquid through the mesh. Our results demonstrated no presence of liquid accumulation below the skin or peri-implant according to clinical and ultrasound evaluation.

The presence of post-operative contamination and infection is a major concern in Plastic Surgery. The rate of complications can increase when two foreign materials are used. It is well known that antibiotics soak the breast implant or mesh in an antibiotic solution before implantation to prevent contamination.[63] Additionally, biodegradable meshes and mesh coatings incorporating silver and antibiotic drugs, including ciprofloxacin,

ampicillin, and vancomycin, have shown effectiveness over extended periods in inhibiting infection *in vitro* and *in vivo.*[307] The incorporation of drug delivery and growth factors to improve tissue regeneration and prevent infection is a current challenge. Our microfibers electrospun PCUU-T have the potential to carry out drugs like antibiotics to release gradually and treat possible contaminations.

Staphylococcus epidermidis is a coagulase-negative staphylococci (CNS) and is a harmless bacterium abundant on the human skin. It is a significant player in maintaining local homeostasis. Also, it may fight against other potentially harmful microorganisms, like Staphylococcus aureus, to keep a balanced skin flora.[308] However, is responsible for most of the foreign body infections (FBI) after prosthetic material implantation. It can form biofilm and implant encapsulation.[309]

Corynebacterium spp. are Gram-positive, aerobic bacteria of the Corynebacteriaceae family and are often part of the normal human and animal skin flora and mucous membranes.[310] In our rat model, the contaminations found were not the same rats who lost the implant. Maybe the result was an external contamination and no infection per se. Furthermore, all tests showed no statistical significance between groups.

The rat model is particularly accepted and used as a correlate of humans' physiological and behavioral dispositions. During adulthood (6 weeks), one day in an animal's life is approximately equivalent to 34.8 human days. One rat month is comparable to 3 human years.[311] Our follow-up was 2 rat months. Considering that all possible rat complications were equal to 6 human years, time is considered enough for significant complication appearance.

Hematological parameters.

The materials used in our study and its components are well-known material, with non-cytotoxicity, and non-carcinogenic effect. Despite this, we checked hematological and serum parameters at preoperative and postoperative 63 days to investigate side effects. The result was not statistically significant.

Several *limitations* of the present report should be mentioned. We could not finish with immunofluorescence process to evaluate macrophages (type 1 and 2) and angiogenesis due to technical protocol reasons. Further investigation with immunofluorescence or immunohistochemical will be necessary to analyze the vessels infiltration and well remodeling outcomes. The lack of long-term implantation to evaluate late complications.

More investigations are required to evaluate for long-term (more than 9 weeks) the PCUU absorption and its behavior on a host tissue.
Finally, considering the key role of collagen formation in tissue integration and mechanical behavior, likely, further studies of collagen I/III ratio could add more information to the density and spacial collagen organization.

The *strengths* of this study were the contribution, knowledge and help in every step of the research provided by specialized Scientifics. The bioengineers teaching, sharing, and attending the process of mechanical tests that provided an accurate result, bio-Pharmaceutics in the elaboration and process of the biomaterial, Plastic surgeons performing the surgeries on the rats ensuring a proper and sensitive technique and sterile protocol.
PCUU-T has a lower inflammatory response, which is important to diminish seroma formation and potential reintervention that are a big challenge in Plastic Surgery.

Further pre-clinical studies in large animals and inserting the mesh beneath the breast are needed to obtain sufficient evidence and continue to the future clinical trial.

Understanding the past of the meshes, this study moved forward with innovative designs, which looked to benefit patients' health and satisfy their aesthetic expectations. To date, significant progress has been achieved in the design of biomaterials for BR; however, multiple challenges remain. These include minimizing the acute and chronic FBR to the implanted material, preventing, and controlling post-operative infection, promoting tissue growth and vascularization, and achieving physiological thickness and mechanical properties.

The present study designed and fabricated a novel blend mesh thorough tissue engineering and characterized electrospun scaffolds for breast implant reconstruction applications. Based on the results of our in vivo pre-clinical research, PCUU-T mesh, achieves supplementary tissue, with less inflammation and chronic reaction proving good host tissue integration and regeneration, which could help to maintain a lasting successful repair, sufficient support, and breast implant positioning. Moreover, it is worth to consider the beneficial cost-efficiency of PCUU-T over ADM.

Thus far, there is no published evidence of PCUU-T nanofiber manufacturing to generate a slow and non-biodegradable mesh, using it as a scaffold in association with a breast implant in a rat model.

CONCLUSION

This research was designed to develop a novel electrospun mesh suitable for native tissue integration, promoting healing, facilitating constructive remodeling tissue, and providing mechanical support for future breast implant reconstruction.

PCUU-T nanofiber partially biodegradable mesh was used as a scaffold in association with a breast implant in a rat model. Also, was compared with partially absorbable Ultrapro™ mesh in the other side of the rat model.

The outcomes of the novel mesh were associated with the lowest foreign body response without giant cells formation, low inflammation, appropriate vascularization and good degree of new collagen deposition and matrix remodeling.

The increasing learning in science, histology process, optical and scanning electron microscope evaluation, mechanical characterization, and continuous research with great scientists, fulfilled the knowledge to finish this project.

The interdisciplinary task in this research clearly showed that the different disciplines (surgeons, scientists, and manufacturers) can improve the result of research in benefit to the science and therefore to the patient.

BIBLIOGRAPHY

[1] https://www.fda.gov/medical-devices/letters-health-care-providers/labeling-updates-bd-mesh-products-letter-health-care-providers?mkt_tok=MTAxLUJTTy05OTMAAAGPXagZkSS2XcTtcz-cl5E0njLgNiDYLhV0im3RPs8y8gLzY7LPE-NLAXxSdJqHo-tIsCHAtYf1xR_M-o94_MQDfWmWdUEDELN70z7oVPadKxkx

[2] Burg KJL, Burg TC. Breast tissue engineering: implantation and three-dimensional tissue test system applications. In: Karen J.L. Burg1 and Timothy C. Burg (eds). *Principles of Tissue Engineering (5th ed).* Kidlington, Oxford (UK): Elsevier Inc. 2020; Chapter 30.

[3] Goldwyn RM. Vincenz Czerny and the beginnings of breast reconstruction. Plast Reconstr Surg. 1978 May;61(5):673-81. doi: 10.1097/00006534-197805000-00003. PMID: 347474.

[4] Frame JD. The waterfall effect in breast augmentation. *Gland Surg*. 2017;6(2):193-202. doi:10.21037/gs.2016.10.01 https://pubmed.ncbi.nlm.nih.gov/28497023/

[5] Iwuagwu FC, Frame JD. Silicone breast implants: complications. *Br J Plast Surg*. 1997;50(8):632-636. doi:10.1016/s0007-1226(97)90509-9 https://pubmed.ncbi.nlm.nih.gov/9613406/

[6] Institute of Medicine (US) Committee on the Safety of Silicone Breast Implants; Bondurant S, Ernster V, Herdman R, editors. Safety of Silicone Breast Implants. Washington (DC): National Academies Press (US); 1999. 2, Silicone Chemistry. Available from: https://www.ncbi.nlm.nih.gov/books/NBK44788/

[7] Cronin TD, Gerow FJ. Augmentation Mammaplasty: A New 'Natural Feel' Prosthesis. En: *Transactions of the Third International Congress of Plastic Surgery.* Amsterdam (Brussels): Excerpta Medica

[8] Ashley FL. A new type of breast prosthesis. Preliminary report. *Plast Reconstr Surg*. 1970;45(5):421-424. doi:10.1097/00006534-197005000-00001 https://pubmed.ncbi.nlm.nih.gov/5438186/

[9] Hartley JH. Specific applications of the double lumen prosthesis. *Clin Plast Surg.* 1976;3(2):247–263. https://doi.org/10.1016/S0094-1298(20)30225-X https://www.sciencedirect.com/science/article/abs/pii/S009412982030225X

[10] Radovan C. Breast reconstruction after mastectomy using the temporary expander. *Plast Reconstr Surg*. 1982;69(2):195-208. doi:10.1097/00006534-198202000-00001 https://pubmed.ncbi.nlm.nih.gov/7054790/

[11] Becker H. Breast reconstruction using an inflatable breast implant with detachable reservoir. *Plast Reconstr Surg*. 1984;73(4):678-683. doi:10.1097/00006534-198404000-00031 https://pubmed.ncbi.nlm.nih.gov/6709750/

[12] Batich C, Williams J, King R. Toxic hydrolysis product from a biodegradable foam implant. *J Biomed Mater Res.* 1989;23(A3 Suppl):311–319. https://doi.org/10.1002/jbm.820231406 https://onlinelibrary.wiley.com/doi/10.1002/jbm.820231406

[13] Hester TR, Ford NF, Gale PJ, et al. Measurement of 2,4-toluenediamine in urine and serum samples from women with Même or Replicon breast implants. *Plast Reconstr Surg.* 1997;100(5):1291–1298. https://doi.org/10.1097/00006534-199710000-00035

[14] Fewtrell L, Bartram J. Water Quality: Guidelines, Standards and Health. IWA Publishing; 2001 Accessed October 17, 2021. https://apps.who.int/iris/handle/10665/42442

[15] United States Food and Drug Administration. FDA breast implant consumer handbook 2004: timeline of breast implant activities. 2004. Disponible en: http://www.professor-graf.de/tl_files/professor-graf/Infos/Aesthetik/fdabreastprosthesis.pdf

[16] US Food and Drug Administration. Saline, silicone gel, and alternative breast implants, guidance for industry and food and drug administration staff. 2020.Disponible en: https://www.fda.gov/media/71081/download

[17] Hedén P, Bronz G, Elberg JJ, et al. Long-term safety and effectiveness of style 410 highly cohesive silicone breast implants. *Aesthet Plast Surg*. 2009;33(3):430–438. doi:10.10 07/s0 0266-0 09-9360-x.

[18] Schleiter KE. Silicone breast implant litigation. *Virtual Mentor*. 2010;12(5):389-394. Published 2010 May 1. doi: 10.1001/virtualmentor.2010.12.5.hlaw1-1005 https://pubmed.ncbi.nlm.nih.gov/23158391/

[19] Atlan M, Nuti G, Wang H, Decker S, Perry T. Breast implant surface texture impacts host tissue response. *J Mech Behav Biomed Mater*. 2018; 88:377-385. doi: 10.1016/j.jmbbm.2018.08.035 https://pubmed.ncbi.nlm.nih.gov/30205325/

[20] Duteille F, Perrot P, Bacheley MH, Bell E, Stewart S. Ten-year safety data for eurosilicone's round and anatomical silicone gel breast implants. Aesthet Surg J Open Forum. 2019;1(2):ojz012 Published 2019 Apr 27. doi:10.1093/asjof/ojz012.

[21] Chao AH, Garza R, Povoski SP. A review of the use of silicone implants in breast surgery. Expert Rev Med Devices. 2016;13(2):143–156. doi:10.1586/17434440.2016.1134310. https://pubmed.ncbi.nlm.nih.gov/26690709/

[22] Monstrey S, Christophe A, Delanghe J, et al. What exactly was wrong with the Trilucent breast implants? A unifying hypothesis. *Plast Reconstr Surg*. 2004;113(3):847-856. doi: 10.1097/01.prs.0000105337.12656.dc https://pubmed.ncbi.nlm.nih.gov/15108875/
[23] Berkel H, Birdsell DC, Jenkins H. Breast augmentation: a risk factor for breast cancer? N Engl J Med. 1992;326(25):1649–1653. doi:10.1056/NEJM199206183262501.
[24] Gabriel SE, O'Fallon WM, Kurland LT, Beard CM, Woods JE, Melton LJ. Risk of connective-tissue diseases and other disorders after breast implantation. N Engl J Med. 1994;330(24):1697–1702. doi:10.1056/NEJM199406163302401.
[25] Sánchez-Guerrero J, Colditz GA, Karlson EW, Hunter DJ, Speizer FE, Liang MH. Silicone breast implants and the risk of connective-tissue diseases and symptoms. N Engl J Med. 1995;332(25):1666–1670. doi:10.1056/NEJM199506223322502.
[26] Watad A, Rosenberg V, Tiosano S, et al. Silicone breast implants and the risk of autoimmune/rheumatic disorders: a real-world analysis. Int J Epidemiol. 2018;47(6):1846–1854. doi:10.1093/ije/dyy217.
[27] Coroneos CJ, Selber JC, Offodile AC, Butler CE, Clemens MW. US FDA breast implant post approval studies: long-term out-comes in 99,993 patients. Ann Surg. 2019;269(1):30–36. doi:10.1097/SLA.0000000000002990 https://pubmed.ncbi.nlm.nih.gov/30222598/
[28] Santanelli di Pompeo F, Paolini G, Firmani G, Sorotos M. History of breast implants: Back to the future. JPRAS Open. 2022 Mar 11; 32:166-177. doi: 10.1016/j.jpra.2022.02.004. PMID: 35434240; PMCID: PMC9006741.
[29] Orel, Y., Noam, C., & Jacky, Y. (2022). Five-Year Safety and Satisfaction With the Lightweight Breast Implant. *Aesthetic Surgery Journal*, *42*(3), 261-272. https://doi.org/10.1093/asj/sjab054
[30] Govrin-Yehudain, J., Dvir, H., Preise, D., Govrin-Yehudain, O., & Govreen-Segal, D. (2015). Lightweight Breast Implants: A Novel Solution for Breast Augmentation and Reconstruction Mammaplasty. *Aesthetic Surgery Journal*, *35*(8), 965-971. https://doi.org/10.1093/asj/sjv080
[31] Jovic, T. H., Combellack, E. J., Jessop, Z. M., & Whitaker, I. S. (2020). 3D Bioprinting and the Future of Surgery. *Frontiers in Surgery*, *7*, 609836. https://doi.org/10.3389/fsurg.2020.609836
[32] https://collplant.com/products/breast-implants/
[33] https://healshape.com
[34] Cheng M, Heald A, Wagels M, Ung O, Hutmacher D. Scaffold-guide breast tissue engineering: the future of breast implants. Australas J Plast Surg. 2023;6(2):71282 https://doi.org/10.34239/ajops.71282
[35] Berkane, Y., Oubari, H., Charlès, L., Lupon, E., McCarthy, M., Bertheuil, N., Uygun, B. E., Smadja, D. M., & Lellouch, A. G. (2024). Tissue engineering strategies for breast reconstruction: A literature review of current advances and future directions. *Annals of Translational Medicine*, *12*(1). https://doi.org/10.21037/atm-23-1724
[36] Nichter, Larry S. MD1; Hardesty, Robert A. MD2; Zimmerman, Terry J. MD3. Ideal Implant Structured Breast Implants: Core Study Results through 10 Years. Plastic and Reconstructive Surgery 152(3): p 424e-432ehttps://www.fda.gov/medical-devices/breast-implants/types-breast-implants#saline, September 2023. | DOI: 10.1097/PRS.0000000000010312
[37] https://www.fda.gov/medical-devices/breast-implants/types-breast-implants#saline
[38] Stein, Michael J. MD, MAS1; Applebaum, Sarah A. MD, MS2; Harrast, John J. MS3; Lipa, Joan E. MD, MSc4,5; Matarasso, Alan MD1; Gosain, Arun K. MD2. Practice Patterns in Primary Breast Augmentation: A 16-Year Review of Continuous Certification Tracer Data from the American Board of Plastic Surgery. Plastic and Reconstructive Surgery 152(6):p 1011e-1021e, December 2023. | DOI: 10.1097/PRS.0000000000010497
[39] Ramião, N. G., S. Martins, D. P., Barroso, M. L., Santos, D. C., & Fernandes, A. A. (2018). In Vitro Degradation of Polydimethylsiloxanes in Breast Implant Applications. *Journal of Applied Biomaterials & Functional Materials*. https://doi.org/10.5301/jabfm.5000354
[40] International Organization for Standardization. 2018. ISO 14607:2018(en) - non-active surgical implants — mammary implants — particular requirements. https://www.iso.org/obp/ui/#iso:std:iso:14607:ed-3:v2:en
[41] Barr S, Hill EW, Bayat A. Functional biocompatibility testing of silicone breast implants and a novel classification system based on surface roughness. *J Mech Behav Biomed Mater*. 2017; 75:75-81. doi: 10.1016/j.jmbbm.2017.06.030 https://pubmed.ncbi.nlm.nih.gov/28697402/
[42] Jaeger, M., Randquist, C., & Gahm, J. (2023). Anatomical Breast Implant Assessment Using Ultrasound: A Case Series from the International Breast Implant Check Clinic. *Plastic and Reconstructive Surgery Global Open*, *11*(12). https://doi.org/10.1097/GOX.0000000000005469

[43] Mayo, Federico MD. Breast Surgery with Smooth Anatomical Implants with Fixation System: A Review of the World's Largest Series of Cases. Plastic and Reconstructive Surgery 151(2):p 207e-213e, February 2023. | DOI: 10.1097/PRS.0000000000009829
[44] Shoenfeld Y, Agmon-Levin N. 'ASIA' - autoimmune/inflammatory syndrome induced by adjuvants. J Autoimmun. 2011 Feb;36(1):4-8. doi: 10.1016/j.jaut.2010.07.003. Epub 2010 Aug 13. PMID: 20708902.
[45] Puskas, J. E., & Luebbers, M. T. (2012). Breast implants: The good, the bad and the ugly. Can nanotechnology improve implants? *Wiley Interdisciplinary Reviews: Nanomedicine and Nanobiotechnology*, *4*(2), 153-168. https://doi.org/10.1002/wnan.164
[46] Ohlinger R, Alwafai Z, Paepke S, Zygmunt M, Nawroth F, Schüler K, Fröhlich P. Patient Quality of Life After Subpectoral Implant-based Breast Reconstruction With Synthetic or Biological Materials. Anticancer Res. 2021 Jun;41(6):3075-3082. doi: 10.21873/anticanres.15091. PMID: 34083300.
[47] Hall-Findlay EJ. Breast implant complication review: double capsules and late seromas. Plast Reconstr Surg. 2011 Jan;127(1):56-66. doi: 10.1097/PRS.0b013e3181fad34d. PMID: 21200201.
[48] Lee, J.H., Ryu, J.Y., Lee, J.S. *et al.* Effect of Topical Tranexamic Acid on Seroma Formation in a Rat Mastectomy Model. *Aesth Plast Surg* 46, 3063–3071 (2022). https://doi.org/10.1007/s00266-022-03032-0
[49] Lese, I.; Tsai, C.; Matter, M.; Wüthrich, T.; Scheer, H.S.; Taddeo, A.; Constantinescu, M.A.; Herrmann, I.K.; Olariu, R. Mixed Metal Oxide Nanoparticle Formulations for the Treatment of Seroma. ACS Biomater. Sci. Eng. 2021, 7, 2676–2686.
[50] Morales-Conde S, Gómez-Menchero J, Alarcón I, Balla A. Retroprosthetic Seroma After Laparoscopic Ventral Hernia Repair Is Related to Mesh Used? J Laparoendosc Adv Surg Tech A. 2020 Mar;30(3):241-245. doi: 10.1089/lap.2019.0646. Epub 2019 Nov 19. PMID: 31742465.
[51] Bengtson B, Brody GS, Brown MH, Glicksman C, Hammond D, Kaplan H, Maxwell GP, Oefelein MG, Reisman NR, Spear SL, Jewell ML; Late Periprosthetic Fluid Collection after Breast Implant Working Group. Managing late periprosthetic fluid collections (seroma) in patients with breast implants: a consensus panel recommendation and review of the literature. Plast Reconstr Surg. 2011 Jul;128(1):1-7. doi: 10.1097/PRS.0b013e318217fdb0. PMID: 21441845.
[52] Lista F, Tutino R, Khan A, Ahmad J. Subglandular breast augmentation with textured, anatomic, cohesive silicone implants: a review of 440 consecutive patients. Plast Reconstr Surg. 2013 Aug;132(2):295-303. doi: 10.1097/PRS.0b013e3182958a6d. PMID: 23584627.
[53] Marcos Sforza, Rodwan Husein, Connor Atkinson, Renato Zaccheddu, Unraveling Factors Influencing Early Seroma Formation in Breast Augmentation Surgery, *Aesthetic Surgery Journal*, Volume 37, Issue 3, 1 March 2017, Pages 301–307, https://doi.org/10.1093/asj/sjw196
[54] Derby, Brian M. M.D.; Codner, Mark A. M.D. Textured Silicone Breast Implant Use in Primary Augmentation: Core Data Update and Review. Plastic and Reconstructive Surgery 135(1):p 113-124, January 2015. | DOI: 10.1097/PRS.0000000000000832
[55] Kuroi K, Shimozuma K, Taguchi T, Imai H, Yamashiro H, Ohsumi S, Saito S. Pathophysiology of seroma in breast cancer. Breast Cancer. 2005;12(4):288-93. doi: 10.2325/jbcs.12.288. PMID: 16286909.
[56] Jordan, Sumanas W. M.D., Ph.D.; Khavanin, Nima B.S.; Kim, John Y. S. M.D. Seroma in Prosthetic Breast Reconstruction. Plastic and Reconstructive Surgery 137(4):p 1104-1116, April 2016. | DOI: 10.1097/01.prs.0000481102.24444.72
[57] Chun YS, Verma K, Rosen H, Lipsitz S, Morris D, Kenney P, Eriksson E. Implant-based breast reconstruction using acellular dermal matrix and the risk of postoperative complications. Plast Reconstr Surg. 2010 Feb;125(2):429-436. doi: 10.1097/PRS.0b013e3181c82d90. PMID: 20124828.
[58] Brzezienski MA, Jarrell JA 4th, Mooty RC. Classification and management of seromas in immediate breast reconstruction using the tissue expander and acellular dermal matrix technique. Ann Plast Surg. 2013 May;70(5):488-92. doi: 10.1097/SAP.0b013e31827eac93. PMID: 23542848.
[59] Parks JW, Hammond SE, Walsh WA, Adams RL, Chandler RG, Luce EA. Human acellular dermis versus no acellular dermis in tissue expansion breast reconstruction. Plast Reconstr Surg. 2012 Oct;130(4):739-746. doi: 10.1097/PRS.0b013e318262f06e. PMID: 23018685.
[60] Mendenhall SD, Anderson LA, Ying J, Boucher KM, Liu T, Neumayer LA, Agarwal JP. The BREAST Trial: stage I. Outcomes from the time of tissue expander and acellular dermal matrix placement to definitive reconstruction. Plast Reconstr Surg. 2015 Jan;135(1):29e-42e. doi: 10.1097/PRS.0000000000000758. PMID: 25539349.
[61] Cootney, R. W. (2001). Ultrasound Imaging: Principles and Applications in Rodent Research. *ILAR Journal*, *42*(3), 233-247. https://doi.org/10.1093/ilar.42.3.233
[62] Schüler K, Paepke S, Kohlmann T, Alwafai Z, Nawroth F, Zygmunt M, Ohlinger R. Postoperative Complications in Breast Reconstruction With Porcine Acellular Dermis and Polypropylene Meshes in

Subpectoral Implant Placement. In Vivo. 2021 Sep-Oct;35(5):2739-2746. doi: 10.21873/invivo.12558. PMID: 34410963; PMCID: PMC8408734.

[63] Adams WP Jr, Culbertson EJ, Deva AK, R Magnusson M, Layt C, Jewell ML, Mallucci P, Hedén P. Macrotextured Breast Implants with Defined Steps to Minimize Bacterial Contamination around the Device: Experience in 42,000 Implants. Plast Reconstr Surg. 2017 Sep;140(3):427-431. doi: 10.1097/PRS.0000000000003575. PMID: 28841597.

[64] Siggelkow W, Faridi A, Spiritus K, Klinge U, Rath W, Klosterhalfen B. Histological analysis of silicone breast implant capsules and correlation with capsular contracture. *Biomaterials*. 2003;24(6):1101-1109. doi:10.1016/s0142-9612(02)00429-5 https://pubmed.ncbi.nlm.nih.gov/12504533/

[65] Ganott MA, Harris KM, Ilkhanipour ZS, Costa-Greco MA. Augmentation mammoplasty: normal and abnormal findings with mammography and US. *Radiographics*. 1992;12(2):281-295. doi:10.1148/radiographics.12.2.1561417 https://pubmed.ncbi.nlm.nih.gov/1561417/

[66] Embrey M, Adams EE, Cunningham B, Peters W, Young VL, Carlo GL. A review of the literature on the etiology of capsular contracture and a pilot study to determine the outcome of capsular contracture interventions. *Aesthetic Plast Surg*. 1999;23(3):197-206. doi:10.1007/s002669900268 https://pubmed.ncbi.nlm.nih.gov/10384019/

[67] Poeppl N, Schreml S, Lichtenegger F, Lenich A, Eisenmann-Klein M, Prantl L. Does the surface structure of implants have an impact on the formation of a capsular contracture? *Aesthetic Plast Surg*. 2007;31(2):133-139. doi:10.1007/s00266-006-0091-y https://pubmed.ncbi.nlm.nih.gov/17205246/

[68] Wick, G., Backovic, A., Rabensteiner, E., Plank, N., Schwendtner, C., & Sgonc, R. (2010). The immunology of fibrosis: Innate and adaptive responses. *Trends in Immunology*, *31*(3), 110. https://doi.org/10.1016/j.it.2009.12.001

[69] Steiert, A. E., Boyce, M., & Sorg, H. (2013). Capsular contracture by silicone breast implants: Possible causes, biocompatibility, and prophylactic strategies. *Medical Devices (Auckland, N.Z.)*, *6*, 211-218. https://doi.org/10.2147/MDER.S49522

[70] Spear SL, Baker JL Jr. Classification of capsular contracture after prosthetic breast reconstruction. Plast Reconstr Surg. 1995 Oct;96(5):1119-23; discussion 1124. PMID: 7568488.

[71] Baker JL Jr. Owsley JQ Jr, Peterson RA, eds. Augmentation mammaplasty. In: Symposium on Aesthetic Surgery of the Breast. 1978: St. Louis: Mosby;256–263.

[72] Filiciani, Sandra M.D.; Siemienczuk, Guillermo F. M.D.; Etcheverry, Mariano G. M.D.. Smooth versus Textured Implants and Their Association with the Frequency of Capsular Contracture in Primary Breast Augmentation. Plastic and Reconstructive Surgery 149(2):p 373-382, February 2022. | DOI: 10.1097/PRS.0000000000008717

[73] Schaub, Timothy A. M.D.; Ahmad, Jamil M.D.; Rohrich, Rod J. M.D. Capsular Contracture with Breast Implants in the Cosmetic Patient: Saline versus Silicone–A Systematic Review of the Literature. Plastic and Reconstructive Surgery 126(6): p 2140-2149, December 2010. | DOI: 10.1097/PRS.0b013e3181f2b5a2

[74] Ricci, J. A., Epstein, S., Momoh, A. O., Lin, S. J., Singhal, D., & Lee, B. T. (2017). A meta-analysis of implant-based breast reconstruction and timing of adjuvant radiation therapy. *Journal of Surgical Research*, *218*, 108-116. https://doi.org/10.1016/j.jss.2017.05.072

[75] Coleman DJ, Sharpe DT, Naylor IL, Chander CL, Cross SE. The role of the contractile fibroblast in the capsules around tissue expanders and implants. Br J Plast Surg. 1993 Oct;46(7):547-56. doi: 10.1016/0007-1226(93)90104-j. PMID: 8252260.

[76] Larsen, A., Rasmussen, L.E., Rasmussen, L.F. *et al.* Histological Analyses of Capsular Contracture and Associated Risk Factors: A Systematic Review. *Aesth Plast Surg* 45, 2714–2728 (2021). https://doi.org/10.1007/s00266-021-02473-3

[77] Bui JM, Perry TA, Ren CD, Nofrey B, Teitelbaum S, Van Epps DE (2015) Histological characterization of human breast implant capsules. Aesthetic Plast Surg 39(3):306–315

[78] Hwang K, Sim HB, Huan F, Kim DJ (2010) Myofibroblasts and capsular tissue tension in breast capsular contracture. Aesthetic Plast Surg 34(6):716–721

[79] Efanov JI, Giot JP, Fernandez J, Danino MA (2017) Breast-implant texturing associated with delamination of capsular layers: a histological analysis of the double capsule phenomenon. Ann Chir Plast Esthet 62(3):196–201

[80] Kamel M, Protzner K, Fornasier V, Peters W, Smith D, Ibanez D (2001) The peri-implant breast capsule: an immunophenotypic study of capsules taken at explantation surgery. J Biomed Mater Res 58(1):88–96

[81] Berry, M., Cucchiara, V., & Davies, D. (2010). Breast augmentation: Part II – adverse capsular contracture. *Journal of Plastic, Reconstructive & Aesthetic Surgery*, *63*(12), 2098-2107. https://doi.org/10.1016/j.bjps.2010.04.011

[82] Moyer KE, Ehrlich HP. Capsular contracture after breast reconstruction: collagen fiber orientation and organization. Plast Reconstr Surg. 2013 Apr;131(4):680-685. doi: 10.1097/PRS.0b013e31828189d0. PMID: 23542241.

[83] de Bakker E, van den Broek LJ, Ritt MJPF, Gibbs S, Niessen FB. The Histological Composition of Capsular Contracture Focussed on the Inner Layer of the Capsule: An Intra-Donor Baker-I Versus Baker-IV Comparison. Aesthetic Plast Surg. 2018 Dec;42(6):1485-1491. doi: 10.1007/s00266-018-1211-1. Epub 2018 Sep 5. PMID: 30187083; PMCID: PMC6280822.

[84] Vascular Endothelial Growth Factor Overexpression Positively Modulates the Characteristics of Periprosthetic Tissue of Polyurethane-Coated Silicone Breast Implant in Rats Vilberto J. Vieira, M.D., M.Sc. Armando J. d'Acampora, M.D., Ph.D. Florianopolis, Santa Catarina, Brazil. Plast. Reconstr. Surg. 126: 1899, 2010.

[85] del Rosario AD, Bui HX, Petrocine S et al (1995) True synovial metaplasia of breast implant capsules: a light and electron microscopic study. Ultrastruct Pathol 19(2):83–93. https://doi.org/10.3109/01913129509014607

[86] https://www.who.int/news-room/fact-sheets/detail/breast-cancer. Last access 04/12/24

[87] Jagsi R, Jiang J, Momoh AO, Alderman A, Giordano SH, Buchholz TA, Kronowitz SJ, Smith BD. Trends and variation in use of breast reconstruction in patients with breast cancer undergoing mastectomy in the United States. J Clin Oncol. 2014 Mar 20;32(9):919-26. doi: 10.1200/JCO.2013.52.2284. Epub 2014 Feb 18. PMID: 24550418; PMCID: PMC4876312.

[88] Albornoz CR, Matros E, Lee CN, Hudis CA, Pusic AL, Elkin E, Bach PB, Cordeiro PG, Morrow M. Bilateral Mastectomy versus Breast-Conserving Surgery for Early-Stage Breast Cancer: The Role of Breast Reconstruction. Plast Reconstr Surg. 2015 Jun;135(6):1518-1526. doi: 10.1097/PRS.0000000000001276. PMID: 26017588; PMCID: PMC4744797.

[89] Dean C, Chetty U, Forrest AP. Effects of immediate breast reconstruction on psychosocial morbidity after mastectomy. Lancet. 1983 Feb 26;1(8322):459-62. doi: 10.1016/s0140-6736(83)91452-6. PMID: 6131178.

[90] Maxwell GP. Iginio Tansini and the origin of the latissimus dorsi musculocutaneous flap. Plast Reconstr Surg. 1980 May;65(5):686-92. doi: 10.1097/00006534-198005000-00027. PMID: 6988856.

[91] Schneider WJ, Hill HL Jr, Brown RG. Latissimus dorsi myocutaneous flap for breast reconstruction. Br J Plast Surg. 1977 Oct;30(4):277-81. doi: 10.1016/0007-1226(77)90117-5. PMID: 338072.

[92] https://www.cancer.org/cancer/types/breast-cancer/reconstruction-surgery/breast-reconstruction-options/breast-reconstruction-after-lumpectomy-or-partial-mastectomy.html. Last access 04/11/24

[93] https://www.cancer.gov/types/breast/reconstruction-fact-sheet. Last access 04/11/24

[94] Rancati A, Angrigiani C, Hammond D, Nava M, Gonzalez E, Rostagno R, Gercovich G. Preoperative digital mammography imaging in conservative mastectomy and immediate reconstruction. Gland Surg. 2016 Feb;5(1):9-14. doi: 10.3978/j.issn.2227-684X.2015.08.01. PMID: 26855903; PMCID: PMC4716857.

[95] Mangialardi, Maria L., Marzia Salgarello, Ilaria Baldelli, and Edoardo Raposio. "Prepectoral Implant Pocket Conversion in Breast Reconstruction." *JPRAS Open 26*, (2020): 12-25. Accessed May 16, 2024. https://doi.org/10.1016/j.jpra.2020.08.001.

[96] Regan JP, Schaffner AD. Breast Reconstruction Expander Implant. [Updated 2022 Dec 11]. In: StatPearls [Internet]. Treasure Island (FL): StatPearls Publishing; 2024 Jan-. Available from: https://www.ncbi.nlm.nih.gov/books/NBK431062/

[97] Rose V, Cooper L, Pafitanis G, Hogben K, Sharma A, Din AH. Single-stage buried autologous breast reconstruction (BABR). J Plast Reconstr Aesthet Surg. 2022 Sep;75(9):2960-2969. doi: 10.1016/j.bjps.2022.04.033. Epub 2022 Apr 25. PMID: 35643594.

[98] Hartrampf CR, Scheflan M, Black PW. Breast reconstruction with a transverse abdominal island flap. Plast Reconstr Surg. 1982 Feb;69(2):216-25. doi: 10.1097/00006534-198202000-00006. PMID: 6459602.

[99] Germann, G., & Öhlbauer, M. (2009). Latissimus dorsi flap. *Flaps and Reconstructive Surgery*, 287-303. https://doi.org/10.1016/B978-0-7216-0519-7.00023-X

[100] https://www.plasticsurgery.org/reconstructive-procedures/breast-reconstruction/techniques. Last access 04/12/24

[101] Angrigiani, Claudio M.D; Grilli, Daniel M.D.; Siebert, John M.D. Latissimus Dorsi Musculocutaneous Flap Without Muscle. Plastic and Reconstructive Surgery 96(7):p 1608-1614, December 1995.

[102] Allen RJ, Treece P. Deep inferior epigastric perforator flap for breast reconstruction. Ann Plast Surg. 1994 Jan;32(1):32-8. doi: 10.1097/00000637-199401000-00007. PMID: 8141534.
[103] Koshima I, Soeda S. Inferior epigastric artery skin flaps without rectus abdominis muscle. Br J Plast Surg. 1989 Nov;42(6):645-8. doi: 10.1016/0007-1226(89)90075-1. PMID: 2605399.
[104] Grünherz, L., Wolter, A., Andree, C. *et al.* Autologous Breast Reconstruction with SIEA Flaps: An Alternative in Selected Cases. *Aesth Plast Surg* 44, 299–306 (2020). https://doi.org/10.1007/s00266-019-01554-8
[105] Spiegel, A. J., & Eldor, L. (2010). SIEA Flap Breast Reconstruction. *Aesthetic and Reconstructive Surgery of the Breast*, 147-159. https://doi.org/10.1016/B978-0-7020-3180-9.00009-3
[106] Martineau J, Scampa M, Viscardi JA, Giordano S, Kalbermatten DF, Oranges CM. Inferior gluteal artery perforator (IGAP) flap in autologous breast reconstruction: A proportional meta-analysis of surgical outcomes. J Plast Reconstr Aesthet Surg. 2023 Sep;84:147-156. doi: 10.1016/j.bjps.2023.05.018. Epub 2023 May 24. PMID: 37329748.
[107] Saad A, Sadeghi A, Allen RJ. The anatomic basis of the profunda femoris artery perforator flap: a new option for autologous breast reconstruction--a cadaveric and computer tomography angiogram study. J Reconstr Microsurg. 2012 Jul;28(6):381-6. doi: 10.1055/s-0032-1313773. Epub 2012 May 15. PMID: 22588791.
[108] Martineau J, Kalbermatten DF, Oranges CM. Safety and Efficacy of the Superior Gluteal Artery Perforator (SGAP) Flap in Autologous Breast Reconstruction: Systematic Review and Meta-Analysis. Cancers (Basel). 2022 Sep 11;14(18):4420. doi: 10.3390/cancers14184420. PMID: 36139580; PMCID: PMC9497191.
[109] Hurley AR, Zoccali G, Tasoulis MK, Chrysopoulo M, Blackburn A, James SE, Morgan MS, Harris P, Nanidis T. Preoperative volume estimation in transverse upper gracilis flap surgery: A pilot study. J Plast Reconstr Aesthet Surg. 2021 Nov;74(11):2891-2898. doi: 10.1016/j.bjps.2021.03.101. Epub 2021 Apr 19. PMID: 34059471.
[110] Chang DW, Barnea Y, Robb GL. Effects of an autologous flap combined with an implant for breast reconstruction: an evaluation of 1000 consecutive reconstructions of previously irradiated breasts. Plast Reconstr Surg. 2008 Aug;122(2):356-362. doi: 10.1097/PRS.0b013e31817d6303. PMID: 18626350.
[111] Coleman SR, Saboeiro AP. Fat grafting to the breast revisited: safety and efficacy. Plast Reconstr Surg. 2007 Mar;119(3):775-85; discussion 786-7. doi: 10.1097/01.prs.0000252001.59162.c9. PMID: 17312477.
[112] Gutowski KA; ASPS Fat Graft Task Force. Current applications and safety of autologous fat grafts: a report of the ASPS fat graft task force. Plast Reconstr Surg. 2009 Jul;124(1):272-280. doi: 10.1097/PRS.0b013e3181a09506. PMID: 19346997.
[113] Spear SL, Wilson HB, Lockwood MD. Fat injection to correct contour deformities in the reconstructed breast. Plast Reconstr Surg. 2005 Oct;116(5):1300-5. doi: 10.1097/01.prs.0000181509.67319.cf. PMID: 16217471.
[114] Martin S, Cai L, Beniwal A, Tevlin R, Lee G, Nazerali RS. Autologous Fat Grafting and the Occurrence of Radiation-Induced Capsular Contracture. Ann Plast Surg. 2021 May 1;86(5S Suppl 3):S414-S417. doi: 10.1097/SAP.0000000000002817. PMID: 33833172.
[115] Rigotti G, Marchi A, Galiè M, Baroni G, Benati D, Krampera M, Pasini A, Sbarbati A. Clinical treatment of radiotherapy tissue damage by lipoaspirate transplant: a healing process mediated by adipose-derived adult stem cells. Plast Reconstr Surg. 2007 Apr 15;119(5):1409-1422. doi: 10.1097/01.prs.0000256047.47909.71. PMID: 17415234.
[116] Zhang X, Cai L, Yin B, Han X, Li F. Total breast reconstruction using large-volume condensed and viable fat grafting after mastectomy. J Plast Reconstr Aesthet Surg. 2021 May;74(5):966-973. doi: 10.1016/j.bjps.2020.10.109. Epub 2020 Nov 26. PMID: 33341385.
[117] Orbay H, Hinchcliff KM, Charvet HJ, Sahar DE. Fat Graft Safety after Oncologic Surgery: Addressing the Contradiction between In Vitro and Clinical Studies. Plast Reconstr Surg. 2018 Dec;142(6):1489-1499. doi: 10.1097/PRS.0000000000004992. PMID: 30489524.
[118] Stillaert FBJL, Lannau B, Van Landuyt K, Blondeel PN. The Prepectoral, Hybrid Breast Reconstruction: The Synergy of Lipofilling and Breast Implants. Plast Reconstr Surg Glob Open. 2020 Jul 23;8(7):e2966. doi: 10.1097/GOX.0000000000002966. PMID: 32802660; PMCID: PMC7413773.
[119] Vona-Davis L, Rose DP. Adipokines as endocrine, paracrine, and autocrine factors in breast cancer risk and progression. Endocr Relat Cancer. 2007 Jun;14(2):189-206. doi: 10.1677/ERC-06-0068. PMID: 17639037.

[120] Krastev TK, Schop SJ, Hommes J, Piatkowski AA, Heuts EM, van der Hulst RRWJ. Meta-analysis of the oncological safety of autologous fat transfer after breast cancer. Br J Surg. 2018 Aug;105(9):1082-1097. doi: 10.1002/bjs.10887. Epub 2018 Jun 5. PMID: 29873061; PMCID: PMC6055707.
[121] Petit, Jean Yves M.D.; Lohsiriwat, Visnu M.D.; Clough, Krishna B. M.D.; Sarfati, Isabelle M.D.; Ihrai, Tarik M.D.; Rietjens, Mario M.D.; Veronesi, Paolo M.D.; Rossetto, Fabio B.S.; Scevola, Anna M.D.; Delay, Emmanuel M.D. The Oncologic Outcome and Immediate Surgical Complications of Lipofilling in Breast Cancer Patients: A Multicenter Study—Milan-Paris-Lyon Experience of 646 Lipofilling Procedures. Plastic and Reconstructive Surgery 128(2):p 341-346, August 2011. | DOI: 10.1097/PRS.0b013e31821e713c
[122] Saiga M, Nakagiri R, Mukai Y, Matsumoto H, Kimata Y. Trends, and issues in clinical research on satisfaction and quality of life after mastectomy and breast reconstruction: a 5-year scoping review. Int J Clin Oncol. 2023 Jul;28(7):847-859. doi: 10.1007/s10147-023-02347-5. Epub 2023 May 9. PMID: 37160493; PMCID: PMC10310584.
[123] Santosa KB, Qi J, Kim HM, Hamill JB, Wilkins EG, Pusic AL. Long-term Patient-Reported Outcomes in Postmastectomy Breast Reconstruction. *JAMA Surg.* 2018;153(10):891–899. doi:10.1001/jamasurg.2018.1677
[124] Momoh AO, Cohen WA, Kidwell KM, Hamill JB, Qi J, Pusic AL, Wilkins EG, Matros E. Tradeoffs Associated With Contralateral Prophylactic Mastectomy in Women Choosing Breast Reconstruction: Results of a Prospective Multicenter Cohort. Ann Surg. 2017 Jul;266(1):158-164. doi: 10.1097/SLA.0000000000001840. PMID: 27355266; PMCID: PMC5459619.
[125] Billroth T. *The Medical Sciences in the German Universities: A Study in the History of Civilization*; New York (USA): Macmillan Ed. 1924.
[126] Chowbey P (ed.). *Endoscopic Repair of Abdominal Wall Hernias (2nd ed.): Revised and Enlarged Edition*. Delhi (India): Byword Books Private Limited. 2012
[127] USHER FC, HILL JR, OCHSNER JL. Hernia repair with Marlex mesh. A comparison of techniques. Surgery. 1959 Oct;46:718-24. PMID: 13840514.
[128] Klinge U, Klosterhalfen B, Birkenhauer V, Junge K, Conze J, Schumpelick V. Impact of polymer pore size on the interface scar formation in a rat model. *J Surg Res*. 2002;103(2):208-214. doi:10.1006/jsre.2002.6358
[129] Bryan N, Battersby C, Smart N, Hunt J. A review of biocompatibility in hernia repair; considerations in vitro and in vivo for selecting the most appropriate repair material. *Hernia*. 2015;19(2):169-178. doi:10.1007/s10029-014-1307-8
[130] Est S, Roen M, Chi T, et al. Multi-directional mechanical analysis of synthetic scaffolds for hernia repair. *J Mech Behav Biomed Mater*. 2017; 71:43-53. doi: 10.1016/j.jmbbm.2017.02.009
[131] Baylón K, Rodríguez-Camarillo P, Elías-Zúñiga A, Díaz-Elizondo JA, Gilkerson R, Lozano K. Past, Present and Future of Surgical Meshes: A Review. *Membranes (Basel)*. 2017;7(3):47. Published 2017 Aug 22. doi:10.3390/membranes7030047
[132] Coda A, Lamberti R, Martorana S. Classification of prosthetics used in hernia repair based on weight and biomaterial. Hernia. 2012 Feb;16(1):9-20. doi: 10.1007/s10029-011-0868-z. Epub 2011 Aug 12. PMID: 21837484.
[133] HerniaSurge Group. International guidelines for groin hernia management. Hernia. 2018 Feb;22(1):1-165. doi: 10.1007/s10029-017-1668-x. Epub 2018 Jan 12. PMID: 29330835; PMCID: PMC5809582.
[134] Bobyn, J. D., Wilson, G. J., MacGregor, D. C., Pilliar, R. M., & Weatherly, G. C. (1982). Effect of pore size on the peel strength of attachment of fibrous tissue to porous-surfaced implants. *Journal of Biomedical Materials Research*, *16*(5), 571-584. https://doi.org/10.1002/jbm.820160505
[135] White RA. The effect of porosity and biomaterial on the healing and long-term mechanical properties of vascular prostheses. ASAIO Transactions. 1988 Apr-Jun;34(2):95-100. DOI: 10.1097/00002480-198804000-00004. PMID: 3285872.
[136] Amid K, Shulman G, Lichtenstein L, Sostrin S, Young J, Hakakha M. Preliminary evaluation of composite materials for the repair of incisional hernias. Ann Chir. 1995;49(6):539-42; discussion 542-3. French. PMID: 8526448.
[137] Klosterhalfen B, Klinge U. Retrieval study at 623 human mesh explants made of polypropylene--impact of mesh class and indication for mesh removal on tissue reaction. J Biomed Mater Res B Appl Biomater. 2013 Nov;101(8):1393-9. doi: 10.1002/jbm.b.32958. PMID: 24591221.
[138] Miao, L., Wang, F., Wang, L., Zou, T., Brochu, G., & Guidoin, R. (2015). Physical Characteristics of Medical Textile Prostheses Designed for Hernia Repair: A Comprehensive Analysis of Select Commercial Devices. *Materials*, *8*(12), 8148-8168. https://doi.org/10.3390/ma8125453

[139] Klinge U, Klosterhalfen B. Mesh implants for hernia repair: an update. Expert Review of Medical Devices. 2018 Oct;15(10):735-746. DOI: 10.1080/17434440.2018.1529565. PMID: 30261148.
[140] Alexander, J. Wesley M.D., ScD.; Kaplan, Jerold Z. B.S.; Altemeier, W. A. M.D. Role of Suture Materials in the Development of Wound Infection. Annals of Surgery 165(2): p 192-199, February 1967.
[141] Law NW, Ellis H. A comparison of polypropylene mesh and expanded polytetrafluoroethylene patch for the repair of contaminated abdominal wall defects--an experimental study. Surgery. 1991 May;109(5):652-5. PMID: 1826970.
[142] Jacombs ASW, Karatassas A, Klosterhalfen B, Richter K, Patiniott P, Hensman C. Biofilms, and effective porosity of hernia mesh: are they silent assassins? Hernia. 2020 Feb;24(1):197-204. doi: 10.1007/s10029-019-02063-y. Epub 2019 Oct 31. PMID: 31673846.
[143] Klinge U, Klosterhalfen B. Modified classification of surgical meshes for hernia repair based on the analyses of 1,000 explanted meshes. Hernia. 2012 Jun;16(3):251-8. doi: 10.1007/s10029-012-0913-6. Epub 2012 May 5. PMID: 22562353; PMCID: PMC3360857.
[144] Mühl T, Binnebösel M, Klinge U, Goedderz T. New objective measurement to characterize the porosity of textile implants. J Biomed Mater Res B Appl Biomater. 2008 Jan;84(1):176-83. doi: 10.1002/jbm.b.30859. PMID: 17497684.
[145] Corduas, F., Lamprou, D.A. & Mancuso, E. Next-generation surgical meshes for drug delivery and tissue engineering applications: materials, design, and emerging manufacturing technologies. *Bio-des. Manuf.* **4**, 278–310 (2021). https://doi.org/10.1007/s42242-020-00108-1
[146] Rodríguez, M., Gómez-Gil, V., Pérez-Köhler, B., Pascual, G., & Bellón, J. M. (2021). Polymer Hernia Repair Materials: Adapting to Patient Needs and Surgical Techniques. *Materials*, *14*(11). https://doi.org/10.3390/ma14112790
[147] Elango, S., Perumalsamy, S., Ramachandran, K., & Vadodaria, K. (2017). Mesh materials and hernia repair. *BioMedicine*, *7*(3). https://doi.org/10.1051/bmdcn/2017070316
[148] Deeken CR, Abdo MS, Frisella MM, Matthews BD. Physicomechanical evaluation of polypropylene, polyester, and polytetrafluoroethylene meshes for inguinal hernia repair. J Am Coll Surg. 2011 Jan;212(1):68-79. doi: 10.1016/j.jamcollsurg.2010.09.012. Epub 2010 Nov 5. PMID: 21115372.
[149] https://en.wikipedia.org/wiki/Anisotropy
[150] Saberski ER, Orenstein SB, Novitsky YW. Anisotropic evaluation of synthetic surgical meshes. Hernia. 2011 Feb;15(1):47-52. doi: 10.1007/s10029-010-0731-7. Epub 2010 Sep 30. PMID: 20882394.
[151] Cobb WS, Kercher KW, Heniford BT. The argument for lightweight polypropylene mesh in hernia repair. *Surg Innov*. 2005;12(1):63-69. doi:10.1177/155335060501200109
[152] Novitsky YW, Harrell AG, Cristiano JA, et al. Comparative evaluation of adhesion formation, strength of ingrowth, and textile properties of prosthetic meshes after long-term intra-abdominal implantation in a rabbit. *J Surg Res*. 2007;140(1):6-11. doi: 10.1016/j.jss.2006.09.015
[153] Harrell AG, Novitsky YW, Cristiano JA, et al. Prospective histologic evaluation of intra-abdominal prosthetics four months after implantation in a rabbit model. *Surg Endosc*. 2007;21(7):1170-1174. doi:10.1007/s00464-006-9147-y
[154] Deeken CR, Matthews BD. Characterization of the Mechanical Strength, Resorption Properties, and Histologic Characteristics of a Fully Absorbable Material (Poly-4-hydroxybutyrate-PHASIX Mesh) in a Porcine Model of Hernia Repair. *ISRN Surg*. 2013; 2013:238067. Published 2013 May 28. doi:10.1155/2013/238067
[155] Guillaume, O., Teuschl, A. H., Gruber-Blum, S., Fortelny, R. H., Redl, H., & Petter-Puchner, A. (2015). Emerging trends in abdominal wall reinforcement: bringing bio-functionality to meshes. *Advanced healthcare materials*, *4*(12), 1763-1789.
[156] https://novusscientific.com/row/wp-content/uploads/sites/3/2023/12/PG-450003-12-TIGR-Matrix-BR-Brochure-Eng_web.pdf
[157] https://www.pfmmedical.com.ar/implantes-de-malla-titanizada/
[158] Williams SF, Martin DP, Moses AC. The History of Galaflex P4HB Scaffold. *Aesthet. Surg J*. 2016;36(suppl 2): S33-S42. doi:10.1093/asj/sjw141
[159] Narayanan M. Nair, Bernd Gerber, Carolin Nestle-Kraemling. Poly-4-Hydroxybutyrate (P4HB) Scaffold Internal Support: Preliminary Experience with Direct Implant Opposition During Complex Breast Revisions. Aesthetic Surgery Journal 2019, 39 (11) 1203-1213. DOI: 10.1093/asj/sjy276
[160] David P. Martin, Jeffrey R. Scott. Journal of Surgical Research 2013, 184, 766-773. Characterization of poly-4-hydroxybutyrate mesh for hernia repair applications.
[161] Jonathan S. Grashow, Ajit P. Yoganathan. Absorbable Material (Poly-4-hydroxybutyrate—PHASIX Mesh). Annals of Biomedical Engineering 2006, Vol. 34, No. 10. 10.1007/s10439-006-9183-8

[162] Brown BN, Badylak SF. Extracellular matrix as an inductive scaffold for functional tissue reconstruction. Transl Res. 2014 Apr;163(4):268-85. doi: 10.1016/j.trsl.2013.11.003. Epub 2013 Nov 8. PMID: 24291155; PMCID: PMC4203714.
[163] Brown BN, Freund JM, Han L, Rubin JP, Reing JE, Jeffries EM, Wolf MT, Tottey S, Barnes CA, Ratner BD, Badylak SF. Comparison of three methods for the derivation of a biologic scaffold composed of adipose tissue extracellular matrix. Tissue Eng Part C Methods. 2011 Apr;17(4):411-21. doi: 10.1089/ten.TEC.2010.0342. Epub 2011 Feb 5. PMID: 21043998; PMCID: PMC3065729.
[164] Keane TJ, Swinehart IT, Badylak SF. Methods of tissue decellularization used for preparation of biologic scaffolds and in vivo relevance. Methods. 2015 Aug;84:25-34. doi: 10.1016/j.ymeth.2015.03.005. Epub 2015 Mar 16. PMID: 25791470.
[165] Burke JF, Yannas IV, Quinby WC Jr, Bondoc CC, Jung WK. Successful use of a physiologically acceptable artificial skin in the treatment of extensive burn injury. Ann Surg. 1981 Oct;194(4):413-28. doi: 10.1097/00000658-198110000-00005. PMID: 6792993; PMCID: PMC1345315.
[166] Moiemen NS, Staiano JJ, Ojeh NO, Thway Y, Frame JD. Reconstructive surgery with a dermal regeneration template: clinical and histologic study. Plast Reconstr Surg. 2001 Jul;108(1):93-103. doi: 10.1097/00006534-200107000-00015. PMID: 11420509.
[167] Reynolds M, Kelly DA, Walker NJ, Crantford C, Defranzo AJ. Use of Integra in the Management of Complex Hand Wounds From Cancer Resection and Nonburn Trauma. Hand (N Y). 2018 Jan;13(1):74-79. doi: 10.1177/1558944717692090. Epub 2017 Feb 14. PMID: 28720057; PMCID: PMC5755867.
[168] Salzberg CA, Ashikari AY, Berry C, Hunsicker LM. Acellular Dermal Matrix-Assisted Direct-to-Implant Breast Reconstruction and Capsular Contracture: A 13-Year Experience. Plast Reconstr Surg. 2016 Aug;138(2):329-337. doi: 10.1097/PRS.0000000000002331. PMID: 27064232.
[169] Wagner RD, Braun TL, Zhu H, Winocour S. A systematic review of complications in prepectoral breast reconstruction. J Plast Reconstr Aesthet Surg. 2019 Jul;72(7):1051-1059. doi: 10.1016/j.bjps.2019.04.005. Epub 2019 Apr 21. PMID: 31076195.
[170] Safran T, Al-Halabi B, Viezel-Mathieu A, Boileau JF, Dionisopoulos T. Direct-to-Implant, Prepectoral Breast Reconstruction: A Single-Surgeon Experience with 201 Consecutive Patients. Plast Reconstr Surg. 2020 Apr;145(4):686e-696e. doi: 10.1097/PRS.0000000000006654. PMID: 32221195.
[171] Pandit AS, Henry JA. Design of surgical meshes – an engineering perspective. Technol Health Care. 2004;12:51–65.
[172] Clanahan JM, Awad MM. How Does Robotic-Assisted Surgery Change OR Safety Culture? AMA J Ethics. 2023 Aug 1;25(8):E615-623. doi: 10.1001/amajethics.2023.615. PMID: 37535506.
[173] Becker H, Lind Ii JG. The Use of Synthetic Mesh in Reconstructive, Revision, and Cosmetic Breast Surgery. Aesthetic Plast Surg. 2020 Aug;44(4):1120-1127. doi: 10.1007/s00266-020-01822-y. Epub 2013 Jul 17. PMID: 32844265.
[174] Mayer, H.F., Piedra Buena, I.T., Martino, S.A., Loustau, H.D. (2020). Synthetic Meshes in Breast Reconstruction. In: Mayer, H. (eds) Breast Reconstruction. Springer, Cham. https://doi.org/10.1007/978-3-030-34603-4_4
[175] Breuing KH, Warren SM. Immediate bilateral breast reconstruction with implants and inferolateral AlloDerm slings. Ann Plast Surg. 2005 Sep;55(3):232-9. doi: 10.1097/01.sap.0000168527.52472.3c. PMID: 16106158.
[176] Bindingnavele V, Gaon M, Ota KS, Kulber DA, Lee DJ. Use of acellular cadaveric dermis and tissue expansion in postmastectomy breast reconstruction. J Plast Reconstr Aesthet Surg. 2007;60(11):1214-8. doi: 10.1016/j.bjps.2007.03.015. Epub 2007 Apr 25. PMID: 17459797.
[177] Topol BM, Dalton EF, Ponn T, Campbell CJ. Immediate single-stage breast reconstruction using implants and human acellular dermal tissue matrix with adjustment of the lower pole of the breast to reduce unwanted lift. Ann Plast Surg. 2008 Nov;61(5):494-9. doi: 10.1097/SAP.0b013e31816d82d9. PMID: 18948774.
[178] Hill JL, Wong L, Kemper P, Buseman J, Davenport DL, Vasconez HC. Infectious complications associated with the use of acellular dermal matrix in implant-based bilateral breast reconstruction. Ann Plast Surg. 2012 May;68(5):432-4. doi: 10.1097/SAP.0b013e31823b6ac6. PMID: 22531395.
[179] Wang, ED; Lanier, ST; Phillips, BT; Arora, BP; Katz, SM; Khan, SU; Dagum, AB; Bui, DT. 29: Risks and rewards of acellular dermal matrix in tissue expander/implant breast reconstruction. Plastic and Reconstructive Surgery 125(6):p 27, June 2010. | DOI: 10.1097/01.prs.0000371765.30020.4a
[180] Brooke, S; Mesa, J; Uluer, M; Michelotti, B; Moyer, K; Mackay, D; Potochny, J. Abstract 24: Complications in Tissue Expander Breast Reconstruction. Plastic and Reconstructive Surgery 130(1S):p 26, July 2012. | DOI: 10.1097/01.prs.0000416112.33447.67

[181] Komorowska-Timek E, Oberg KC, Timek TA, Gridley DS, Miles DAG. The effect of AlloDerm envelopes on periprosthetic capsule formation with and without radiation. Plast Reconstr Surg. 2009 Mar;123(3):807-816. doi: 10.1097/PRS.0b013e318199eef3. PMID: 19319043.
[182] Dieterich M, Angres J, Stubert J, Stachs A, Reimer T, Gerber B. Patient-Reported Outcomes in Implant-Based Breast Reconstruction Alone or in Combination with a Titanium-Coated Polypropylene Mesh - A Detailed Analysis of the BREAST-Q and Overview of the Literature. Geburtshilfe Frauenheilkd. 2015 Jul;75(7):692-701. doi: 10.1055/s-0035-1546218. PMID: 26257406; PMCID: PMC4520995.
[183] Pukancsik D, Kelemen P, Gulyás G, Újhelyi M, Kovács E, Éles K, Mészáros N, Kenessey I, Pálházi P, Kovács T, Kásler M, Mátrai Z. Clinical experiences with the use of ULTRAPRO® mesh in single-stage direct-to-implant immediate postmastectomy breast reconstruction in 102 patients: A retrospective cohort study. Eur J Surg Oncol. 2017 Jul;43(7):1244-1251. doi: 10.1016/j.ejso.2017.01.236. Epub 2017 Feb 6. PMID: 28215734.
[184] József, Z.; Újhelyi, M.; Ping, O.; Domján, S.; Fülöp, R.; Ivády, G.; Tislér, R.; Rubovszky, G.; Mészáros, N.; Kenessey, I.; et al. Long-Term Dynamic Changes in Cosmetic Outcomes and Patient Satisfaction after Implant-Based Postmastectomy Breast Reconstruction and Contralateral Mastopexy with or without an Ultrapro Mesh Sling Used for the Inner Bra Technique. A Retrospective Correlational Study. *Cancers* **2021**, *13*, 73. https://doi.org/10.3390/cancers13010073
[185] Spear, Scott L. M.D.; Carter, Mary Ella M.D.; Ganz, Jason C. M.D. The Correction of Capsular Contracture by Conversion to "Dual-Plane" Positioning: Technique and Outcomes. Plastic and Reconstructive Surgery 112(2):p 456-466, August 2003. | DOI: 10.1097/01.PRS.0000070987.15303.1A
[186] McGregor JC, Bahia H. A possible new way of managing breast implant rippling using an autogenous fascia lata patch. Br J Plast Surg. 2004 Jun;57(4):372-4. doi: 10.1016/j.bjps.2003.11.028. PMID: 15145746.
[187] Becker H, Shaw KE, Kara M. Correction of symmastia using an adjustable implant. Plast Reconstr Surg. 2005 Jun;115(7):2124-6. doi: 10.1097/01.prs.0000164682.07583.a8. PMID: 15923866.
[188] Spear, Scott L. M.D.; Seruya, Mitchel M.D.; Clemens, Mark W. M.D.; Teitelbaum, Steven M.D.; Nahabedian, Maurice Y. M.D. Acellular Dermal Matrix for the Treatment and Prevention of Implant-Associated Breast Deformities. Plastic and Reconstructive Surgery 127(3):p 1047-1058, March 2011. | DOI: 10.1097/PRS.0b013e31820436af
[189] Maxwell GP, Gabriel A. Use of the acellular dermal matrix in revisionary aesthetic breast surgery. Aesthet Surg J. 2009 Nov-Dec;29(6):485-93. doi: 10.1016/j.asj.2009.09.007. PMID: 19944993.
[190] Logan Ellis H, Asaolu O, Nebo V, Kasem A. Biological and synthetic mesh use in breast reconstructive surgery: a literature review. World J Surg Oncol. 2016 Apr 21;14:121. doi: 10.1186/s12957-016-0874-9. PMID: 27102580; PMCID: PMC4839154.
[191] Pompei S, Evangelidou D, Arelli F, Ferrante G. The Use of TIGR Matrix in Breast Aesthetic and Reconstructive Surgery: Is a Resorbable Synthetic Mesh a Viable Alternative to Acellular Dermal Matrices? Clin Plast Surg. 2018 Jan;45(1):65-73. doi: 10.1016/j.cps.2017.08.005. Epub 2017 Sep 18. PMID: 29080661.
[192] Atiyeh B, Ghieh F, Chahine F, Oneisi A. Ptosis and Bottoming out Following Mastopexy and Reduction Mammoplasty. Is Synthetic Mesh Internal Breast Support the Solution? A Systematic Review of the Literature. Aesthetic Plast Surg. 2022 Feb;46(1):25-34. doi: 10.1007/s00266-021-02398-x. Epub 2021 Jul 23. PMID: 34297171.
[193] Adams Jr, W. P., Baxter, R., Glicksman, C., Mast, B. A., Tantillo, M., & Van Natta, B. W. (2018). The use of poly-4-hydroxybutyrate (P4HB) scaffold in the ptotic breast: a multicenter clinical study. *Aesthetic surgery journal*, *38*(5), 502-518.
[194] Góes, J. C. S., Landecker, A., Lyra, E. C., Henríquez, L. J., Góes, R. S., & Godoy, P. M. (2004). The application of mesh support in periareolar breast surgery: clinical and mammographic evaluation. *Aesthetic plastic surgery*, *28*, 268-274.
[195] Choi YS, You HJ, Lee TY, Kim DW. Comparing Complications of Biologic and Synthetic Mesh in Breast Reconstruction: A Systematic Review and Network Meta-Analysis. Arch Plast Surg. 2023 Feb 6;50(1):3-9. doi: 10.1055/a-1964-8181. PMID: 36755646; PMCID: PMC9902089.
[196] Dellacherie M, Seo B, Mooney D. Macroscale biomaterials strategies for local immunomodulation. *Nature Reviews Materials*(2019), *4* (6), 379-397. https://doi.org/10.1038/s41578-019-0106-3
[197] Kämmerling, L., Fisher, L. E., Antmen, E., Simsek, G. M., Rostam, H. M., Vrana, N. E., & Ghaemmaghami, A. M. (2021). Mitigating the foreign body response through 'immune-instructive' biomaterials. *Journal of Immunology and Regenerative Medicine*, *12*, 100040. https://doi.org/10.1016/j.regen.2021.100040

[198] Overed-Sayer, C., Rapley, L., Mustelin, T., & Clarke, D. L. (2013). Are mast cells instrumental for fibrotic diseases? *Frontiers in Pharmacology*, *4*. https://doi.org/10.3389/fphar.2013.00174
[199] Franz S, Rammelt S, Scharnweber D, Simon JC. Immune responses to implants - a review of the implications for the design of immunomodulatory biomaterials. Biomaterials. 2011 Oct;32(28):6692-709. doi: 10.1016/j.biomaterials.2011.05.078. Epub 2011 Jun 28. PMID: 21715002.
[200] Acharya KR, Ackerman SJ. Eosinophil granule proteins: form and function. J Biol Chem. 2014 Jun 20;289(25):17406-15. doi: 10.1074/jbc.R113.546218. Epub 2014 May 6. PMID: 24802755; PMCID: PMC4067173.
[201] Wang J, Arase H. Regulation of immune responses by neutrophils. Ann N Y Acad Sci. 2014 Jun;1319:66-81. doi: 10.1111/nyas.12445. Epub 2014 May 21. PMID: 24850053.
[202] Londono, R., Badylak, S.F. Biologic Scaffolds for Regenerative Medicine: Mechanisms of *In vivo* Remodeling. *Ann Biomed Eng* **43**, 577–592 (2015). https://doi.org/10.1007/s10439-014-1103-8
[203] Anderson JM, Rodriguez A, Chang DT. Foreign body reaction to biomaterials. Semin Immunol. 2008 Apr;20(2):86-100. doi: 10.1016/j.smim.2007.11.004. Epub 2007 Dec 26. PMID: 18162407; PMCID: PMC2327202.
[204] Brown, B. N., Ratner, B. D., Goodman, S. B., Amar, S., & Badylak, S. F. (2012). Macrophage polarization: An opportunity for improved outcomes in biomaterials and regenerative medicine. *Biomaterials*, *33*(15), 3792-3802. https://doi.org/10.1016/j.biomaterials.2012.02.034
[205] Machaidze Z, D'Amore A, Freitas RCC, Joyce AJ, Bayoumi A, Rich K, Brown DW, Aikawa E, Wagner WR, Rego BV, Mayer JE Jr. Tissue formation and host remodeling of an elastomeric biodegradable scaffold in an ovine pulmonary leaflet replacement model. J Biomed Mater Res A. 2024 Feb;112(2):276-287. doi: 10.1002/jbm.a.37622. Epub 2023 Sep 29. PMID: 37772456; PMCID: PMC11034854.
[206] Wynn, TA. "Cellular and Molecular Mechanisms of Fibrosis." *The Journal of Pathology 214*, no. 2 (2008): 199-210. Accessed May 9, 2024. https://doi.org/10.1002/path.2277.
[207] Chen, S., Malliaras, G. G., & Barone, D. G. (2021). Foreign Body Reaction to Implanted Biomaterials and Its Impact in Nerve Neuroprosthetics. *Frontiers in Bioengineering and Biotechnology*, *9*, 622524. https://doi.org/10.3389/fbioe.2021.622524
[208] Duffield JS. Cellular and molecular mechanisms in kidney fibrosis. J Clin Invest. 2014 Jun;124(6):2299-306. doi: 10.1172/JCI72267. Epub 2014 Jun 2. PMID: 24892703; PMCID: PMC4038570.
[209] Bonner, J. C. (2004). Regulation of PDGF and its receptors in fibrotic diseases. *Cytokine & growth factor reviews*, *15*(4), 255-273.
[210] Galli SJ, Borregaard N, Wynn TA. Phenotypic and functional plasticity of cells of innate immunity: macrophages, mast cells and neutrophils. Nat Immunol. 2011 Oct 19;12(11):1035-44. doi: 10.1038/ni.2109. PMID: 22012443; PMCID: PMC3412172.
[211] Luttikhuizen, D. T., Harmsen, M. C., & Luyn, M. J. V. (2006). Cellular and molecular dynamics in the foreign body reaction. *Tissue engineering*, *12*(7), 1955-1970.
[212] Jones, K. (2015). Fibrotic Response to Biomaterials and all Associated Sequence of Fibrosis. *Host Response to Biomaterials*, 189-237. https://doi.org/10.1016/B978-0-12-800196-7.00009-8
[213] Novitsky YW, Rosen MJ. The biology of biologics: basic science and clinical concepts. Plast Reconstr Surg. 2012 Nov;130(5 Suppl 2):9S-17S. doi: 10.1097/PRS.0b013e31825f395b. PMID: 23096994.
[214] Amid, P.K. Classification of biomaterials and their related complications in abdominal wall hernia surgery. *Hernia* **1**, 15–21 (1997). https://doi.org/10.1007/BF02426382
[215] Klinge U, Park JK, Klosterhalfen B. 'The ideal mesh?'. Pathobiology. 2013;80(4):169-75. doi: 10.1159/000348446. Epub 2013 May 6. PMID: 23652280.
[216] Klinge U, Klosterhalfen B, Müller M, Schumpelick V. Foreign body reaction to meshes used for the repair of abdominal wall hernias. Eur J Surg. 1999 Jul;165(7):665-73. doi: 10.1080/11024159950189726. PMID: 10452261.
[217] Ward WK, Slobodzian EP, Tiekotter KL, Wood MD. The effect of microgeometry, implant thickness and polyurethane chemistry on the foreign body response to subcutaneous implants. Biomaterials. 2002 Nov;23(21):4185-92. doi: 10.1016/s0142-9612(02)00160-6. PMID: 12194521.
[218] King Jr, T. E., Bradford, W. Z., Castro-Bernardini, S., Fagan, E. A., Glaspole, I., Glassberg, M. K., ... & Noble, P. W. (2014). A phase 3 trial of pirfenidone in patients with idiopathic pulmonary fibrosis. *New England journal of medicine*, *370*(22), 2083-2092.
[219] Astolfi, L., Guaran, V., Marchetti, N., Olivetto, E., Simoni, E., Cavazzini, A., Jolly, C., & Martini, A. (2014). Cochlear implants and drug delivery: In vitro evaluation of dexamethasone release. *Journal of*

Biomedical Materials Research Part B: Applied Biomaterials, *102*(2), 267-273. https://doi.org/10.1002/jbm.b.33004

[220] Mosser, D. M., & Edwards, J. P. (2008). Exploring the full spectrum of macrophage activation. *Nature Reviews Immunology*, *8*(12), 958-969. https://doi.org/10.1038/nri2448

[221] Hinz, B., Phan, S. H., Thannickal, V. J., Prunotto, M., Desmoulière, A., Varga, J., De Wever, O., Mareel, M., & Gabbiani, G. (2012). Recent Developments in Myofibroblast Biology: Paradigms for Connective Tissue Remodeling. *The American Journal of Pathology*, *180*(4), 1340-1355. https://doi.org/10.1016/j.ajpath.2012.02.004

[222] Cox N, Pilling D, Gomer RH. Serum amyloid P: a systemic regulator of the innate immune response. J Leukoc Biol. 2014 Nov;96(5):739-43. doi: 10.1189/jlb.1MR0114-068R. Epub 2014 May 7. PMID: 24804675; PMCID: PMC6607997.

[223] Avula, M. N., Rao, A. N., McGill, L. D., Grainger, D. W., & Solzbacher, F. (2013). Modulation of the foreign body response to implanted sensor models through device-based delivery of the tyrosine kinase inhibitor, masitinib. *Biomaterials*, *34*(38), 9737-9746. https://doi.org/10.1016/j.biomaterials.2013.08.090

[224] Pyne, N. J., Dubois, G., & Pyne, S. (2013). Role of sphingosine 1-phosphate and lysophosphatidic acid in fibrosis. *Biochemical et Biophysical Acta (BBA) - Molecular and Cell Biology of Lipids*, *1831*(1), 228-238. https://doi.org/10.1016/j.bbalip.2012.07.003

[225] Love, R. J., & Jones, K. S. (2013). Transient inhibition of connective tissue infiltration and collagen deposition into porous poly(lactic-co-glycolic acid) discs. *Journal of Biomedical Materials Research Part A*, *101*(12), 3599-3606. https://doi.org/10.1002/jbm.a.34648

[226] Moroni, L., De Wijn, J.R. and Van Blitterswijk, C.A. Integrating Novel Technologies to Fabricate Smart Scaffolds, J. Biomater. Sci. Polym. Ed., 2008: 19: 543–572.

[227] Bendrea, D., Cianga, L., & Cianga, I. (2011). Review paper: Progress in the Field of Conducting Polymers for Tissue Engineering Applications. Journal of Biomaterials Applications. https://doi.org/10.1177/0885328211402704

[228] Ma, P.X. Biomimetic Materials for Tissue Engineering, Adv. Drug. Deliv. Rev., 2008: 60: 184–198.

[229] Mano, J.F., Silva, G.A., Azevedo, H.S., Malafaya, P.B., Sousa, R.A., Silva, S.S., et al. Natural Origin Biodegradable Systems in Tissue Engineering and Regenerative Medicine: Present Status and Some Moving Trends, J. R. Soc. Interface., 2008: 4: 999–1030.

[230] Rosso, F., Marino, G., Giordano, A., Barbarisi, M., Parmeggiani, D. and Barbarisi, A. Smart Materials as Scaffolds for Tissue Engineering, J. Cell. Phys., 2005: 203: 465–470.

[231] Asadi, N., Del Bakhshayesh, A. R., Davaran, S., & Akbarzadeh, A. (2020). Common biocompatible polymeric materials for tissue engineering and regenerative medicine. Materials Chemistry and Physics, 242, 122528. https://doi.org/10.1016/j.matchemphys.2019.122528

[232] Williams, D. F. (2008). On the mechanisms of biocompatibility. *Biomaterials*, *29*(20), 2941-2953. https://doi.org/10.1016/j.biomaterials.2008.04.023

[233] Zhang, X., & Williams, D. (Eds.). (2019). *Definitions of biomaterials for the twenty-first century*. Elsevier.

[234] Bauer, S., Schmuki, P., Von der Mark, K., & Park, J. (2013). Engineering biocompatible implant surfaces: Part I: Materials and surfaces. *Progress in Materials Science*, *58*(3), 261-326. https://doi.org/10.1016/j.pmatsci.2012.09.001

[235] Yi Hong, Jianjun Guan, Kazuro L. Fujimoto, Ryotaro Hashizume, Anca L. Pelinescu, William R. Wagner. Tailoring the degradation kinetics of poly(ester carbonate urethane)urea thermoplastic elastomers for tissue engineering scaffolds. Biomaterials, Volume 31, Issue 15, 2010, Pages 4249-4258. ISSN 0142-9612, https://doi.org/10.1016/j.biomaterials.2010.02.005.

[236] Gostev, A. A., Shundrina, I. K., Pastukhov, V. I., Shutov, A. V., Chernonosova, V. S., Karpenko, A. A., & Laktionov, P. P. (2020). In Vivo Stability of Polyurethane-Based Electrospun Vascular Grafts in Terms of Chemistry and Mechanics. *Polymers*, *12*(4), 845. https://doi.org/10.3390/polym12040845

[237] Szycher M. Biostability of Polyurethane Elastomers: A Critical Review. Journal of Biomaterials Applications. 1988;3(2):297-402. doi:10.1177/088532828800300207

[238] Rolińska, K., Bakhshi, H., Balk, M., Blocki, A., Panwar, A., Puchalski, M., Wojasiński, M., & Mazurek-Budzyńska, M. (2023). Electrospun Poly(carbonate-urea-urethane) s Nonwovens with Shape-Memory Properties as a Potential Biomaterial. *ACS Biomaterials Science & Engineering*, *9*(12), 6683-6697. https://doi.org/10.1021/acsbiomaterials.3c01214

[239] Salacinski, H., Tai, N., Punshon, G., Giudiceandrea, A., Hamilton, G., & Seifalian, A. (2000). Optimal Endothelialisation of a New Compliant Poly(Carbonate-Urea)Urethane Vascular Graft with Effect of Physiological Shear Stress. *European Journal of Vascular and Endovascular Surgery*, *20*(4), 342-352. https://doi.org/10.1053/ejvs.2000.1185

[240] Tan A, Farhatnia Y, Seifalian AM. Polyhedral oligomeric silsesquioxane poly(carbonate-urea) urethane (POSS-PCU): applications in nanotechnology and regenerative medicine. Crit Rev Biomed Eng. 2013;41(6):495-513. PMID: 24940662.
[241] Punshon G, Vara DS, Sales KM, Kidane AG, Salacinski HJ, Seifalian AM. Interactions between endothelial cells and a poly(carbonate-silsesquioxane-bridge-urea)urethane. Biomaterials. 2005 Nov;26(32):6271-9. doi: 10.1016/j.biomaterials.2005.03.034. PMID: 15913770.
[242] Yan, B., Zhang, Y., Li, Z., Zhou, P., & Mao, Y. (2022). Electrospun nanofibrous membrane for biomedical application. Sn Applied Sciences, 4(6). https://doi.org/10.1007/s42452-022-05056-2
[243] Detta N, Errico C, Dinucci D, *et al.* Novel electrospun polyurethane/gelatin composite meshes for vascular grafts. *J Mater Sci: Mater Med* 2010 21, 1761–1769. https://doi.org/10.1007/s10856-010-4006-8
[244] Bélanger MC, Marois Y, Roy R, Mehri Y, Wagner E, Zhang Z, King MW, Yang M, Hahn C, Guidoin R. Selection of a polyurethane membrane for the manufacture of ventricles for a totally implantable artificial heart: blood compatibility and biocompatibility studies. Artif Organs. 2000 Nov;24(11):879-88. doi: 10.1046/j.1525-1594.2000.06504.x. PMID: 11119076.
[245] McGuigan, A. P., & Sefton, M. V. (2007). The influence of biomaterials on endothelial cell thrombogenicity. *Biomaterials*, *28*(16), 2547. https://doi.org/10.1016/j.biomaterials.2007.01.039
[246] Yang, Z., Song, Z., Nie, X., *et al.* A smart scaffold composed of three-dimensional printing and electrospinning techniques and its application in rat abdominal wall defects. *Stem Cell Res Ther* 11, 533 (2020). https://doi.org/10.1186/s13287-020-02042-6
[247] Xue J, Wu T, Dai Y, Xia Y (2019) Electrospinning and Electrospun nanofibers: methods, materials, and applications. Chem Rev 1198:5298–5415. https://doi.org/10.1021/acs.chemrev.8b00593
[248] Mei L, Wang Y, Tong A, Guo G (2016) Facile electrospinning of an efficient drug delivery system. Expert Opin Drug Deliv 135:741–753. https://doi.org/10.1517/17425247.2016.1142525
[249] Park SH, Kim TG, Kim HC, Yang DY, Park TG. Development of dual-scale scaffolds via direct polymer melt deposition and electrospinning for applications in tissue regeneration. Acta Biomater. 2008;4(5):1198–207.
[250] Kurpinski, K.T., Stephenson, J.T., Janairo, R.R.R., Lee, H., Li, S., 2010. The effect of fiber alignment and heparin coating on cell infiltration into nanofibrous PLLA scaffolds. Biomaterials 31, 3536–3542. https://doi.org/10.1016/j.biomaterials.2010.01.062
[251] Hu, X., Liu, S., Zhou, G., Huang, Y., Xie, Z., & Jing, X. (2014). Electrospinning of polymeric nanofibers for drug delivery applications. Journal of Controlled Release, 185, 12-21. https://doi.org/10.1016/j.jconrel.2014.04.018
[252] Sridhar R, Lakshminarayanan R, Madhaiyan K, Amutha Barathi V, Lim KH, Ramakrishna S (2015) Electrosprayed nanoparticles and electrospun nanofibers based on natural materials: applications in tissue regeneration, drug delivery, and pharmaceuticals. Chem Soc Rev 443:790–814.
[253] Adamo, A., Bartolacci, J. G., Pedersen, D. D., Traina, M. G., Kim, S., Pantano, A., Ghersi, G., Watkins, S. C., Wagner, W. R., & Badylak, S. F. (2022). Continuous Microfiber Wire Mandrel-Less Biofabrication for Soft Tissue Engineering Applications. Advanced Healthcare Materials, 11(13), 2102613. https://doi.org/10.1002/adhm.202102613
[254] Bhardwaj, N., & Kundu, S. C. (2010). Electrospinning: A fascinating fiber fabrication technique. *Biotechnology Advances*, *28*(3), 325-347. https://doi.org/10.1016/j.biotechadv.2010.01.004
[255] D'Amore, A., Luketich, S. K., Raffa, G. M., Olia, S., Menallo, G., Mazzola, A., D'Accardi, F., Grunberg, T., Gu, X., Pilato, M., Kameneva, M. V., Badhwar, V., & Wagner, W. R. (2018). Heart valve scaffold fabrication: Bioinspired control of macro-scale morphology, mechanics, and microstructure. Biomaterials, 150, 25-37. https://doi.org/10.1016/j.biomaterials.2017.10.011
[256] Mabrouk, M., Beherei, H. H., & Das, D. B. (2020). Recent progress in the fabrication techniques of 3D scaffolds for tissue engineering. Materials Science and Engineering: C, 110, 110716. https://doi.org/10.1016/j.msec.2020.110716
[257] Wang, J., & Windbergs, M. (2017). Functional electrospun fibers for the treatment of human skin wounds. *European Journal of Pharmaceutics and Biopharmaceutics*, *119*, 283-299. https://doi.org/10.1016/j.ejpb.2017.07.001
[258] https://polytech-health-aesthetics.com/en/pro/products/breast-implants/
[259] https://www.ncbi.nlm.nih.gov/books/NBK54050/
[260] https://www.noselab-ats.com/en/products/plastic-and-rubber-testing/specimen-preparation/fustellatrice-manuale/
[261] Amoroso, N. J., Hong, Y., Wagner, W. R., & Sacks, M. S. (2011). Elastomeric Electrospun Polyurethane Scaffolds: The Interrelationship Between Fabrication Conditions, Fiber Topology, and Mechanical Properties. Advanced Materials, 23(1), 106-111. https://doi.org/10.1002/adma.201003210

[262] Sánchez-Palencia, D. M., D'Amore, A., González-Mancera, A., Wagner, W. R., & Briceño, J. C. (2014). Effects of fabrication on the mechanics, microstructure, and micromechanical environment of small intestinal submucosa scaffolds for vascular tissue engineering. *Journal of Biomechanics*, *47*(11), 2766-2773. https://doi.org/10.1016/j.jbiomech.2014.04.048
[263] https://www.ncbi.nlm.nih.gov/pmc/articles/PMC2855340/pdf/nihms-184610.pdf
[264] Arrúa Báez, W., Centurión Quintana, J. R., Montalbetti Moreno, Y., & Heinichen Almada, O. Y. (2023). Determinación de parámetros bioquímicos de animales del Bioterio de la Facultad de Ciencias Químicas de la Universidad Nacional de Asunción. *Revista De La Sociedad Científica Del Paraguay*, *28*(1), 126–140. https://doi.org/10.32480/rscp.2023.28.1.126
[265] Thammitiyagodage, M. G., Rathnayake, C., Karunakaran, R., WGSS, K., Gunatillka, M. M., Ekanayaka, N., Galhena, B. P., & Thabrew, M. I. (2020). Biochemical and histopathological changes in Wistar rats after consumption of boiled and un-boiled water from high and low disease prevalent areas for chronic kidney disease of unknown etiology (CKDu) in north Central Province (NCP) and its comparison with low disease prevalent Colombo, Sri Lanka. *BMC Nephrology*, *21*. https://doi.org/10.1186/s12882-020-1693-3
[266] Fluke, L. M., Restrepo, R. D., Patel, S., Hoagland, B. D., Krevetski, L. M., & Stephenson, J. T. (2016). Strength and histology of a nanofiber scaffold in rats. *Journal of Surgical Research*, *205*(2), 432-439. https://doi.org/10.1016/j.jss.2016.06.057
[267] https://imagej.net/ij/download.html
[268] https://github.com/landinig/IJ-Colour_Deconvolution2/blob/main/colour_deconvolution2.jar
[269] https://imagej.nih.gov/ij
[270] Quantification of equine dermal collagen by two morphometric techniques: point counting and color segmentation. S. Bedoya, Souza. Arq. Bras. Med. Vet. Zootec., v.71, n.3, p.761-769, 2019
[271] K.L. Fujimoto, J. Guan, H. Oshima, T. Sakai, W.R. Wagner, Vivo evaluation of a porous, elastic, biodegradable patch for reconstructive cardiac procedures, Ann. Thorac. Surg. 83 (2007) 648e654.
[272] R. Hashizume, Y. Hong, K. Takanari, K.L. Fujimoto, K. Tobita, W.R. Wagner, The effect of polymer degradation time on functional outcomes of temporary elastic patch support in ischemic cardiomyopathy, Biomaterials 34 (2013) 7353e7363.
[273] Bernardini, R., Varvaras, D., Bielli, A., Scioli, M. G., Coniglione, F., Rossi, P., Buonomo, O. C., Petrella, G., Mattei, M., & Orlandi, A. (2020). Biological acellular pericardial mesh regulated tissue integration and remodeling in a rat model of breast prosthetic implantation. *Journal of Biomedical Materials Research Part B: Applied Biomaterials*, *108*(2), 577-590. https://doi.org/10.1002/jbm.b.34413
[274] https://www.plasticsurgery.org/documents/News/Statistics/2022/plastic-surgery-statistics-report-2022.pdf
[275] Weyhe, D., Belyaev, O., Müller, C., Meurer, K., Bauer, H., Papapostolou, G., & Uhl, W. (2007). Improving Outcomes in Hernia Repair by the Use of Light Meshes—A Comparison of Different Implant Constructions Based on a Critical Appraisal of the Literature. *World Journal of Surgery*, *31*(1), 234-244. https://doi.org/10.1007/s00268-006-0123-4
[276] Silvestre AC, de Mathia GB, Fagundes DJ, Medeiros LR, Rosa MI. Shrinkage evaluation of heavyweight and lightweight polypropylene meshes in inguinal hernia repair: a randomized controlled trial. Hernia. 2011 Dec;15(6):629-34. doi: 10.1007/s10029-011-0853-6. Epub 2011 Jul 12. PMID: 21748479.
[277] Utiyama EM, Rosa MB, Andres Mde P, Miranda JS, Damous SH, Birolini CA, Damous LL, Montero EF. Polypropylene and polypropylene/polyglecaprone (Ultrapro®) meshes in the repair of incisional hernia in rats. Acta Cir Bras. 2015 Jun;30(6):376-81. doi: 10.1590/S0102-865020150060000001. PMID: 26108024.
[278] Taylor DF, Smith FB. Porous methyl methacrylate as an implant material. J Biomed Mater Res. 1972;6(1):467-79. doi: 10.1002/jbm.820060112. PMID: 5014905.
[279] Bilsel Y, Abci I. The search for ideal hernia repair; mesh materials and types. Int J Surg. 2012;10(6):317-21. doi: 10.1016/j.ijsu.2012.05.002. Epub 2012 May 12. PMID: 22588090.
[280] Roman S, Mangir N, Bissoli J, Chapple CR, MacNeil S. Biodegradable scaffolds designed to mimic fascia-like properties for the treatment of pelvic organ prolapse and stress urinary incontinence. J Biomater Appl. 2016 May;30(10):1578-88. doi: 10.1177/0885328216633373. Epub 2016 Feb 18. PMID: 26896234.
[281] Abdul-Al, M., Zaernia, A., & Sefat, F. (2020). Biomaterials for breast reconstruction: Promises, advances, and challenges. *Journal of Tissue Engineering and Regenerative Medicine*, *14*(11), 1549-1569. https://doi.org/10.1002/term.3121

[282] Ibrahim, Ahmed M.S. MD; Ayeni, Olubimpe A. MD, MPH, FRCSC; Hughes, Kenneth B. MD; Lee, Bernard T. MD; Slavin, Sumner A. MD; Lin, Samuel J. MD. Acellular Dermal Matrices in Breast Surgery: A Comprehensive Review. Annals of Plastic Surgery 70(6): p 732-738, June 2013. | DOI: 10.1097/SAP.0b013e31824b3d30

[283] DeLong M.; Tandon V.; Bertrand A., MacEachern M.; Goldberg M.; Salibian A.; Pusic A.; Festekjian J. Wilkins E. Review of Outcomes in Prepectoral Prosthetic Breast Reconstruction with and without Surgical Mesh Assistance. Plastic and Reconstructive Surgery 147(2): p 305-315, February 2021. | DOI: 10.1097/PRS.0000000000007586

[284] Laschke, M. W., Häufel, J. M., Thorlacius, H., & Menger, M. D. (2005). New experimental approach to study host tissue response to surgical mesh materials in vivo. *Journal of Biomedical Materials Research Part A*, *74A* (4), 696-704. https://doi.org/10.1002/jbm.a.30371

[285] Klinge U. Mesh for hernia repair. Br J Surg. 2008 May;95(5):539-40. doi: 10.1002/bjs.6159. PMID: 18344188.

[286] Agarwal, S., Wendorff, J. H., & Greiner, A. (2008). Use of electrospinning technique for biomedical applications. *Polymer*, *49*(26), 5603-5621.

[287] Madden LR, Mortisen DJ, Sussman EM, Dupras SK, Fugate JA, Cuy JL, Hauch KD, Laflamme MA, Murry CE, Ratner BD. Proangiogenic scaffolds as functional templates for cardiac tissue engineering. Proc Natl Acad Sci U S A. 2010 Aug 24;107(34):15211-6. doi: 10.1073/pnas.1006442107. Epub 2010 Aug 9. PMID: 20696917; PMCID: PMC2930533.

[288] Wright LD, Young RT, Andric T, Freeman JW. Fabrication and mechanical characterization of 3D electrospun scaffolds for tissue engineering. Biomed Mater. 2010 Oct;5(5):055006. doi: 10.1088/1748-6041/5/5/055006. Epub 2010 Sep 15. PMID: 20844321.

[289] McCullen SD, Gittard SD, Miller PR, Pourdeyhimi B, Narayan RJ, Loboa EG. Laser ablation imparts controlled micro-scale pores in electrospun scaffolds for tissue engineering applications. Ann Biomed Eng. 2011 Dec;39(12):3021-30. doi: 10.1007/s10439-011-0378-2. Epub 2011 Aug 17. PMID: 21847685.

[290] Hashizume R, Fujimoto KL, Hong Y, Amoroso NJ, Tobita K, Miki T, Keller BB, Sacks MS, Wagner WR. Morphological and mechanical characteristics of the reconstructed rat abdominal wall following use of a wet electrospun biodegradable polyurethane elastomer scaffold. Biomaterials. 2010 Apr;31(12):3253-65. doi: 10.1016/j.biomaterials.2010.01.051. Epub 2010 Feb 6. PMID: 20138661; PMCID: PMC3182828.

[291] Hall Barrientos, I. J., Paladino, E., Szabó, P., Brozio, S., Hall, P. J., Oseghale, C. I., Passarelli, M. K., Moug, S. J., Black, R. A., Wilson, C. G., Zelkó, R., & Lamprou, D. A. (2017). Electrospun collagen-based nanofibres: A sustainable material for improved antibiotic utilization in tissue engineering applications. *International Journal of Pharmaceutics*, *531*(1), 67-79. https://doi.org/10.1016/j.ijpharm.2017.08.071

[292] Amoroso NJ, D'Amore A, Hong Y, Rivera CP, Sacks MS, Wagner WR. Microstructural manipulation of electrospun scaffolds for specific bending stiffness for heart valve tissue engineering. Acta Biomater. 2012 Dec;8(12):4268-77. doi: 10.1016/j.actbio.2012.08.002. Epub 2012 Aug 10. PMID: 22890285; PMCID: PMC4398312.

[293] Zamani M, Prabhakaran MP, Ramakrishna S. Advances in drug delivery via electrospun and electrosprayed nanomaterials. Int J Nanomedicine. 2013;8:2997-3017. doi: 10.2147/IJN.S43575. Epub 2013 Aug 9. PMID: 23976851; PMCID: PMC3746732.

[294] Chen, S., Li, R., Li, X., & Xie, J. (2018). Electrospinning: An enabling nanotechnology platform for drug delivery and regenerative medicine. *Advanced Drug Delivery Reviews*, *132*, 188-213. https://doi.org/10.1016/j.addr.2018.05.001

[295] Takanari, K., Hong, Y., Hashizume, R., Huber, A., Amoroso, N. J., D'Amore, A., ... & Wagner, W. R. (2016). Abdominal wall reconstruction by a regionally distinct biocomposite of extracellular matrix digest and a biodegradable elastomer. *Journal of tissue engineering and regenerative medicine*, *10*(9), 748-761.

[296] Arrabito G, Ferrara V, Bonasera A, Pignataro B. Artificial Biosystems by Printing Biology. Small. 2020 Jul;16(27):e1907691. doi: 10.1002/smll.201907691. Epub 2020 Jun 8. PMID: 32511894.

[297] Gladman AS, Matsumoto EA, Nuzzo RG, Mahadevan L, Lewis JA. Biomimetic 4D printing. Nat Mater. 2016 Apr;15(4):413-8. doi: 10.1038/nmat4544. Epub 2016 Jan 25. PMID: 26808461.

[298] Mîra A, Carton AK, Muller S, Payan Y. A biomechanical breast model evaluated with respect to MRI data collected in three different positions. Clin Biomech (Bristol, Avon). 2018 Dec;60:191-199. doi: 10.1016/j.clinbiomech.2018.10.020. Epub 2018 Oct 17. PMID: 30408760.

[299] Sivaraman, S., Amoroso, N., Gu, X., Purves, J. T., Wagner, W. R., & Nagatomi, J. (2019). Evaluation of Poly (Carbonate-Urethane) Urea (PCUU) Scaffolds for Urinary Bladder Tissue Engineering. *Annals of Biomedical Engineering*, *47*(3), 891. https://doi.org/10.1007/s10439-018-02182-0

[300] Farmer, Z., Domínguez-Robles, J., Mancinelli, C., Larrañeta, E., & Lamprou, D. A. (2020). Urogynecological surgical mesh implants: New trends in materials, manufacturing, and therapeutic approaches. *International Journal of Pharmaceutics*, *585*, 119512. https://doi.org/10.1016/j.ijpharm.2020.119512

[301] Coyan GN, da Mota Silveira-Filho L, Matsumura Y, Luketich SK, Katz W, Badhwar V, Wagner WR, D'Amore A. Acute In Vivo Functional Assessment of a Biodegradable Stentless Elastomeric Tricuspid Valve. J Cardiovasc Transl Res. 2020 Oct;13(5):796-805. doi: 10.1007/s12265-020-09960-z. Epub 2020 Feb 10. PMID: 32040766.

[302] Zakeri Z, Salehi R, Mahkam M, Rahbarghazi R, Abbasi F, Rezaei M. Electrospun POSS integrated poly(carbonate-urea)urethane provides appropriate surface and mechanical properties for the fabrication of small-diameter vascular grafts. J Biomater Sci Polym Ed. 2022 Aug;33(11):1415-1434. doi: 10.1080/09205063.2022.2059741. Epub 2022 Apr 5. PMID: 35380915.

[303] Arbeiter, D., Lebahn, K., Reske, T., Senz, V., Eickner, T., Schmitz, K., Grabow, N., & Oschatz, S. (2022). Comparison of accelerated and enzyme-associated real-time degradation of HMW PLLA and HMW P3HB films. *Polymer Testing*, *107*, 107471. https://doi.org/10.1016/j.polymertesting.2021.107471

[304] Kalaba S, Gerhard E, Winder JS, Pauli EM, Haluck RS, Yang J. Design Strategies and Applications of Biomaterials and Devices for Hernia Repair. Bioact Mater. 2016 Sep;1(1):2-17. doi: 10.1016/j.bioactmat.2016.05.002. Epub 2016 May 30. PMID: 28349130; PMCID: PMC5365083.

[305] Fischer, S., Hirche, C., Reichenberger, M. A., Kiefer, J., Diehm, Y., Srinivasan Mukundan, J., Alhefzi, M., Bueno, E. M., Kneser, U., & Pomahac, B. (2015). Silicone Implants with Smooth Surfaces Induce Thinner but Denser Fibrotic Capsules Compared to Those with Textured Surfaces in a Rodent Model. *PLoS ONE*, *10*(7). https://doi.org/10.1371/journal.pone.0132131

[306] Huang SQ, Chen Y, Zhu Q, Zhang YM, Lei ZY, Zhou X, Fan DL. In Vivo and In Vitro Fibroblasts' Behavior and Capsular Formation in Correlation with Smooth and Textured Silicone Surfaces. Aesthetic Plast Surg. 2022 Jun;46(3):1164-1177. doi: 10.1007/s00266-022-02769-y. Epub 2022 Mar 2. PMID: 35237878.

[307] Labay C, Canal JM, Modic M, Cvelbar U, Quiles M, Armengol M, Arbos MA, Gil FJ, Canal C. Antibiotic-loaded polypropylene surgical meshes with suitable biological behaviour by plasma functionalization and polymerization. Biomaterials. 2015 Dec;71:132-144. doi: 10.1016/j.biomaterials.2015.08.023. Epub 2015 Aug 19. PMID: 26322724.

[308] Yu, X., Chen, T., Huang, N., Jin, Y., & Yang, L. (2022). Skin Commensal Bacteria Modulates the Immune Balance of Mice to Alleviate Atopic Dermatitis-Induced Damage. *Evidence-Based Complementary and Alternative Medicine: ECAM*, *2022*. https://doi.org/10.1155/2022/4731675

[309] Agalar, c., Ozdogan, m., Agalar, f., Saygun, o., Aydinuraz, k., Akkuş, a., Ceken, s., & Akturk, s. (2006). A rat model of polypropylene graft infection caused by staphylococcus epidermidis. *Anz journal of surgery*, *76*(5), 387-391. https://doi.org/10.1111/j.1445-2197.2006.03728.x

[310] Byrd, A., Belkaid, Y. & Segre, J. The human skin microbiome. *Nat Rev Microbiol* 16, 143–155 (2018). https://doi.org/10.1038/nrmicro.2017.157

[311] Sengupta, P. (2013). The Laboratory Rat: Relating Its Age With Human's. *International Journal of Preventive Medicine*, *4*(6), 624-630. https://www.ncbi.nlm.nih.gov/pmc/articles/PMC3733029/